REFERENCE ONLY

UNIVERSITY OF LONDON THESIS

Degree PhD Year 2005 Name of Author AHMAD, M.

Synaptotagmin IV function in secretory granule maturation in neuroendocrine cells

Malika Ahras

A thesis submitted for the degree of Doctor of Philosophy at the University of London

September 2005

Secretory Pathways Laboratory

Cancer Research UK
London Research Institute
Lincoln's Inn Fields

ProQuest LLC
789 East Eisenhower Parkway
P.O. Box 1346
Ann Arbor, MI 48106-1346

Abstract

In neuroendocrine cells, immature secretory granules (ISGs) bud from the trans Golgi network (TGN), and then undergo a maturation process that includes ISG-ISG homotypic fusion, removal of excess membranes via clathrin-coated vesicles (CCVs) and acidification of the granules. These mature secretory granules (MSGs) can then fuse with the plasma membrane upon receiving an external signal, and finally release their content in the extracellular space.

In this thesis, I will present evidence that Synaptotagmin IV (Syt IV) is one of the components involved in the regulation of granule maturation in neuroendocrine cells.

Syt IV is a neuron and neuroendocrine cell-specific isoform, which belongs to the synaptotagmin family of membrane trafficking proteins. After confirming that Syt IV is localised on ISGs and absent from MSGs in PC12 cells, I investigated whether Syt IV is involved in ISG homotypic fusion by adding the purified Syt IV cytoplasmic domain into an in vitro assay, where it functions as a dominant negative. Addition of this domain, but not a similar domain from Syt I, resulted in a dose-dependent inhibition of ISG-ISG fusion. Furthermore, I found that Syt IV binds to the ISG-SNARE Syntaxin 6 (Stx6), suggesting that the two proteins might be part of the same machinery that regulates ISG maturation.

In addition, I used an in vivo approach based on the processing of secretogranin II (SgII) into its degradation product p18, which occurs during ISG maturation, to assay Syt IV function. I show that the Syt IV cytoplasmic domain, as well as siRNA-mediated knockdown of Syt IV inhibits SgII processing by prohormone convertase 2 (PC2). Interestingly, PC2 is found mostly in the pro-form, suggesting that activation of PC2 is also inhibited. We conclude that Syt IV is an essential component for the process of secretory granule maturation.

Lastly, I found that Syt IV binds preferentially to membrane-bound clathrin adaptor protein-1 (AP-1). This suggests that Syt IV might be sorted from maturing SGs in a complex, possibly via an ISG-SNARE protein that interacts directly with AP-1.

Dedication

This thesis is dedicated to my husband, Salah, without whom all this would not have been possible. He has given me courage and perseverance to continue in what was a difficult journey.

Acknowledgements

I would like to thank my supervisor Sharon Tooze for her advices and continuous support and for believing in me.

Thanks to Dr Mitsunori Fukuda for sending me antibodies and various constructs and to Dr Giampietro Schiavo for all the suggestions and interest in my project.

A very special thank you to Grant Otto for reading my whole thesis (very quickly), he really has avoided me a huge stress, also for his very valued scientific discussions and suggestions. Also I would like to thank Or Kakhlon for his comments and always being ready to discuss my project.

Thanks to past and present members of the lab: Franz, John, Robert, Andrew, Wen, Harold and Ed (for reading part of my thesis).

I also would like to thank Natalie for being such a good friend and always being there for me. Also, thanks to Katrin for always being helpful, to Tracy Hatfield for teaching me various tricks in Word.

Thanks to CR-UK services: light microscopy, EM, FACS, Equipement park, Library staff for their help with the project.

Table of contents

List of Figures

Abbreviation

Ab	Antibody
AP	Adaptor protein
ATP	Adenosine triphosphate
BAMC	Bovine adrenal medulla cytosol
BAPTA	1,2-bis (o-aminophenoxy) ethane-N,N,N',N'-tetraacetic acid
BFA	Brefeldin A
CBD	Calmodulin binding domain
CCVs	Clathrin coated vesicles
CD-MPR	Cation-dependent mannose-6-phosphate receptor of 46 KDa
CDNA	Complementary DNA
CgB	Chromogranin B
CI-MPR	Cation-independent mannose-6-phosphate receptor of 300 KDa
CSVs	Constitutive secretory granules
CR-UK	Cancer Research UK
C-terminus	Carboxy terminus
DAMP	3-(2,4-dinitroanilino)-3'-amino-*N*-methyldipropylamine
DMEM	Dulbecco's modified Eagle medium
DTT	Dithiothreiol
EDTA	Ethylene diamine tetra acetic acid
EEA 1	Early endosomal antigene
ELISA	Enzyme-linked immunosorbent assay
EM	Electron microscopy
ER	Endoplasmic reticulum
FB	Fusion buffer
FPLC	Fast performance liquid chromatography
GST	Glutathione-S-transfecrase
H	Hour
HA	Hemagglutinine
HB	Homogenisation buffer
Hepes	4-(-2-hydroxyl)-1-piperazine ethane sulphonic acid

HRP	Horseradish peroxidase
hsPG	Heparan sulphate proteoglycan
IF	Immunofluorescence
IP	Immunoprecipitation
IPTG	Isopropyl-β-D-thiogalactopyranoside
ISGs	Immature secretory granules
kDa	Kilo Dalton
LAMP	Lysosomal associated membrane protein
M6PR	Mannose 6 phosphate receptor
mab	Monoclonal antibody
MES	(2-[N-Morpholino]ethannesulfonic acid
Min	Minute
MSGs	Mature secretory granules
MW	Molecular weight
NSF	N-ethylmaleimide sensitive factor
N-terminus	Amino-terminus
OD	Optical density
pab	polyclonal antibody
PAGE	Polyacrylamide gel electrophoresis
PBS	Phosphate buffered saline
PC	Prohormone convertase
PC12	Rat pheochromocytoma cell line
PCR	Polymerase chain reaction
PFA	Paraformaldehyde
PMSF	Polymethylsulphonyl fluoride
PNS	Postnuclear supernatant
POMC	Pro-opicomelanocortin
RPM	Round per minute
RT	Room temperature
SDS	Sodium dodecyl sulphate
SEM	Standard error of the mean
SgI	Secretogranin I
SgII	Secretogarnin II

siRNA	Small inhibitory RNA
SNAP	Soluble NSF attachment protein
SNAP 25	Synaptosome associated protein of 25 kDa
SNARE	SNAP-receptor
STI	Soy bean trypsin inhibitor
Stx	Syntaxin
Syt	Synaptotagmin
TAP	Tandem affinity purification
TBS	Tris buffered saline
TCA	Trichlor acetic acid
TEMED	N,N,N',N'-tetramethyl-ethylenediamine
TEV	Tobacco etch virus
TGN	trans-Golgi network
Tris	2-amino-2-(hydroxymethyl)-1,3-propanediol
VAMP	Vesicle associated membrane protein
WB	Western blotting
wt	Wild type

Publications

Ahras, M and Tooze, S.A. Synaptotagmin IV is necessary for maturation of secretory granules in PC12 cells. *Journal of Cell Biology, in revision*

1 Chapter 1: Introduction

1.1 Vesicular transport along the secretory pathway

A eukaryotic cell is subdivided into functionally distinct, membrane-enclosed compartments or organelles. Each compartment contains its own characteristic set of proteins and unique functional properties. Proteins entering the secretory pathway start their route in the endoplasmic reticulum (ER), and move in an anterograde direction towards the Golgi complex, with a final destination in the plasma membrane, lysosomes, endosomes or the exterior of the cell. Proteins are transported via vesicular transport from their site of synthesis to their specific residence (Palade, 1975). Indeed, the work of Palade *et al* has established that the transfer of cargo molecules between organelles of the secretory pathway is mediated by shuttling transport vesicles. Two highly controlled steps define the vesicular transport of cargo along the secretory pathway: budding and fusion. Vesicles bud from a "donor compartment" (vesicle budding), excluding resident proteins of the donor compartment (protein sorting). The budded vesicles are then targeted to a specific "acceptor compartment", into which they unload their cargo upon fusion of their membranes (vesicle fusion). The budding of transport vesicles and the selective incorporation of cargo into the forming vesicles are both mediated by protein coats, whereas membrane fusion is mediated by SNAREs (soluble N-ethylmaleimide sensitive factor attachment protein receptor) and their regulatory proteins (Bonifacino and Glick, 2004).

Proteins containing an ER-signal sequence are translocated across the ER membrane through an aqueous ER-translocon pore complex (Rapoport, 1992). In the ER, protein chaperones facilitate the correct folding and assembly of protein complexes. In addition to the correct folding of newly synthesised proteins, a series of post-translational modifications, such as N-glycosylation and the generation of disulphide bonds, occur. Only correctly folded proteins can exit the ER and are transported to the Golgi complex. Transport from ER to the Golgi is mediated via vesicles that contain coatomer protein II (COP II) coats. After transport vesicles have budded from the ER, they fuse together forming vesicular tubular clusters (VTCs), also called the ER-Golgi intermediate compartment (ERGIC) (Duden, 2003). The ERGIC transports the proteins to the Golgi complex, where they fuse and deliver their contents. Proteins enter the Golgi on its *cis* side and exit from the *trans* side before export to their final destinations. Proteins that have escaped the quality control in the ER are returned from the *cis* Golgi in COP I-coated vesicles. During the transport of proteins though the Golgi stacks, the majority of post-translational modifications, such as O-glycosylation, trimming of N-linked oligosaccharides, added in the ER, and sulphation, occur.

Once in the trans-Golgi network (TGN), proteins are sorted for delivery to distinct destinations (Farquhar and Palade, 1981). Indeed, various trafficking routes emanate from the TGN, including pathways to lysosomes, endosomes, and the plasma membrane via constitutive secretory vesicles or via secretory granules in the regulated secretory pathway, although the latter vesicles are found only in specialised cell types, such as endocrine, neuroendocrine and exocrine cells.

Two major sorting mechanisms occur in the TGN: *sorting for entry* and/or *sorting by retention. Sorting for entry* describes a mechanism by which sorting signals mediate the sorting of proteins into the nascent vesicles. For example, sorting of lysosomal enzymes

destined for delivery to lysosomes is mediated by mannose 6-phosphate (M6P) groups, recognised by the M6P-receptor (M6PR). The MPR contains motifs, such as tyrosine or dileucine-based motifs that will bind the adaptor protein 1 (AP-1) and GGAs (Golgi associated, γ ear-containing, ADP-ribosylation factor (ARF) binding protein). These adaptor proteins recruit clathrin lattices to the budding site. This will mediate the inclusion of the lysosomal hydrolases into clathrin-coated vesicles (CCVs) that are targeted specifically to lysosomes (Kornfeld and Mellman, 1989).

Sorting by retention is used for the retention of proteins in their correct compartments, for example, the one used by the TGN-resident proteins or immature secretory granules proteins (ISGs) (Kuliawat and Arvan, 1994).

The transport of cargo along the secretory pathway, described herein, is anterograde transport (towards the plasma membrane). However, to balance this directional movement of cargo, organelle homeostasis requires the retrieval of transport machinery components back to the corresponding donor compartment for re-use (retrograde transport), a process that also occurs by vesicular transport (Figure 1 shows the intracellular transport between different organelles in the cell) (Bonifacino and Glick, 2004).

For delivery of their content, the formed vesicles have to be targeted to the right compartment, where they undergo membrane fusion. In the cell, specific proteins such as tethering factors ensure that these carriers recognise and fuse with the specific organelle. These processes help maintain the identity of each compartment in the cell.

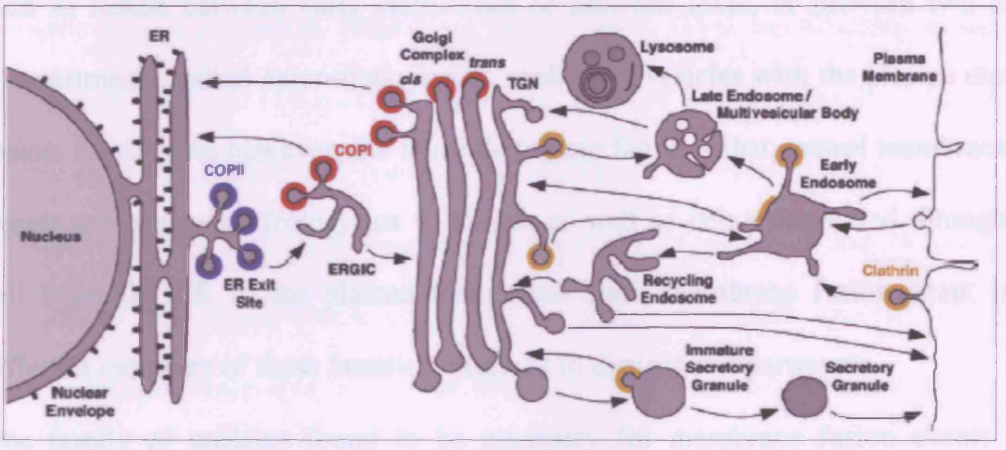

Figure 1: Intracellular transport pathways.

The scheme shows the vesicular transport between different compartments within the cell (indicated by arrows). Budding of vesicles uses coat proteins, COPII (blue), COPI (red), clathrin (orange) (Bonifacino, 2004).

1.2 Membrane fusion and SNARE proteins

Membrane fusion is an important process and allows the passage of molecules from one compartment to another within the cell or their release to the extracellular space. This process must be carefully controlled and regulated to ensure specificity. Membrane fusion can occur between similar compartments, called *homotypic fusion*, such as fusion between early endosomes or between ISGs, or between two different compartments, called *heterotypic fusion*, such as of vesicles with the plasma membrane fusion. In all cases however, the multiple protein families that control membrane fusion events are conserved from yeast to human as well as being conserved throughout the cell from the ER to the plasma membrane. Each membrane fusion event involves different members of these families localised to distinct compartments.

One family of proteins found to be necessary for membrane fusion events are the SNARE (soluble N-ethylmaleimide sensitive factor attachment protein receptor) proteins. SNAREs are small proteins of around 100-300 amino acids in length. Around 36 distinct SNAREs are found in mammalian cells and 24 in yeast (Bock et al., 2001). Syntaxin 1 (Stx1) (Bennett et al., 1992), SNAP-25 (25 kDa synaptosome-associated protein) (Oyler et al., 1989) and VAMP2 (vesicle-associated membrane protein) (Trimble et al., 1988), the first identified SNAREs, are abundantly expressed in neuronal cells and are involved in exocytosis. Since their identification, a multitude of other SNARE proteins, which localise to distinct subcellular compartments and contribute to the regulation of specific membrane fusion events, were identified (Chen and Scheller, 2001). SNAREs were originally classified as t-SNAREs, associated with the target compartment, such as Stx1 and SNAP-25, and v-SNAREs, associated with

the vesicular compartment, such as VAMP-2 (Sollner et al., 1993). To avoid confusion in the case of homotypic membrane fusion, where target and vesicular SNAREs are undistinguishable, SNAREs have been reclassified as R-SNARE or Q-SNARE, depending on the presence of an arginine (R) or glutamine (Q) in the SNARE motif (Fasshauer et al., 1998). The middle of the SNARE bundle is defined as the "0" layer, where there is interaction of three Q residues, contributed by Stx1 (termed Qa SNARE), the N-terminal domain of SNAP-25 (termed Qb-SNARE), and the C-terminal domain of SNAP-25 (termed Qc SNARE) and one R residue (contributed by VAMP-2) in the synaptic SNARE complex (Fasshauer et al., 1998). This classification is now more widely used than the previous one, and it is believed that one member of each family contribute a single SNARE motif, resulting in the Qa-Qb-Qc-R configuration of a SNARE complex (Figure 2 shows the subcellular localisation and classification of mammalian SNAREs) (Bock et al., 2001). Crystal structure analysis showed that SNARE proteins assemble into a four-helical bundle, with each helix contributed by the SNARE motif of Stx1, N-terminal SNARE motif of SNAP-25, C-terminal SNARE motif of SNAP-25 and VAMP-2, forming the SNARE complex, that is resistant to SDS denaturation (Hayashi et al., 1994) and heat stable up to 90 °C (Fasshauer et al., 1997) (Figure 3 represents SNARE complex organisation) (Sutton et al., 1998).

Although considerable advances in our understanding of the molecular mechanisms governing membrane fusion have been made, how membrane fusion occurs or how precisely SNAREs act is not fully understood.

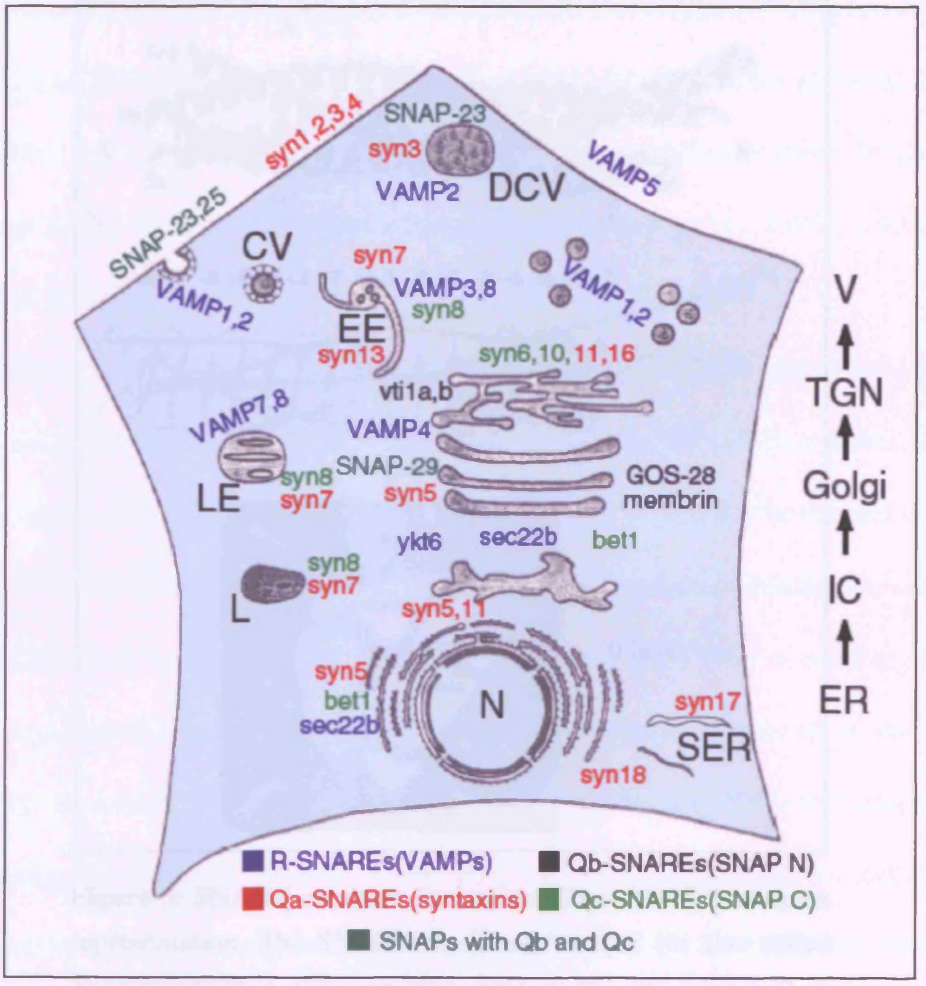

Figure 2: Subcellular localisation and classification of mammalian SNAREs. The scheme represents the different subcelluar localisation of the identified mammalian SNAREs. Syntaxins (classified as QaSNAREs) are represented in red, N-terminal domain of SNAP-25 homologues (Qb-SNAREs) in black, C-terminal of SNAP-25 homologues (Qc-SNAREs) in light green. Proteins such as SNAP-25 have two SNARE domains (Qbc-SNAREs) are represented in dark green (Bock, 2001).

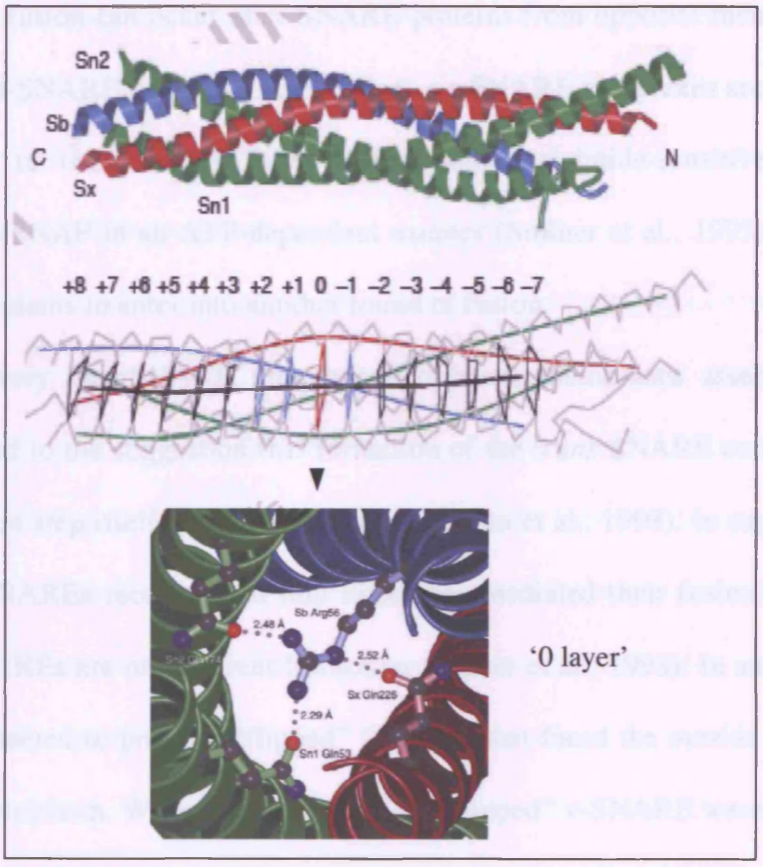

Figure 3: SNARE complex formation. Top: SNARE complex representation. The SNARE motifs of Vamp-2 (or also called Synaptobrevin-II, (Sb)) in blue, Stx1 in red and SNAP-25 in green (Sn1 and Sn2) assemble into a four-helical bundle, which is the core of the SNARE complex. Middle: organisation of the backbone of the SNARE complex into layers, with the "0 layer" in the middle (red) and 15 hydrophobic layers (black). Bottom: '0 layer' of the SNARE complex. Q-SNAREs and R-SNAREs are characterised by by glutamine (Q) or arginine (R) residue, respectively, in the central layer of the SNARE complex, (Sutton, R et al, 1998).

Membrane fusion occurs in successive steps. First, tethering factors ensure that vesicles are transported and linked to its cognate target membranes. After tethering, vesicles and target compartments are brought in close apposition, a process called docking. Finally, membrane fusion can occur after SNARE proteins from opposite membranes assemble into a trans-SNARE complex. After fusion, cis-SNARE complexes are disassembled by the action of the AAA ATPase, NSF (N-ethylmaleimide-sensitive factor) and its cofactor □-SNAP in an ATP-dependent manner (Sollner et al., 1993). This will allow SNARE proteins to enter into another round of fusion.

The discovery that SNARE proteins on opposite membranes assemble into a core complex led to the suggestion that formation of the *trans*-SNARE complex is involved in the fusion step itself, i.e. bilayer mixing (Sutton et al., 1998). In support of this idea, purified SNAREs reconstituted into liposomes mediated their fusion, provided that Q and R-SNAREs are on different liposomes (Weber et al., 1998). In another study, cells were engineered to produce "flipped" SNAREs that faced the outside of the cell rather than the cytoplasm. When cells containing a "flipped" v-SNARE were mixed with cells containing the cognate "flipped" t-SNAREs, efficient cell-cell fusion occurred (Hu et al., 2003). A different study conducted in permeabilised PC12 cells found that inhibition of exocytosis after treatment with botulinum neurotoxin E (BoNT/E), which cleaves SNAP-25, could be rescued by the addition of a soluble C-terminal "SNARE domain" of SNAP-25, but not with SNAP-25 carrying mutations in the hydrophobic residues along its carboxy-terminal coil domain (Chen et al., 1999). Moreover, the irreversible assembly of the SNARE core complex occurred only after the arrival of calcium (Chen et al., 1999). This confirms that the formation of the core complex, which occurs after calcium entry, is crucial for SNARE function. SNARE complex formation is believed to occur by "zippering" of the coiled-coil domains from their N-terminal membrane-distal

to their C-terminal membrane-proximal ends (Mayer, 2001). Indeed, the replacement of the transmembrane domains of SNARE proteins with phospholipids that do not span the lipid bilayer prevent fusion of liposomes (McNew et al., 2000). It was therefore suggested that SNARE complex formation would bring the two opposite membranes in close proximity, and this will promote spontaneous fusion between lipid bilayers by excluding water from the membrane interface. This model places the role of SNARE proteins in the final step of fusion.

Another model, the fusion pore model, emerged following studies conducted mainly in yeast vacuole fusion. This hypothesis suggests that the close membrane apposition mediated by SNAREs brings multimeric protein complexes on both membranes together, allowing the assembly of a pore connection between the opposite membranes, which will induce fusion (Mayer, 2001). This model disputes the role of SNAREs in triggering bilayer mixing, and rather suggests that these proteins are involved in the docking of the opposite membranes.

Homotypic fusion of yeast vacuoles involves the formation of a SNARE complex between the v-SNAREs (Nyv1p, Ykt6p) and the t-SNAREs (Vam3p, Vam7p, Vti1p). It was shown that the pairing of these SNAREs is important for vacuole docking, but not fusion itself (Ungermann et al., 1998). Indeed, the disassembly of the SNARE complex following the addition of excess NSF did not affect content mixing of the vacuoles, suggesting that fusion occurred. In addition, antibody inhibition studies indicated that SNARE proteins are required only up to the docking stage of fusion (Nichols et al., 1997). Together, these data demonstrate that SNARE complex formation is not required for the fusion step, but rather that the SNARE pairing may induce signals to downstream factors, leading to fusion that is controlled by other protein components. The pairing of SNAREs may invoke an efflux of calcium from the vacuole lumen,

which then recruits calmodulin to the membranes, which is part of a protein complex involved in triggering membrane fusion of yeast vacuoles (Peters and Mayer, 1998). Indeed, calmodulin interacts with the V_0 sector of the vacuolar H^+-ATPase (V-ATPase) on vacuoles, and this interaction was found to occur after trans-SNARE pairing (Peters et al., 2001). Moreover, when reconstituted into liposomes, V_0 was shown to form complexes between opposing membranes in a calcium-dependent manner (Peters et al., 2001). These complexes form sealed channels, which expand to form aqueous pores between opposite membarnes. Additional data showed that vacuole membranes from Δvph1 yeast deficient in one of the V_0 subunits- were capable of docking and trans-SNARE pairing, but did not fuse, even when only one of the fusion partners was devoid of Vph1p (Bayer et al., 2003), thus establishing a role for V_0 as an important component in vacuole fusion downstream of trans-SNARE pairing. These data support a model where the V_0 sectors on opposing membranes assemble to form a continuous pore composed of multiple subunits and enable membrane fusion.

In conclusion, both the pore and proximity models could be valid, and might predominate depending on the type of membrane fusion, homotypic versus heterotypic fusion.

Although the function of SNAREs in membrane fusion is incontestably important, increasing lines of evidence suggest that other proteins, such as, Rabs, tethering factors, SM proteins, Synaptotagmins and others, that also distribute to distinct cellular compartments and interact with SNAREs, participate in regulating a single or multiple stages of membrane fusion, as well as help to ensure membrane identity, suggesting that membrane fusion is a more complex than previously thought.

1.3 Rab proteins and their effectors

Rab proteins constitute a large family of conserved monomeric small GTPases. More than 60 Rab proteins were identified in humans and ~11 Ypt/Sec4 (Rab homologues) in yeast. Like SNAREs, Rab proteins are distributed to distinct intracellular compartments. Several studies have established that Rab proteins are involved in the tethering of vesicles to their target compartments, establishing the importance of Rab proteins in membrane fusion. Additionally, Rabs have also been implicated in vesicle budding and vesicle transport along the cytoskeleton, elevating this family of proteins to key players in different membrane trafficking events (Zerial and McBride, 2001).

Rab proteins do not have a transmembrane domain, but are attached to target membranes via two C-terminal geranylgeranyl groups. Rab escort proteins (REPs) bind newly synthesised Rab proteins, which are then prenylated upon the action of geranylgranyltransferase (Andres et al., 1993). REPs deliver the prenylated Rabs to their target membrane, where the complex dissociates. On membranes, Rabs can enter the GEF-and GAP-mediated GTPase cycle, where Rab proteins oscillate between "active" GTP- and "inactive" GDP-bound states. GDP-bound Rabs are cytosolic and are found in a complex with GDP dissociation inhibitor (GDI). GDI solubilises Rab-GDP proteins by enveloping the geranylgeranyl groups, releasing them into the cytosol. Specific guanine-nucleotide exchange factors (GEFs) target GDP-Rab proteins to membranes and activate the GDP-Rab proteins by GDP to GTP exchange. Activated Rabs can then interact with several effectors that connect the two opposed membranes. After fusion, a Rab GTPase-activating protein (GAP) triggers GTP hydrolysis to GDP, which results in the dissociation of Rab-effector molecule complexes. The GDP bound

Rab is then recognised by GDI, which removes it from membranes and recycles it to another GTPase cycle.

The ability of Rab proteins to act as GTP-dependent switches allows them to control the activity of effector molecules that function as tethering factors (Zerial and McBride, 2001) (Whyte and Munro, 2002). The function of the tethering factors is to allow close positioning of the vesicles with the target compartment, which will facilitate the subsequent trans-SNARE pairing followed by fusion. One well-studied example is the multimeric complex of proteins involved in the tethering reaction during fusion of early endosomes. On early endosomes, Rab5 was found to bind these membranes and to regulate their fusion *in vitro* (Gorvel et al., 1991). Later, Rab5 was found to interact with several down-stream effectors, such as EEA1, on early endosomes, revealing a more complex machinery (Christoforidis et al., 1999a). Rab5 was found to interact with hVPS34, a phosphatidylinositol-3-OH-kinase (PI(3)K), which preferentially phosphorylates phosphatidylinositol (PtIns) to PtIns(3)P, thus coupling PtIns(3)P production to Rab5 localisation (Christoforidis et al., 1999b). The concomitant presence of Rab5 and PtIns(3)P on early endosomes allows the recruitment of the tethering factor EEA1. EEA1 binds to both PtIns(3)P through its FYVE finger, and to Rab5 through a Rab5-binding site located immediately upstream of the FYVE finger (Simonsen et al., 1998). EEA1 was shown be involved in the tethering of endosomes (Christoforidis et al., 1999a). Moreover, EEA1 interacts with the SNARE machinery, and was shown to interact with Stx13, a SNARE protein involved in endosome-endosome fusion (McBride et al., 1999). This interaction was suggested to mediate the homotypic fusion of early endosomes. The link between tethering molecules and SNARE proteins was also found in other membranes, suggesting that this mechanism is conserved. Indeed, the Golgi tethering factor, p115, was found to interact directly with the Golgi-SNAREs,

Stx5 and GS28 (Shorter et al., 2002). The discovery that components of the Rab machinery interact with the fusion machinery allowed for a link between Rab-dependent membrane tethering, docking and finally membrane fusion. In addition, molecular interactions of SNARE proteins within Rab-enriched domains of membranes might result in the selective enrichment of SNARE complexes at their site of function. The involvement of large complexes, such as Rabs and their ever-growing list of effectors, during different steps of fusion, might contribute in achieving high fidelity during membrane fusion.

1.4 Sec1/Munc18 (SM) proteins

SM proteins constitute another family of proteins that was found to regulate membrane fusion reactions. They are hydrophilic proteins of 60-70 kDa (Jahn and Sudhof, 1999). There are four known SM proteins in yeast (Sec1p, Sly1p, Vps33p and Vps45p), and 7 in mammals (Munc18-1, Munc18-2, Munc18-3, VPS33A, VPS33B, VPS45 and SLY1). Munc18-1, Munc18-2 and Munc18-3 are functionally homologous to yeast Sec1p and function in the regulation of vesicle fusion with the plasma membrane. The neuronal-specific Munc18-1 is the most studied SM protein, and is involved in synaptic vesicle fusion. VPS33A and VPS33B are homologous to the yeast Vps33p, and are involved the endocytic pathway. VPS45 and SLY1 correspond to yeast Vps45p and Sly1p, and are involved in traffic at the Golgi (Gerst, 2003).

Although a role of SM proteins as essential factors in membrane fusion is established, their exact mode of function and at which stage they act is still under study. The controversy over the precise role of SM proteins in membrane fusion stems mainly from the conflicting data obtained from studies using neuronal SM proteins compared to their yeast orthologues. All SMs share a common property in that they bind to the Stx family

of proteins. However, SM proteins interact with the Qa-SNAREs via different mechanisms, not all of which involve direct binding. SM proteins, such as the neuron-specific Munc18-1, bind directly to the monomeric Stx1. This binding requires that Stx1 be in the "closed" conformation, in which the N-terminus, termed the Habc domain, folds back onto the SNARE motif (Misura et al., 2000). In contrast to Munc18, its yeast orthologue, Sec1p, does not bind directly to the monomeric Qa-SNARE Sso1p, that also adopts a closed conformation, but only to the fully assembled SNARE complex (Munson et al., 2000). These different modes of binding might be a mechanism to prevent binding of SM proteins to non-cognate Stxs, and to provide specificity to membrane fusion.

Studies using yeast SM proteins suggest that they positively regulate the formation of SNARE complexes. It was demonstrated, for example, that Golgi-SNARE complexes do not assemble in the absence Vps45p (Bryant and James, 2001). Furthermore, Sly1p, an SM protein operating in ER to Golgi fusion, prevents promiscuous SNARE assembly *in vitro* (Peng and Gallwitz, 2002). Together, these results obtained from yeast studies suggest a positive role of SM proteins in regulating fusion and, more precisely, in promoting the incorporation of Stxs into cognate SNARE complexes.

In contrast, a different role for SM proteins as negative regulators of fusion has been proposed from data demonstrating that Munc18-1 binding to Stx1 blocks SNARE complex formation *in vitro* (Pevsner et al., 1994). Moreover, the crystal structure showed that Munc18 stabilises Stx1 in its closed conformation (Misura et al., 2000). These observations suggested that Munc18-1 hinders the SNARE motif of Stx1, therefore preventing SNARE complex formation.

However, other studies have suggested instead that Munc18-1 acts positively to regulate membrane fusion. For example, mice lacking Munc18-1 exhibit an inhibition of

neurotransmitter release (Verhage et al., 2000). Moreover, large dense-core vesicle-mediated exocytosis from chromaffin cells was inhibited in the absence of Munc18-1, and stimulated by its overexpression (Voets et al., 2001). These results suggest that Munc18-1, in contrast to previous studies, plays a positive role in the regulation of exocytosis. Analysis of cells from Munc18-1-deficient mice revealed that these proteins could function in more than one step during membrane fusion. In chromaffin cells from these mice, a reduction in the number of docked dense core granules was observed, suggesting a role for SM proteins in the docking of vesicles (Voets et al., 2001). In contrast, synaptic vesicle docking in these mice was normal, suggesting that Munc18-1 has a role in a post-docking stage of fusion in neurons (Verhage et al., 2000). A recent study showed that Stx1 levels are reduced by 70% in Munc18-1 knock-out mice, which is due to a decrease in Stx1 stability (Toonen et al., 2005). However, in these cells residual Stx1 was correctly targeted to synapses, and was capable of forming a SNARE complex. Based on the complete lack of neurotransmitter release in Munc18-1 knock-out mice, it is possible that SM proteins may also function after SNARE complex assembly. This study suggested that binding to Stx1 is not the only function of SM proteins. In fact, it was proposed that SM proteins could also regulate fusion independently of their interaction with Stxs. In agreement with this, it was shown that Munc18-1 mutants displaying normal binding to Stx1 affected both early and late steps of exocytosis (Ciufo et al., 2005). These results were attributed to the fact that in addition to Stx1, Munc18-1 binds to a multitude of other proteins involved in exocytosis, such as Mints.

In conclusion, SM proteins are an important family of proteins involved in the regulation of membrane fusion in concert with SNAREs. However, their role in the

regulation of fusion is not limited to their binding to Stxs, but clearly the role of these proteins in fusion is more varied.

1.5 Synaptotagmins

1.5.1 Synaptotagmin I

Synaptotagmins (Syts) belong to the C-terminal-type tandem C2 protein family, and are involved in membrane trafficking events. All Syt isoforms share the same domain structure. They are characterised by a short N-terminal luminal domain, a single transmembrane domain, a variable length spacer domain, and C2A and C2B domains (Tucker and Chapman, 2002).

Synaptotagmin I (Syt I) was the first identified and is the best characterised Syt isoform. It is a neuronal and neuroendocrine-specific isoform, and is localised on synaptic vesicles as well as MSGs called large dense core vesicles (LDCVs) (Matthew et al., 1981) (Walch-Solimena et al., 1993). The crystal structure of the C2 domain of Syts shows that they are compact, rigid eight-stranded β-sandwiches. Flexible loops protrude from the ends of these domains, two of which coordinate the binding of three calcium ions in C2A (Sutton et al., 1995) (Ubach et al., 1998) and two calcium ions in C2B domain (Fernandez et al., 2001) (Figure 4 shows the domain structure of Syt I and the crystal structure of Syt I-C2 domains).

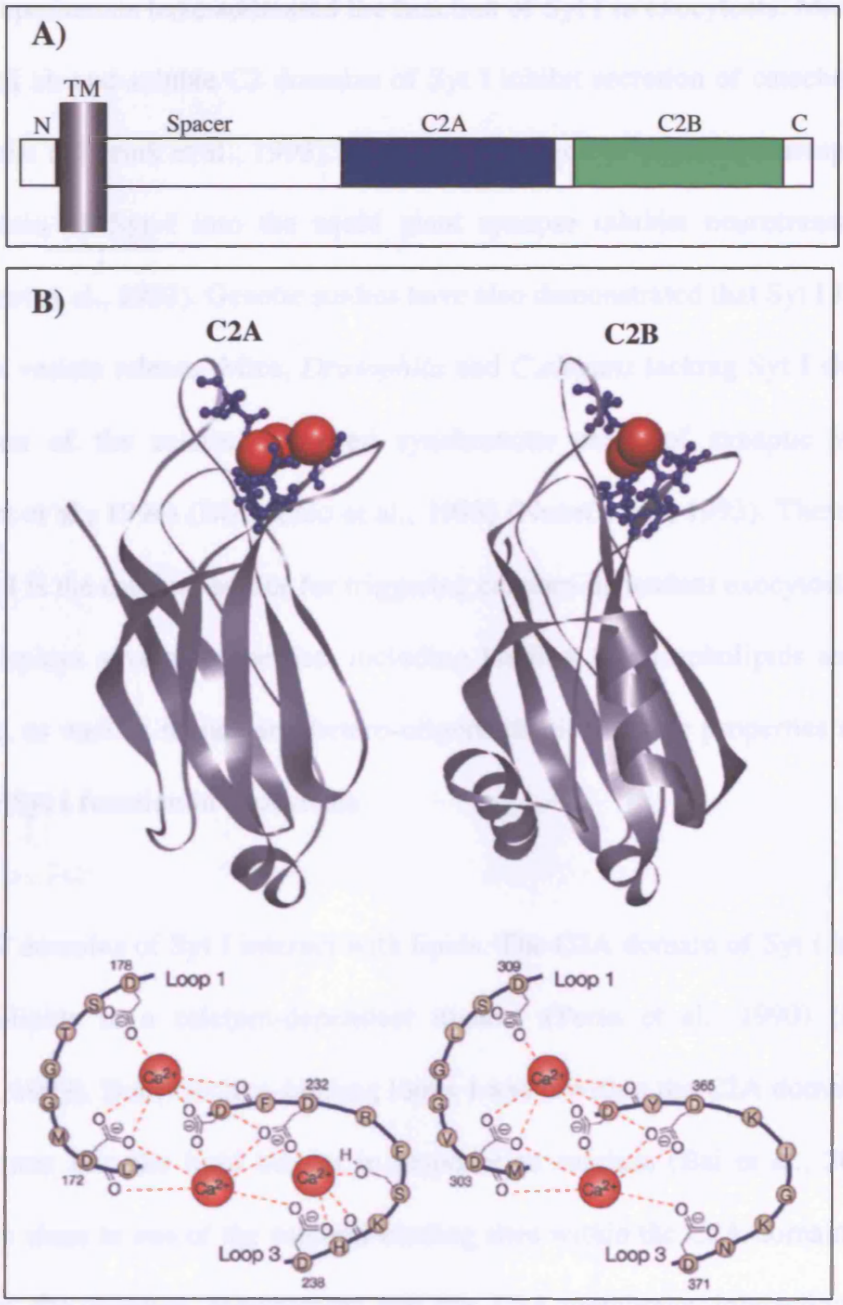

Figure 4: Syt I structure. A) Schematic representation of Syt I domain structure. Syt I has a short lumenal N-terminal domain, a single transmembrane domain, a spacer domain, the C2A (blue), C2B domains (green) and a small C-terminal domain. B) Ribbon diagrams of the C2A and C2B domains of Syt I. Each domain is formed by eight-stranded-β-sandwich motif. Calcium-binding loops protrude from the top surface of each motif. A total of five calcium ions (red) bind to loops 1 and 3 of both domains via calcium binding residues (blue) (Top). Five acidic residues in both C2A and C2B domains coordinate the binding of three and two calcium ions,espectively (Bottom).
(Chapman et al, 2002)

Initial experiments have addressed the function of Syt I in exocytosis. Microinjection of anti-Syt I ab and soluble C2 domains of Syt I inhibit secretion of catecholamines from PC12 cells (Elferink et al., 1993). Moreover, injection of peptides corresponding to the C2 domain of Syt I into the squid giant synapse inhibits neurotransmitter release (Bommert et al., 1993). Genetic studies have also demonstrated that Syt I is important in synaptic vesicle release. Mice, *Drosophila* and *C.elegans* lacking Syt I show a specific disruption of the calcium-triggered synchronous phase of synaptic vesicle fusion (Geppert et al., 1994) (DiAntonio et al., 1993) (Nonet et al., 1993). These data suggest that Syt I is the calcium-sensor for triggering calcium-dependent exocytosis.

Syt I displays several properties, including binding to phospholipids and to SNARE proteins, as well as homo- and hetero-oligomerisation. These properties are thought to mediate Syt I function in exocytosis.

Both C2 domains of Syt I interact with lipids. The C2A domain of Syt I binds to acidic phospholipids in a calcium-dependent manner (Perin et al., 1990) (Davletov and Sudhof, 1993). Both calcium-binding loops 1 and 3 within the C2A domain were found to penetrate into the lipid bilayer in response to calcium (Bai et al., 2000). A point mutation close to one of the calcium-binding sites within the C2A domain decreases by two-fold the calcium requirement for the C2A-membrane interaction (Fernandez-Chacon et al., 2001). Knock-in mice harbouring this mutation show a similar two-fold reduction in exocytosis, suggesting that this property in important for fusion (Fernandez-Chacon et al., 2001). The C2B domain of Syt I was also shown to bind acidic phospholipids, but only when tethered to the C2A domain, suggesting a cooperative function between the two domains (Bai et al., 2002).

In addition to acidic phospholipids, the C2B domain of Syt I binds phosphatidylinositol (4,5)-bisphosphate (PIP2) (Schiavo et al., 1996). Recently, it was shown that the C2B domain of Syt I displays two modes of binding to PIP2. In the absence of calcium, Syt I-C2B domain binds to PIP2 weakly. Increases in calcium concentration drive the reorientation of C2B and its insertion into the lipid bilayer (Bai et al., 2004a). These findings prompted a model in which the Syt I inserts into PIP2-rich domains in the plasma membrane to help pull the bilayers together and to accelerate calcium-triggered membrane fusion. This ability to bind lipids in a calcium-dependent manner has put the function of Syt I at the last step of fusion (Chapman, 2002).

In addition to binding lipids, Syts, including Syt I, are able to interact with SNARE proteins. Syt I was found to interact with Stx1 and SNAP-25, and the affinity of this interaction increased in the presence of calcium (Chapman et al., 1995) (Gerona et al., 2000) (Earles et al., 2001). Syt I-SNARE interactions are important for the regulation of membrane fusion. Mutations in SNAP-25 that affect interactions with Syt I reduce exocytosis (Zhang et al., 2002). Both C2A and C2B domains of Syt I are required for binding to t-SNAREs and for fusion, suggesting that they cooperate in the regulation of fusion events (Earles et al., 2001) (Bai et al., 2004b). Syt I was shown to stimulate the fusion of reconstituted v-and t-SNARE-containing liposomes in the presence of calcium. The loss of calcium-dependent SNARE-binding activity correlated with a loss of calcium-dependent simulation of liposome fusion, suggesting that Syt I and SNAREs are essential components of the fusion machinery (Tucker et al., 2004). It is not known whether Syt I-SNAREs interactions occur at one or multiple stages of fusion. One study showed that Syt I-SNAP-25 interactions have a role in docking of secretory vesicles in AtT-20 cells (Chieregatti et al., 2002). These findings suggested that one role of Syt I

during membrane fusion might be to facilitate vesicle docking. In contrast, a different study showed that the binding of Syt I to t-SNAREs is important for a later stage of fusion. Indeed, loss of Syt I-SNARE interaction resulted in the destabilisation of fusion pores, suggesting that this interaction controls fusion pore dynamics (Bai et al., 2004b). Although calcium increases the affinity of Syt I to t-SNARES, there is some degree of calcium-independent interactions (Zhang et al., 2002) (Rickman and Davletov, 2003), with still unclear functional relevance. It is thought that these calcium-independent interactions exist to increase the speed of calcium-induced changes in the complex that result in high affinity binding. These data place Syt function at multiple stages of membrane fusion

Some Syts, including Syt I, display homo- and hetero-oligomerisation properties. Both homo-and hetero-oligomerisation can occur in a calcium-dependent and –independent manner. A region within the N-terminal domain was shown to mediate the calcium-independent oligomerisation of Syts *in vitro* (Fukuda et al., 1999) (Fukuda and Mikoshiba, 2000b) (Fukuda and Mikoshiba, 2000a). However, the functional relevance of the calcium-independent oligomerisation of Syts *in vivo* is still unknown.

In addition to calcium-independent oligomerisation, some Syt isoforms, such as Syt I, were shown to form calcium-dependent homo-and hetero-oligomers (Chapman et al., 1996) (Sugita et al., 1996) (Osborne et al., 1999) (Fukuda and Mikoshiba, 2000a). The calcium-dependent oligomerisation of Syt I was found to depend on the presence of lipids, where the C2B domains form ring-like heptameric oligomers (Wu et al., 2003). Consistent with an important role for calcium-dependent oligomerisation, a mutation in the C2B domain of Syt I that inhibited calcium-triggered oligomerisation resulted in the inhibition of secretion, suggesting that this property is important for triggering

membrane fusion (Desai et al., 2000) (Littleton et al., 2001). How Syt oligomerisation regulates fusion is still unclear. It was suggested, however, that the calcium-dependent oligomerisation might influence fusion pore kinetics. Indeed, the overexpression of Syt I or Syt IV, a calcium- and phospholipid-independent binding isoform, in PC12 cells affected the stability and opening time of fusion pores (Wang et al., 2001) (discussed in section 1.5.2). In addition, it was shown that Syt isoforms display different sensitivities to calcium (Sugita et al., 2002), leading to the suggestion that the association of different Syt isoforms might regulate the calcium-dependence of membrane fusion. A recent study showed that the upregulation of Syt VII, which possess a higher sensitivity to calcium than Syt I and IX, resulted in the targeting of this isoform into MSGs, which resulted in an increase in calcium sensitivity for catecholamine release in PC12 cells (Wang et al., 2005). These data suggest that the calcium requirement for exocytosis is determined by the precise ratio of different Syt isoforms. However, because endogenous Syt VII is not detectable in PC12 cells (Tucker et al., 2003), the localisation and function of the overexpressed protein remains controversial (Fukuda et al., 2004) (Sugita et al., 2001).

In addition to exocytosis, Syt I was shown to function in endocytosis. Indeed, two independent studies showed that in *Drosophila* and mice lacking Syt I, synaptic vesicles recycling from the plasma membrane is affected (Poskanzer et al., 2003) (Nicholson-Tomishima and Ryan, 2004). Recently, a role of oligomerisation in endocytosis has also been highlighted (Grass et al., 2004). The recognition of the double lysine within the C2B domain of Syt I by AP-2 was shown to depend on the multimerisation of Syt I-C2B domain. Interestingly, the same double lysine motif within the C2B domain was found to mediate both oligomerisation as well as binding to AP-2 (Chapman et al.,

1998). Thus, whether Syt I adopts a multimeric state to regulate both exocytosis and endocytosis remains to be elucidated.

Many different models to explain the possible role of Syt I during exocytosis exist (Chapman, 2002). One preferred model is as follows: First, Syt I interacts weakly with SNAREs and membranes in preparation for fusion. Following the entry of calcium, the calcium-binding loops integrate into PIP2 raft domains in the opposite membrane, and the oligomerisation of Syts occur. This helps bring the two membranes in close apposition, and stabilises the SNARE complex, followed by complete fusion. This model only describes a role for Syt I, PIP2 and SNAREs, and it is very likely that other factors are involved (Figure 5).

In conclusion, it is without doubt that Syt I is an important component of the fusion machinery. Available data suggest that Syts participate in more than one step during membrane fusion. This ability is probably achieved via Syt I interactions with multiple effectors during membrane fusion.

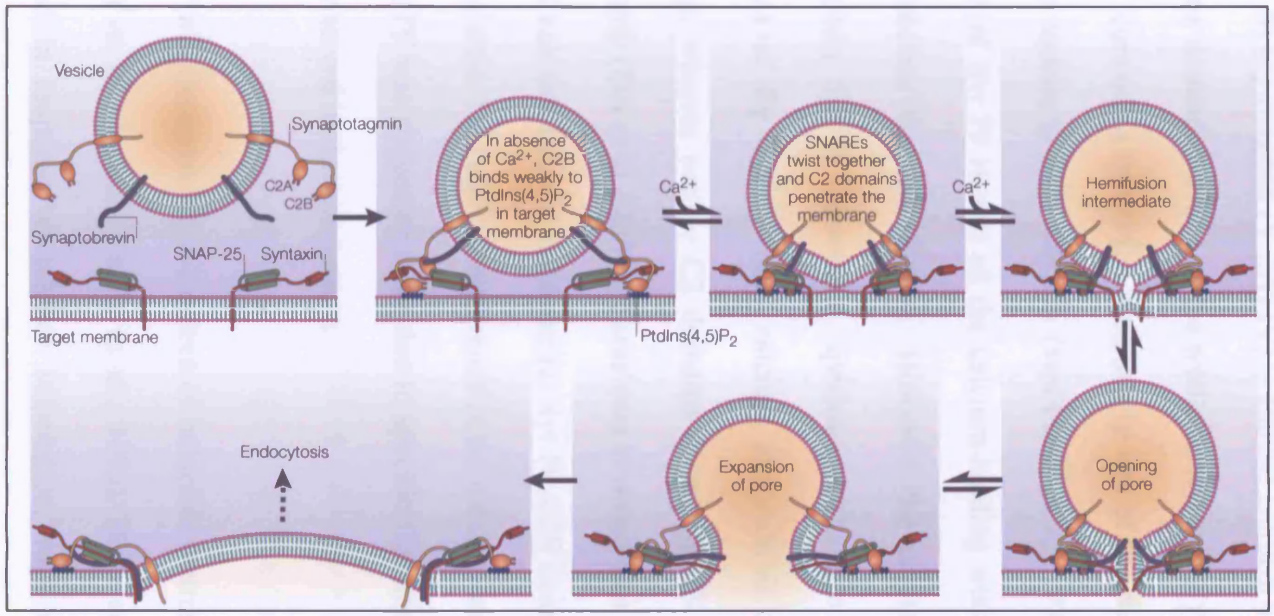

Figure 5: A model for Syt I function during exocytosis. One of the working models describing the function of Syt I during exocytosis. Syt I is shown in orange, SNAP-25 in green, Stx1 in red, VAMP2 in blue and PIP2 shown as blue ovals on the target-membrane surface. Syt I interacts weakly with the SNARE proteins and PIP2 before the arrival of calcium. Upon calcium entry, Syt I inserts into lipid domains via its C2B domain. This probably help bring the two membranes into close apposition and stabilise the SNARE complex. All these steps will drive membrane fusion (Chapman E, 2002).

1.5.2 Synaptotagmin IV

Synaptotagmin IV (Syt IV) is another isoform of the Syt family of proteins, with the same domain structure as the well-characterised SytI. However, the C2A domain of Syt IV contains a conserved mutation in one of the calcium-binding sites, making this domain unable to bind calcium (von Poser et al., 1997). On the other hand, the C2B domain of Syt IV retains all the calcium-binding sites and it was thought that Syt IV bind calcium via this domain. However, the crystal structure of mammalian and *Drosophila* Syt IV showed a species-specific calcium-binding property. Both C2 domains of fly Syt IV bind calcium and exhibit calcium-dependent phospholipid binding, whereas neither C2 domains of rat Syt IV bind calcium or phospholipids efficiently (Dai et al., 2004). These data revealed that the orientation and flexibility of critical calcium ligands make the rat Syt IV C2B domain unable to form full calcium-binding sites. This marked difference in the calcium-binding properties between fly and rat Syt IV was suggested to be due to specific features determined by residues that are not conserved in their sequences.

Syt IV was first isolated in a screen of inducible neuron-specific immediate-early genes (IEGs) in PC12 cells (Vician et al., 1995). IEGs are genes whose transcription is induced in response to cellular stimulation, such as depolarisation and forskolin stimulation, in the presence of a protein synthesis inhibitor, cycloheximide. Forskolin is a stimulator of protein kinase A, which plays a role in the activation of the cyclic AMP response element-binding protein (CREB) transcription pathway, which in turn is involved in the development of learning and memory. Disruption of CREB and the

CREB activation pathway disrupt long-term memory (Yin et al., 1994). Forskolin was found to up-regulate Syt IV expression in PC12 cells (Vician et al., 1995), and interestingly, a concensus CREB element has been reported in the promoter of Syt IV (Ferguson et al., 2000).

Syt IV is expressed in the brain, mostly in the hippocampus, and in neuroendocrine tissues (Vician et al., 1995). Kainic acid, a glutamate agonist, induces seizures in mice, and results in elevated Syt IV message (Vician et al., 1995). Interestingly, Syt IV expression is developmentally regulated in brain during periods which correlate with synaptic plasticity and remodelling (Ibata et al., 2000). Together these findings made Syt IV a good candidate for proteins whose induction might play a role in the modulation of synaptic function.

To examine the role of Syt IV in neuronal plasticity *in vivo*, Syt IV (-/-) mutant mice were generated and analysed (Ferguson et al., 2000). Syt IV null mutant mice are viable, but they exhibit deficits in motor coordination and hippocampal-related learning and memory. Thus, Syt IV may play a role in stabilising memories after they are initially established. That is, like kainic acid-induced seizures (Vician et al., 1995), learning may trigger changes in Syt IV expression that are critical for memory consolidation.

In studies of the molecular mechanisms underlying the possible function of the inducible Syt IV in the brain, PC12 cells are often used as a model system. PC12 cells are derived from a rat pheochromocytoma tumour, and they share some properties of neurons in that they contain small synaptic vesicles, called synaptic-like microvesicles (SLMVs), and mature secretory granules, also referred to as large-dense core vesicles (LDCVs). When PC12 cells are stimulated by depolarisation, they release their vesicle

contents in a calcium-dependent fashion. PC12 cells, like neurons, thus undergo calcium-dependent neurotransmitter release from synaptic vesicles.

The subcellular localisation of Syt IV has long been a matter of debate. Initially, Syt IV, similarly to Syt I, was characterised as a synaptic vesicle protein, as well as being on MSGs (or LDCVs) (Ferguson et al., 1999). Moreover, Syt IV was found to form calcium-dependent hetero-oligomers with Syt I (Thomas et al., 1999). Following these results, it was suggested that the role of Syt IV, perhaps in concert with Syt I, was to modulate synaptic vesicle fusion with the plasma membrane.

In contrast, it was shown using indirect immunofluorescence that Syt IV displays a predominantly perinuclear localisation in PC12 cells, and was found in the distal part of neurites in NGF-differentiated PC12 cells, and that these signals were distinct from that of Syt I (Ibata et al., 2000). Moreover, using subcellular fractionation of rat cerebellar-homogenates, it was shown that Syt IV is not found in the synaptic-vesicle enriched fractions, suggested that Syt IV and Syt I localise to distinct populations of neuronal transport vesicles (Berton et al., 2000). Subcellular fractionation of AtT-20 and PC12 cells also demonstrated that Syt IV is localised on ISGs and not MSGs (Eaton et al., 2000) (Fukuda et al., 2003). Moreover, it was shown *in vitro* that the calcium-dependent and -independent oligomerisation activities of Syt IV are very weak compared to those of Syt I, indicating that hetero-oligomerisation of Syt IV and Syt I is very unlikely *in vivo* (Fukuda and Mikoshiba, 2000a) (Osborne et al., 1999) (Fukuda et al., 2004).

These discrepancies in localisation were attributed to the difference in the specificity of the abs used in the first studies, where the anti-Syt IV ab recognised a higher molecular weight band in addition to that of Syt IV. More importantly, an often overlooked reason is that Syt IV localisation was assessed in forskolin-and NGF-treated PC12 cells in the

studies by Thomas *et al.* (1999) and Ferguson *et al.* (1999), whereas Ibata *et al.* (2000) and Fukuda *et al.* (2003) studied the localisation of the endogenous Syt IV in untreated PC12 cells. In fact, more recent studies showed that the treatment of PC12 cells with NGF and forskolin, as well as the overexpression of Syt IV, induces the sorting of Syt IV into MSGs, where it is involved in calcium-regulated exocytosis (Fukuda et al., 2003) (Fukuda and Yamamoto, 2004) (Wang et al., 2003a).

As with its localisation, the function of the inducible Syt IV remains controversial. Functional studies suggest that one role of the inducible Syt IV is to modulate vesicle fusion with the plasma membrane, but whether it is a negative or positive regulator of exocytosis is under debate. Work from Littleton *et al.* (1999) showed that the overexpression of Syt IV, but not Syt I, in *Drosophila* inhibited evoked transmission in the fly neuromuscular junction (Littleton et al., 1999). Overexpression of Syt IV in AtT-20 and PC12 cells also caused a decrease in ACTH and hGH exocytosis, respectively (Eaton et al., 2000) (Machado et al., 2004). Furthermore, electrophysiological measurements in PC12 cells showed that increasing the copy number of Syt IV by overexpression shortened the fusion pore opening time, whereas overexpression of Syt I prolonged this time (Wang et al., 2001). In contrast, the overexpression of Syt IV in pancreatic MIN6-β cells allowed full release to occur, suggesting that fusion pores were stable and remained open (Tsuboi and Rutter, 2003). These different results could be attributed to the use of different cell lines. A more recent electrophysiological study showed that overexpression of Syt IV favours "kiss-and-run" fusion, in which fusion pores initiate but do not dilate effectively, whereas the overexpression of Syt I favours full fusion (Wang et al., 2003a). Syt IV was shown to bind to SNAP-25 and Stx1 in a calcium-independent manner, suggesting that this interaction might drive the kiss-and-

run fusion events (Wang et al., 2003a). Moreover, overexpression of a Syt IV-C2B domain harbouring a mutation in one of the acidic residue previously thought to mediate binding to calcium abolished the ability of C2B to mediate kiss-and-run fusion, leading Wang *et al.* to suggest that Syt IV mediates kiss-and-run events via calcium-binding through its C2B domain (Wang et al., 2003a). This calcium-dependent role of Syt IV was later put into question after the finding that the C2B domain of Syt IV does not bind calcium, although all the calcium-binding residues are conserved (Dai et al., 2004). It is thought that Syt IV functions similarly in the brain. During seizures, Syt IV is upregulated in neurons, and this will allow the slow release of neurotransmitters through the small pore size. The continuous slow release will increase the concentration of neurotransmitter in the synaptic space, which was suggested to desensitize postsynaptic receptors without generating synaptic responses (Klyachko and Jackson, 2002). The upregulation of Syt IV could then render the synapse silent to counteract hyperexitability during seizures. Thus, the seizure-induced upregulation of Syt IV may be a conserved mechanism to down-regulate neuronal activity. This upregulation could also be a mechanism for controlling long-term plasticity in the brain, consistent with the defects observed in Syt IV null mice.

In contrast, others have suggested that instead of its inhibitory roles, Syt IV may promote neurotransmitter release. Expression of Syt IV in a *Drosophila* Syt I-null mutant restored synaptic transmission (Robinson et al., 2002). This discrepancy was attributed to the possibility that when synapses have no Syt I, Syt IV may substitute for Syt IV and promote vesicle fusion. However, recent crystallography data have shown that rat and *Drosophila* Syt IV, although conserved in their primary sequence, differ in their calcium binding properties. Indeed, the *Drosophila* Syt IV, in contrast to the rat Syt IV, is a calcium- and phospholipid- binding protein (Dai et al., 2004). This data,

although they do not explain the results of Littleton *et al.*, suggests that *Drosophila* Syt IV, in contrast to the rat isoform, promotes synaptic vesicle fusion.

There are no available data regarding the function of endogenous Syt IV in neuroendocrine cells relating to its distribution on ISGs and not MSGs, (Eaton et al., 2000) (Fukuda et al., 2003). Syt IV displays a similar localisation to Stx6 and VAMP4, two SNARE proteins involved in secretory granule maturation in PC12 cells (Wendler et al., 2001) (Hinners et al., 2003). Although a role of Syt IV in granule maturation was suggested, it has never been demonstrated.

1.5.3 Controversies in Synaptotagmin function

The Syt family is now the largest of the C-terminal-type tandem C2 protein families. A recent genomic analysis has revealed that sixteen isoforms exist in mammals, five in plants, and seven in *Drosophila* and *C. elegans*, suggesting that Syts, like SNAREs or Rabs, may regulate various trafficking events (Craxton, 2004). It was previously thought that Syts do not exist in yeast, but a recent study identified three Syt-like proteins containing three C2-domains, called tricalbins (Schulz and Creutz, 2004) (Creutz et al., 2004). Although the function of the synaptic vesicle protein Syt I as a calcium sensor in neurotransmitter release has been well documented, the localisation and function of the other isoforms is still controversial. Several observations suggest that most Syt isoforms with different calcium sensitivities, such as Syt VII, IX and X, cooperate to regulate the same exocytic process, including that of dense core vesicle fusion in PC12 cells (Saegusa et al., 2002) (Tucker et al., 2003). However, since only Syt I, IV and IX are found at detectable levels in those cells, this hypothesis is difficult

to confirm. Another hypothesis is that each Syt isoform may participate in a distinct membrane trafficking pathway. Supporting this model, several Syts display different localisation than Syt I. In PC12 cells, Syt IV was found to localise in the perinuclear area (Ibata et al., 2000). In other cell lines, several Syt isoforms also localised to different compartments. For example, in mast cells, Syt III was shown to localise on early endosomes as well as secretory granules, and was shown to be involved in the delivery of internalised cargo to the perinuclear endocytic recycling compartment, as well as having a role in secretory granule maturation (Grimberg et al., 2003). Syt IX, however, was localised on the endocytic recycling compartment, and is required for trafficking to the plasma membrane (Haberman et al., 2003). Moreover, a recent study in *Drosophila* showed that Syt isoforms localise to non-overlapping subcellular compartments, further supporting the idea that Syts function in different membrane trafficking steps (Adolfsen et al., 2004).

The availability of specific antibodies and tools to characterise the localisation and function of the endogenous synaptotagmins will help answer some of these questions, and reveal whether this family of proteins contributes to the identity of cellular compartments.

1.6 Biogenesis of secretory granules in neuroendocrine cells.

Eukaryotic cells are capable of secreting components into the extracellular space. Two secretion pathways have been described: the constitutive pathway, common to all cells, where proteins are transferred in small vesicles from the TGN to the plasma membrane and released outside the cell in a spontaneous manner. In contrast to the constitutive pathway, the regulated secretory pathway is unique to specialised cells such as exocrine, endocrine, neuroendocrine and neuronal cells. In these cells, specialised organelles called secretory granules (also termed large dense core vesicles or LDCVs), package hormones and bioactive molecules at the TGN, and transport them in highly selective events involving active sorting and targeting to the plasma membrane. After a series of changes and upon external stimulation, these vesicles fuse with the plasma membrane and exocytose their content into the extracellular space. Some cells of the haematopoietic lineage or melanocytes contain organelles, called secretory lysosomes, that also undergo regulated secretion (Blott and Griffiths, 2002). For example, cytotoxic T cells (CTLs) and natural killer cells recognise infected or tumourigenic cells and destroy them by secreting cytolytic proteins, which are stored in the secretory lysosomes.

1.6.1 Secretory granule formation

Secretory granules initiate their life at the TGN, where the packaging of regulated secretory proteins occurs. In neuroendocrine and endocrine cells, the budded granule is the intermediate compartment between the TGN and the mature secretory

granule (MSG), called immature secretory granule (ISG). Morphological data observed a "lace-like" coat in the TGN-areas where secretory proteins accumulate prior to budding (Ladinsky et al., 1994). The nature of this coat, or whether secretory granule budding from the TGN is coat-mediated, is still unknown.

The sorting of secretory proteins into the nascent granule from the TGN was suggested to occur via a "sorting for entry" mechanism, where the soluble secretory proteins are sorted by binding to specific receptors, or by forming aggregates that would exclude proteins not destined for the regulated secretory pathway. One such described receptor is carboxypeptidase E (CPE), which was suggested to function as a "sorting receptor" for pro-opiomelanocortin (POMC) (Cool et al., 1997). Studies performed on Cpe^{fat}/Cpe^{fat} mice, which express a CPE point mutant that missfolds and fails to be exported from the ER, contradicted this suggestion. Indeed, in these mice, pro-insulin is not processed to insulin, due to the absence of the pro-peptidase CPE in the secretory granules, which results in hyperglycemia and obesity. However, pro-insulin is sorted properly into vesicles, suggesting that CPE is not responsible for the sorting of secretory proteins (Irminger et al., 1997).

In contrast to receptor-mediated sorting, it was proposed that secretory proteins are sorted to the regulated pathway via aggregation. Granins are a family of soluble proteins found in secretory granules and expressed in most neuroendocrine and endocrine cells. This family of proteins includes Chromogranin A (CgA), CgB, also called Secretogranin I (SgI), SgII, SgIII and Secretogranin IV (called 7B2). The granins are able to aggregate, and this is favoured by a low pH and high calcium concentrations (Gerdes et al., 1989). This ability to aggregate was suggested to mediate the sorting of secretory granins into the nascent vesicles forming from the TGN (Chanat and Huttner, 1991), thus excluding proteins not destined for constitutive secretion. It was shown that

the overexpression of CgB in AtT-20 cells promoted the efficient sorting of POMC into secretory granules (Natori and Huttner, 1996). Studies have suggested that an amphipathic disulfide loop in the N-terminus of the secretory proteins chromogranin A and B, is necessary for their correct sorting. However, it is not known whether this sequence exerts its effect on sorting via aggregation or via binding to membranes. Using a vaccinia virus expression system in PC12 cells, the expression of a mutant CgB lacking the N-terminal disulfide bond loop, in the absence of endogenous protein synthesis, resulted in the missorting of the mutated protein and an inability to enter the regulated secretory pathway (Kromer et al., 1998). The mutant CgB was expressed in conditions where the endogenous protein synthesis was inhibited to abolish co-aggregation with endogenous wild type protein, suggesting that the disulphide loop of CgB mediates its sorting via aggregation (Kromer et al., 1998). A different study showed that the incubation of PC12 cells with DTT, which disrupts the disulfide bond of CgB, also resulted in its missorting to the constitutive pathway (Chanat et al., 1993). However, the DTT treatment did not affect the aggregative property of CgB, suggesting that sorting is independent of the aggregation of CgB (Chanat et al., 1994).

Another hypothesis is that the sorting of regulated secretory proteins happens in a later compartment. It was suggested that proteins are included in the forming vesicles by default. Proteins destined for the regulated pathway are kept in the vesicle, whereas other proteins are removed. This hypothesis defines the "sorting by retention" mechanism (Arvan and Castle, 1998). In pancreatic β-cells, sorting of insulin from other proteins, such the lysosomal hydralases, occurs in the ISG (Kuliawat et al., 1997). Moreover, it was shown that in PC12 cells, proteins such as furin, a secretory granule

protein, are sorted from the maturing granule (Dittie et al., 1997). The sorting from the ISG involves clathrin and its adaptor protein-1 (AP-1) (discussed later).

Although the mechanism of sorting of secretory proteins into the regulated secretory pathway is still under debate, it is possible that both mechanisms function, so that "sorting for entry" first occurs in the TGN to exclude some proteins, and later a second "sorting by retention" step occurs in the ISG to retain the secretory proteins destined for the regulated pathway, and remove other proteins not needed for this route. The sorting mechanism could also depend on the cell type. In PC12 cells, the constitutively secreted heparan sulphate proteoglycan (hsPG) is not found in ISGs, suggesting that sorting from the regulated pathway into constitutive vesicles occurred in the TGN (Tooze and Huttner, 1990). A second sorting step, via clathrin, in the ISG removes other proteins not found on the MSG (Dittie et al., 1997). In contrast, in pancreatic β-cells, most of the sorting appears to happen in the ISG, where proteins such as the C-peptide are removed form the ISG and secreted via a constitutive-like pathway (Kuliawat and Arvan, 1992).

1.7 Maturation of secretory granules

1.7.1 Homotypic fusion of ISGs

After budding from the TGN, ISGs undergo several changes including an increase in size upon homotypic fusion, acidification of their lumen, prohormone processing and the removal of unnecessary proteins, to give rise to an MSG, (Figure 6 is a working model of secretory granule maturation in PC12 cells), (Tooze et al., 2001).

Initial observations in mammotroph cells of the anterior pituitary using EM showed the presence of an irregular-shaped delimiting membrane containing several dense cores,

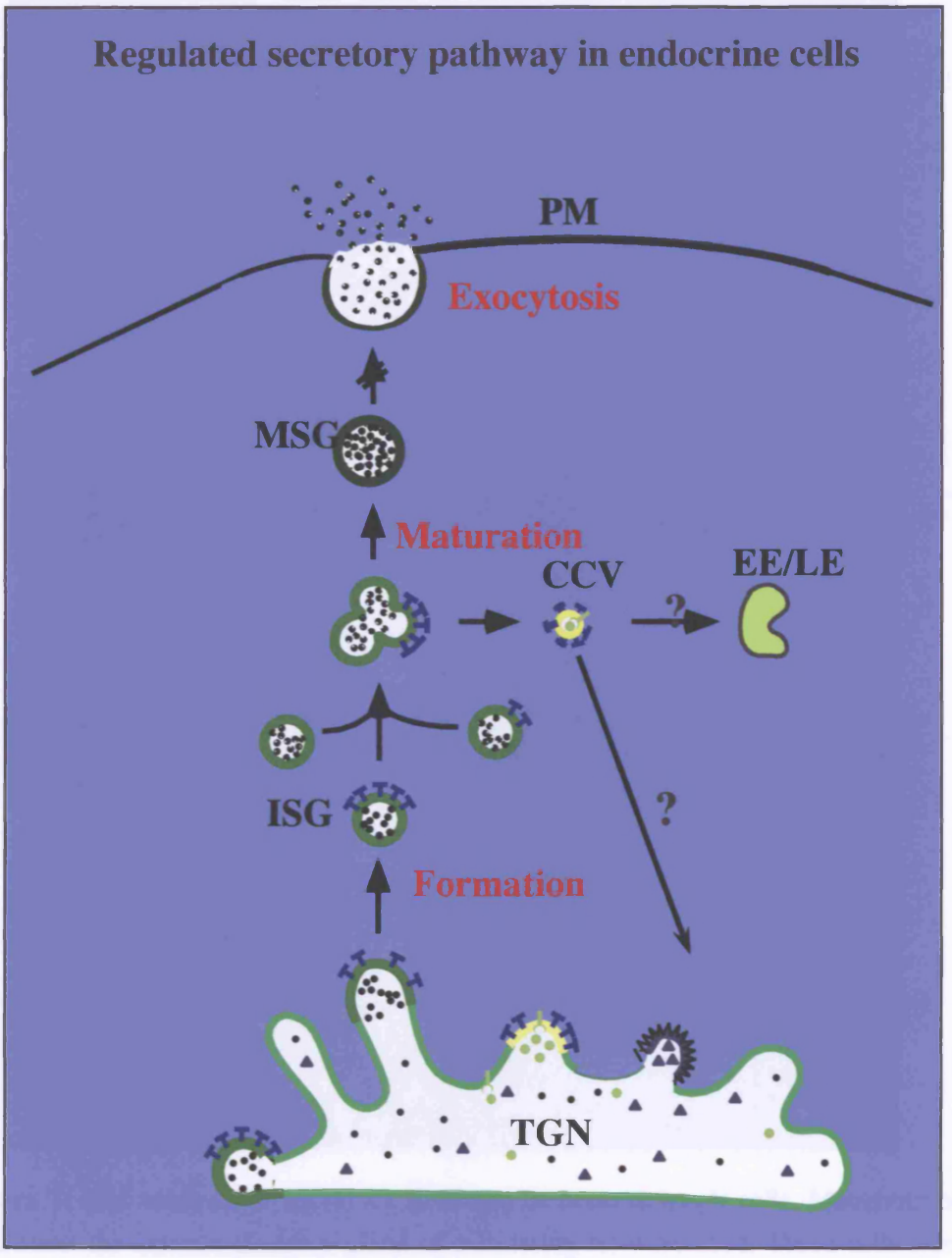

Figure 6: Model of regulated secretory pathway in neuroendocrine cells.
Schematic representation of a model for secretory granule biogenesis in PC12 cells. Immature secretory granules (ISGs) bud from the TGN and undergo a maturation process, which includes homotypic fusion of ISGs, membrane removal of unnecessary proteins via clathrin coated vesicles (CCVs). This maturation process give rise to a mature secretory granule (MSG). In response to a stimulus, MSGs fuse with the plasma membrane and deliver their contents into the extracellular space.

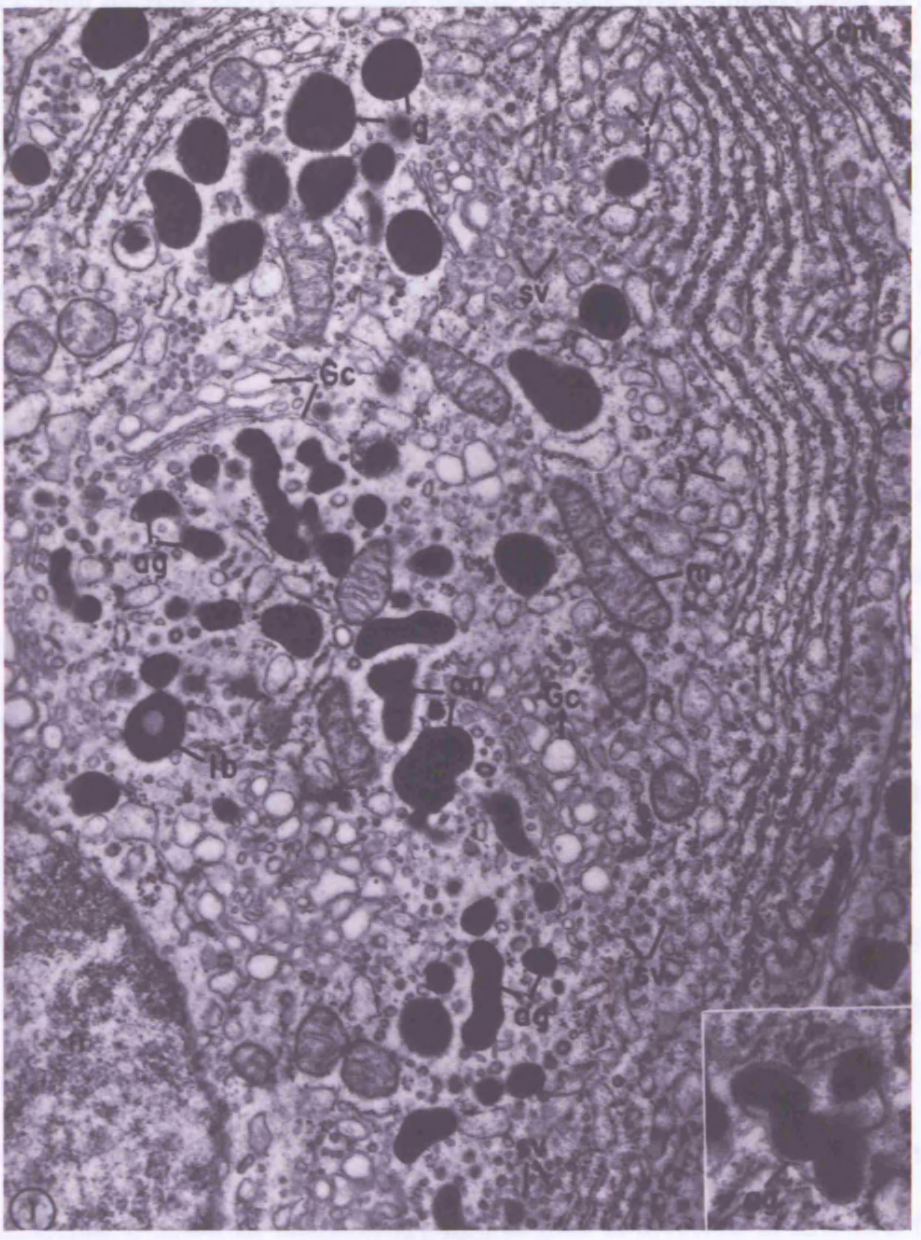

Figure 7: EM analysis of secretory granules in mammotroph cells. Mammotroph cells from the anterior pituitary gland of a lactating rat were used. These cells were fixed in 1% OsO_4 inophosphate buffer (pH 7.6) and embedded in Araldite. Sections were doubly stained with uranyl acetate and lead citrate. x24,000; inset,x40,000. In the cell, the rough-ER (er) close to the cell membrane (cm). as well as the Golgi complex (GC) can be observed. Forming granules (aggregating granules are marked (ag)), mature granules (sg) and (sg'), with a rounded and uniform in size are also seen. Immature secretory granules vary in size and shape and are close to the Golgi. The inset shows several small cores, or vesicles, delimited by one membrane. This polymorphous granule seems to be formed by the fusion of these smaller vesicle. (j), junctional elements of the ER; (sv), smooth-ER. (lb), lytic body (Smith and Farquahar, 1966).

which then become an ovoid-shaped mature granule, that is bigger than an ISG (Smith and Farquhar, 1966) (Figure 7 shows an EM picture of secretory granules in mammotroph cells, as well as progression through different shapes of secretory granules) (The inset in Figure 7 shows several dense cores within one delimiting membrane. In PC12 cells, the measured dense core of the characterised ISG was smaller (~80 nm) compared to that of an MSG (~120 nm) (Tooze et al., 1991). These observations led to the hypothesis that 3 to 5 ISGs undergo homotypic fusion, followed by the removal of excess membranes, to generate an MSG (Tooze et al., 1991). An *in vitro* assay has shown that indeed ISGs undergo homotypic fusion (Urbe et al., 1998). ISG-ISG fusion was found to require ATP, GTP, the ATPase NSF and α-SNAP (Urbe et al., 1998). Homotypic fusion of ISGs was not inhibited by the addition of botulinum neurotoxins, suggesting that plasma membrane SNAREs, although present on ISGs, do not participate in this fusion event (Urbe et al., 1998).

So far the only SNARE protein directly shown to be involved in the regulation of ISG-ISG fusion is Stx6 (Wendler et al., 2001). Interestingly, Stx6 was found in a SNARE complex with SNAP-25, SNAP-29 (GS32) and VAMP4 (Wendler et al., 2001). However, as ISG-ISG fusion is resistant to botulinum neurotoxin treatment, it is unlikely that a SNAP25-Stx6-containing complex is involved in ISG-ISG fusion. This result was surprising, because Stx6 is classified as a Qc-SNARE (Bock et al., 1997), and so a canonical Qabc SNARE complex containing SNAP-25 and SNAP-29, both of which are considered Qbc-SNAREs, would lack a Qa SNARE. A possible explanation is that because Stx6 has an N-terminal domain similar to that of Stx1 (Misura et al., 2002) Stx6 may behave as a Qa-SNARE in a complex containing either SNAP-25 and VAMP-4, or SNAP-29 and VAMP-4. Others have found Stx6 in a complex with Stx16, vti1a, and VAMP4 (Kreykenbohm et al., 2002) (Mallard et al., 2002), where it would be

predicted to function as a Qc SNARE. All these SNARE proteins were found in ISG-containing fractions from PC12 cells, making this complex a potential candidate to study in ISG homotypic fusion (Wendler et al., 2001) (Wendler, F. Unpublished observations).

The search for other proteins involved in regulating the homotypic fusion of ISGs continues, and should give us more insight into the molecular mechanisms underlying this membrane fusion event.

1.7.2 Membrane remodelling

It was suggested that, following the fusion of ISGs, excess membrane is generated, which is then removed via a CCV pathway (Arvan and Castle, 1998) (Tooze et al., 2001). Indeed, using EM, clathrin patches were observed on ISGs and not MSGs, suggesting that ISG-localised proteins are sorted into the budding vesicles (Orci et al., 1984) (Orci et al., 1985) (Tooze and Tooze, 1986).

Clathrin coats were found to be associated with ISG membranes through the adaptor protein-1 (AP-1), which was demonstrated to bind ISG membranes (Dittie et al., 1996). AP-1 coats were suggested to include proteins to be removed form the maturing granules, through binding a sorting signals in their cytoplasmic tails. Proteins such as CI-MPR and furin were found to be on ISGs and absent from MSGs (Klumperman et al., 1998) (Dittie et al., 1997). Moreover, these two proteins were found to bind AP-1, and this interaction was enhanced by a casein kinase II (CKII)-mediated phosphorylation of their cytoplasmic tails (Dittie et al., 1997). Additional proteins have been found on ISGs and not on MSGs, such as VAMP4, Stx6, and Syt IV, suggesting

that proteins that are not needed on the MSG are being removed (Wendler et al., 2001) (Eaton et al., 2000) (Fukuda et al., 2003) (present study, Chapter 3). Recently, VAMP4 was also found to bind to the μ1 subunit of AP-1 via a dileucine motif in the cytoplasmic tail of VAMP4 (Peden et al., 2001) (Hinners et al., 2003). A CK2-mediated phosphorylation within an acidic cluster adjacent to the dileucine motif enhanced this interaction (Hinners et al., 2003). Expression of VAMP-4 harbouring mutations in the dileucine motif and the phosphorylation site within the acidic cluser, prevented its removal from the maturing granule in AtT-20 cells (Hinners et al., 2003). It was suggested that the removal of proteins, such as VAMP4 and Syt IV, from MSGs is necessary for the granules to acquire their exocytic abilities (Eaton et al., 2000). This is an interesting observation, and one can hypothesise that proteins involved in the regulation of ISG maturation, such as proteins involved in homotypic fusion, are not needed for later stages, and they must be removed in order for the MSG to become a mature granule capable of exocytic activity.

1.7.3 Granule acidification and hormone processing

Hormones and granins, generated as large precursors, are subjected to endoproteolytic cleavage during granule maturation. Early studies provided the first evidence for the conversion of proinsulin into active insulin (Steiner et al., 1967). It was later reported that insulin secretory granules contained two endoproteases, which converted proinsulin into insulin in a calcium and pH-dependent manner (Davidson et al., 1988).

Other endoproteases have been subsequently identified, and now classified as Prohormone Convertases (PCs), which include PC1/PC3, PC2, PACE4, PC4, PC5/PC6

and PC7. The endoproteolytic cleavage of prohormones usually occurs at dibasic amino acid sites, although cleavage can also take place at a single basic residue (Seidah and Prat, 2002). PCs cleave different precursor hormones and granins into their active form; for example, in pituitary cells, PC1/PC3 mediates the initial processing of pro-opiomelanocortin (POMC) into corticotropin (ACTH) and β-lipotropic hormone (β-LPH), then PC2 converts β-LPH into β-melanocyte-stimulating hormone and β-endorphin (Benjannet et al., 1991). In PC12/PC2 cells, and during the maturation of ISGs, SgII is cleaved by PC2 into a final 18 KDa product (p18) (Dittie and Tooze, 1995).

PC2 itself is found as a 75 KDa precursor in the TGN, and is endoproteolytically cleaved to the 65 KDa mature form during granule maturation in a pH-dependent manner (Urbe et al., 1997) (Lamango et al., 1999). The transport and activation of PC2 depend on its association with the chaperone, 7β2 (Muller et al., 1997) (Mbikay et al., 2001). The site where the initiation of processing occurs is controversial. Some suggest that it starts in the TGN (Xu and Shields, 1993), whereas others found that processing starts in the ISG, and continues during granule maturation (Orci et al., 1987) (Tooze et al., 1987).

Early studies have revealed that luminal pH of secretory granules in neuroendocrine and endocrine cells is acidic and ranges between pH 5.0 and 5.5 (Johnson and Scarpa, 1976) (Carty et al., 1982) (Hutton, 1982). The acidification of many organelles, including secretory granules, is carried out by the vacuolar-type proton ATPase (V-ATPase), which uses the energy of ATP hydrolysis to transport protons across membranes. The V-ATPase belongs to the family of multi-subunit ATP-dependent proton pumps, and consists of two major functional sectors, V_1, which contains three catalytic sites for ATP hydrolysis, and Vo, responsible for proton translocation across the membranes

(Sun-Wada et al., 2004). The V-ATPase inhibitor, bafilomycin A1, inhibited processing of POMC, PC2 and SgIII in primary *Xenopus* intermediate pituitary cells (Schoonderwoert et al., 2000). Moreover, inhibition of the V-ATPase by another inhibitor, concanamycin A, abolished SgII processing in isolated PC12-ISGs (Urbe et al., 1997), suggesting that the acidification of granules, important for hormone processing, is dependent on the activation of the V-ATPase.

It is not well understood how acidification in secretory granules exactly occurs. It was demonstrated that acidification of granules along the secretory pathway is solely dependent on the rates of H^+ pumping and the rates of H^+ leackage, and not membrane potential (Wu et al., 2001). It was suggested that the acidification from ISGs to MSGs is accomplished by progressively increasing the density of active V-ATPase while decreasing the density of H^+ leaks (Wu et al., 2001). In contrast, the acidification of the endosomes is regulated by the Na^+/K^+-ATPase (Cain et al., 1989) (Fuchs et al., 1989). This latter produces an interior positive membrane potential in early endosomes, preventing maximal acidification by the V-ATPase. In this model, the acidification from early to late endosome was suggested to occur by the removal of the Na^+/K^+-ATPase. These results suggest that the mechanism for acidification along the secretory pathway differs from that previously proposed for the endocytic pathway.

The different steps described above, including homotypic fusion, membrane remodelling, acidification and hormone processing, are highly controlled and regulated. The identification of proteins involved in these processes, and the mechanism by which they do so, will increase our understanding of how the regulated secretory pathway in specialised cells is controlled.

1.8 Objective of the thesis

Work from Eaton and colleagues have shown that Syt IV is localised on ISGs and not MSGs in AtT-20 cells (Eaton et al., 2000). Two SNARE proteins, VAMP4 and Stx6, were similarly shown to localise on ISGs and be removed from granules during maturation in AtT-20 cells (Wendler et al., 2001). Moreover, Stx6 was directly shown to be involved in the regulation of ISG-ISG homotypic fusion (Wendler et al., 2001). Although a direct involvement of VAMP4 in ISG homotypic fusion was never demonstrated, it was found in complex with Stx6 on ISGs, and it was suggested that this complex is involved in the regulation of ISG-ISG fusion. A hypothesis emerged that proteins involved in the regulation of ISG maturation (i.e. homotypic fusion) are being removed from MSGs.

Studies have shown that Syts are involved in the regulation of membrane fusion events. Moreover, Syts were shown to interact with the SNARE proteins, making this family of proteins important components of the fusion machinery.

The purpose of the thesis was to investigate whether Syt IV is involved in the maturation of ISGs in PC12 cells. After I confirmed that endogenous Syt IV is localised on ISGs and not MSGs in PC12 cells, I asked whether it is involved in the regulation of ISG maturation. To investigate this question, I used an *in vitro* assay that reconstitutes ISG-ISG fusion (Urbe et al., 1998), and tested the effect of soluble Syt IV cytoplasmic domain in this membrane fusion event. The inhibition of ISG homotypic fusion obtained with the addition of the cytoplasmic domain suggested that Syt IV is involved in this process.

Morover, the Syt IV cytoplasmic domain, and siRNA against Syt IV, affected SgII maturation in PC12 cells, confirming the role of Syt IV in granule maturation *in vivo*.

The finding that Syt IV is involved in ISG homotypic fusion led me to ask whether it interacts with the SNARE protein Stx6, and further to hypothesise that these two proteins are in the same complex that regulates ISG-ISG fusion.

Finally, many proteins removed from the maturing granule, including VAMP4, were shown to bind to AP-1, which recruits clathrin to ISG membranes. As mentioned above, Syt IV is found on ISGs and not MSGs, suggesting that it is also removed during maturation. I hypothesised that the sorting of Syt IV from MSG could occur in the same manner. Following this hypothesis, I tested whether Syt IV interacts with AP-1.

In conclusion, the determination of whether or not Syt IV is an additional component regulating granule maturation, and in particular homotypic fusion of ISGs, will give us more clues about the mechanisms underlying this membrane fusion event, and in particular the function of this large family of proteins in membrane trafficking. The involvement of Syt IV in the regulation of ISG-ISG fusion provides additional evidence to support the notion that Syts, like SNAREs or Rabs, regulate distinct membrane fusion events.

2 Chapter 2: Materials and Methods

2.1 Materials

2.1.1 Chemicals

All chemicals were purchased from the following companies unless otherwise stated: Sigma; Bohringer Manheim; Amersham Pharmacia; BDH; Fluka; Roche; Invitrogen; Calbiochem or Pierce. 1,2-bis (o-aminophenoxy) ethane-N,N,N',N'-tetraacetic Acid (BAPTA) was purchased from Calbiochem; [3-(2,4-dinitroanilio-3'-amino-N-methyldipropylamine] (DAMP) was from Oxford Biomedical Research; [^{35}S]-Sulphate 48.3 mCi/ml was from Amersham Pharmacia; Protein G was either from Amersham Pharmacia or Roche. Horse serum and foetal calf serum were from Sigma.

Molecular biology reagents were from Promega; New England Biolabs; Invitrogen or Qiagen.

Phosphate buffered saline (PBS), LB-medium for bacterial growth, LB-agar, E4 (Dulbecco's modified eagle medium), E4 without antibiotics, E4 without sulphate medium for mammalian cell culture, trypsin, versene and glutamine were supplied by Cancer Research UK laboratory services.

2.1.2 Antibodies

Primary antibodies

Antibody	Antigen	Species	Applications/Dilution	Supplier
Anti-Syt IV	Syt IV	rabbit pab	WB, IF (1:1000)	M.Fukuda Japan
Anti-Syt I	Syt I	mouse mab	WB, IF (1:1000)	Synaptic Systems
STO 112	Syntaxin 6	rabbit pab	WB (1:500) IF (1:200)	S.Tooze CRUK
Clone 30	Syntaxin 6	mouse mab	IF (1:200)	Transduction laboratories
175	SgII(C-term)	rabbit pab	WB (1:1000)	Dittie and Tooze, 1995
6β1	p18	mouse mab	IF (1:200) IP	Dittie and Tooze, 1995
Clone 88	γ-adaptin	mouse mab	WB (1:500) IF (1:200)	Transduction laboratories
100/3	γ-adaptin	mouse mab	WB (1:200)	Sigma
Anti-PC2	PC2	rabbit pab	WB, IF (1:1000)	B.Eipper University of Connecticut
Anti-Myc	Myc tag	rabbit pab	IP	Abcam
9E10	Myc tag	mouse mab	WB (1:500)	CR-UK
12CA5	HA tag	mouse mab	WB, IF (1:500), IP	CR-UK
Anti-HA	HA tag	rat mab	IF (1:500)	Roche
Anti-DNP	DAMP	mouse mab	EM (1:10)	Oxford biomedical research

Secondary antibodies

Antibody	Antigen	Species	Application	Supplier
Alexa 488	rabbit,mouse and rat IgG	goat,Alexa488-conjugated	IF (1:1000)	Transduction laboratories
Alexa 555	rabbit,mouse and rat IgG	goat,Alexa555-conjugated	IF (1:1000)	Transduction laboratories
Alexa 633	rabbit,mouse	goat,Alexa-633conjugated	IF (1:1000)	Transduction laboratories
Anti-mouse Cy3	mouse IgG	sheep,Cy3-conjugated	IF (1:1000)	Jackson Immunoresearch
Anti-guinea pig Cy3	guinea pig IgG	goat, Cy3-conjugated	IF (1:500)	Abcam

Anti-goat Rhodamine	Goat IgG	rabbit, rhodamine-conjugated	IF (1:500)	Pierce
Anti-rabbit Alexa 647	rabbit IgG	goat, Alexa 647-conjugated	FACS (1:100)	Transduction labortories
Anti-mouse-HRP	mouse IgG	sheep,HRP-conjugated	WB (1:2500)	Amersham
Anti-rabbit-HRP	rabbit IgG	donkey, HRP-conjugated	WB (1:2500)	Amersham
Anti-guinea pig HRP	guinea pig IgG	rabbit, HRP-conjugated	WB (1:2500)	Abcam

2.1.3 Oligonucleotides

All oligonucleotides were synthesised and purified by Cancer Research UK oligonucleotide services.

Primer's name	**Oligouncleotide sequence**
SytIV-cytoplasmic domain	5'TCCCCCGGGTGCCAGAGAAGATCCGCTAAGTCCAACAAG3' 3'AAGGAAAAAAAGCGGCCGCCTAACCATCACAGAGCATATG5'
SytIV-C2A domain	5'TCCCCCGGGTGCCAGAGAAGATCCGCTAAGTCCAACAAG3' 3'AAGGAAAAAAAGCGGCCGCTGTGGCACCCAGGACCAACCG5'
Syt IV-C2B domain	5'TCCCCCGGGTCTTCTGGACGGGGTGAACTTCTGGTCTCC3' 3'AAGGAAAAAAAGCGGCCGCTGTGGCACCCAGGACCAACCG5'
HA-Syt IV cytoplasmic domain	5'CCCAAGCTTGCCAGCATGGCATACCCATACGACGTCCCAGAC TACGCTGCTCCTATCAACACCAGCCGGGTG3' 3'CCGGAATTCCTAACCATCACAGAGCATATG5'
HA-Syt IV C2A domain	5'CCCAAGCTTGCCAGCATGGCATACCCATACGACGTCCCAGAC TACGCTAAACAAGAGAAGCTGGGCACTCTC3' 3'CCGGAATTCCTAAAGAGGAACGAGGACTTCTCCAATGAC5'
HA-syt IV	5'CCCAAGCTTGCCAGCATGGCATACCCATACGACGTCCCA

C2B domain	GACTACGCTGCTAAGAAGTCTTCTGGACGGGGT3' 3'CCGGAATTCCTAACCATCACAGAGCATATG5'
pGEX	5'GGGCTGGCAAGCCACGTTTGGTG3' 3'CCCGGGAGCTGCATGTGTCAGAGG5'
T3	5'AATTAACCCTCACTAAAGGG3'
T7	5'GTAATACGACTCACTATAGGGC3'

2.1.4 Synaptotagmin IV siRNA sequences

Smart pool consisting of 4 pooled siRNAs duplexes specific for rat Syt IV were synthesised by Dharmacon. The sequences are as follow:

5'-GAAGAAAGCAUUUGUGGUG-3'
5'-GGAGACAAAUUGCUAAGUG-3'
5'-CAACAAGACUCCUCCAUAC-3'
5'-UAAAGGAGUUGAUAUCUAC-3'

2.1.5 Constructs

Bacterial expression vectors

Name	Vector	Origin	Fusion protein
GST-Syt IV cytoplasmic domain	pGEX-4T2	This study	soluble
GST-Syt IV C2A domain	pGEX-4T2	This study	low expression
GST-Syt IV C2B domain	pGEX-4T2	This study	insoluble
GST-Syt I cytoplasmic domain	PGEX-KG	G. Schiavo CRUK	soluble
GST-Vamp4 cytoplasmic domain	PGEX-KG	Ina Hinners CRUK	soluble

Mammalian expression vectors

Name	Vector	Origin
HA-Syt IV cytoplasmic domain	pcDNA 3.1	This study
HA-SytIV C2A domain	pcDNA 3.1	This study
HA-SytIV C2B domain	pcDNA 3.1	This study
T7-SytIV FL	pEF-BOS	M.Fukuda Japan
PC2	pRC-CMV	N.Seidah (Montreal)
Myc-Syntaxin6 FL	pCDNA3.1	F.Wendler CRUK
GFP	pEGFP	Clontech

Adenoviral expression vectors

Name	Vector	Origin
HA-Syt IV cytoplasmic domain-VQ	VQAd5CMVK-NpA	Viraquest

2.2 Methods

2.2.1 Tissue culture techniques

2.2.1.1 Mammalian cells lines

PC12 cells are a neuroendocrine cell line derived from a pheochromocytoma of rat-adrenal medulla gland. They are used as a model to study the regulated secretory pathway. PC12 cells, clone 251, were originally from Dr.H.Thoenen (Martnsried, Germany) (Heumann et al., 1983). PC12/PC2 cell-line is a PC12 cell line that stably expresses the prohormone convertase, PC2 (Dittie and Tooze, 1995). AtT-20 cells

(AtT20 D16V) were originally obtained from R.Kelly (Gumbiner and Kelly, 1981). HEK-293A cells (Human Embryonic Kidney cells) were purchased from Invitrogen.

2.2.1.2 Maintenance of mammalian cells

Solutions: Phosphate-buffered saline (PBS): (137mM NaCl, 3.35 mM KCl, 10 mM Na_2HPO_4, 1.84 mM KH_2PO_4, PH 7.2); trypsin/versene:(0.05% trypsin (w/v), 0.02% EDTA (w/v), 1% phenol red in PBS); E4 (Dulbecco's MEM); glutamine (250 mM stock); were provided by Cancer Research UK, Central Cell Services. Horse serum and foetal calf serum were from Sigma and were batch tested.

All cells were used between passage 9 and 23 and were grown at 37 °C in humidified incubators at 10% CO_2.

PC12 cells and PC12/PC2 cells were maintained in E4 supplemented with 10% horse serum, 5% FCS, 4mM glutamine. HEK cells were maintained in E4 supplemented with 10% FCS and 4.8 mM glutamine. Cells were grown up to 80 % confluency. For passaging, cells were washed once in PBS and incubated for 5 min in trypsin/versene until cells detached from the plastic. Cells were collected into a 50 ml polypropylene centrifuge tube (Falcon) containing growth media and spun at 1000 rpm for 5 min in a swing bucket centrifuge (Heraeus). To obtain a single cell suspension, the pellet was resuspended in 1 ml media using a Pasteur pipette that has been flamed to narrow the opening. Cells were plated at the desired dilution into flasks, dishes or plates.

2.2.1.3 Storage and recovery of mammalian cells

For storage, the cell pellet was prepared as described above, and resuspended in growth medium supplemented with 10% sterile DMSO and 1 ml aliquots were dispensed into cryovials (Nunc). Aliquots of these cells were frozen at – 80 °C for one week, before

long term storage in liquid nitrogen. For recovery, an aliquot was rapidly thawed at 37 °C and plated into a 70 cm^2 tissue culture flask, containing growth medium. The medium was replaced the following day, after the cells had attached to the plastic.

2.2.2 Molecular biology techniques

2.2.2.1 Extraction of total RNA from PC12 cells

Isolation of total RNA from PC12 cells was performed using the RNeasy Mini Kit (Qiagen) according to the manufacturer's instructions. Briefly a maximum of 10^7 PC12 cells are first lysed and homogenised in the presence of a highly denaturing guanidium isothiocyanate (GITC)-containing buffer which immediately inactivates RNAses to ensure isolation of intact RNA. Ethanol is added to provide appropriate binding conditions and the sample is then applied to an RNeasy mini spin column where the total RNA binds to the membrane and contaminants are efficiently washed away. Total RNA is then eluted in 30 µl or more, of RNAse-free water. RNA concentration is determined at OD_{260} using a spectrophotometer and finally total RNA was aliquoted and stored at –80 °C to avoid degradation.

2.2.2.2 cDNA synthesis from total RNA

PC12 cDNA synthesis from isolated total RNA was performed using the thermoscript TM RT-PCR system (Life Technologies) following the manufacturer's instructions. Briefly, a mixture of 1 µg of total RNA and oligo (dT)20 primer (50pmol/reaction) was denatured by incubating at 65 °C for 5 min. cDNA is then synthesised by adding thermoscript RT (15units/µl), 10mM dNTP mix, 0.1 M DTT and 1x cDNA synthesis

buffer, to the previous total RNA-containing mix at 50°C for 60 min. The cDNA synthesis reaction was stored at –20 °C or used for PCR immediately.

To amplify specific genes, 2 µl of the cDNA was mixed with gene-specific primers (2 µM each) and PCR reaction was performed as described in (2.2.2.3).

2.2.2.3 Amplification of DNA by polymerase chain reaction (PCR)

DNA was routinely amplified using the following 50 µl reaction mixture: 1-50 ng of template DNA, 2 µM primer (each), 200 µM dNTPs (Promega), 2.5 units Pfu polymerase (Stratagene), 1x Pfu buffer. When amplifying cDNA from reverse transcription reactions, 2µl cDNA was used. PCR reactions were performed in a thermal cycler with the following conditions:

- denaturation: 94 °C, 5 min
- denaturation: 94 °C, 1 min
- annealing: 55-65 °C, 1 min x 30 cycles
- extension: 72 °C, 1 min
- final extention: 72 °C, 12 min

2.2.2.4 Quantitation of DNA and RNA

DNA or RNA was placed in a quartz cuvette with a path length of 1 cm and absorbance at wavelength 260 nm was read in a spectrophotometer. An OD_{260} of 1 corresponds to 50 µg/ml double stranded DNA, 40 µg/ml RNA and 33 µg/ml single stranded DNA.

2.2.2.5 Restriction digest of plasmid DNA and DNA fragments

Typically, 0.2-2 μg of DNA was digested using 10 U of the appropriate digestion enzyme and 1x enzyme buffer in a 20-50 μl total reaction. Reactions were incubated at the enzyme's working temperature (typically 37 °C) for 1-4 h.

2.2.2.6 DNA agarose gel electrophoresis and extraction

Typically, 1% agarose was disolved in 1x TAE buffer (40 mM Tris, pH 8, 20 mM acetic acid, 1mM EDTA). Ethidium bromide was then added to a final concentration of 0.5 μg/ml. DNA samples were resuspended in loading buffer (60% (w/v) sucrose, 0.1% bromophenol blue (w/v), 0.1 % xylene cyanol (w/v) in TAE) and run at 5-20V/cm in 1xTAE buffer.

DNA was routinely purified using QIA quick gel extraction Kit following manufacturer's instructions. Briefly, the gel slice containing the fragment of interest was solubilised and applied to the reservoir of silica-gel membrane column. During centrifugation, the DNA attaches to the silica membrane whilst the dissolved agarose and other impurities pass through the column. Bound DNA was washed in buffer containing ethanol and eluted in 10 mM Tris-HCL, pH 8.5 or in dH_2O. All buffers were provided in the kit.

2.2.2.7 Ligation of DNA

100-500 ng of digested and gel purified vector DNA were mixed with an excess of purified insert DNA (typically 1:3 plasmid to insert ratio); 200 units T4 DNA ligase and 1x DNA ligase buffer (New England biolabs) in a total volume of 10 μl. DNA was ligated for 1h at room temperature.

2.2.2.8 Bacterial transformation

100 µl chemically competent bacteria , DH5-α (Invitrogen) or XL-1 blue (Stratagene), were mixed with 10 µl ligation reaction or 10-50 ng of supercoiled plasmid DNA and incubated for 40 sec at 42 °C then immediately returned on ice for 2 min. 900 µl of SOC medium was added and bacteria were incubated for 1h at 37 °C. Transformed bacteria were plated onto LB-agar plates with the appropriate selection antibiotics (typically 50-100 µg/ml antibiotic). Plates were incubated O/N at 37 °C.

2.2.2.9 DNA Sequencing

DNA sequencing was carried out using the ABI dye Terminator sequencing kit (Applied Biosystems). 20 µl sequencing reactions contained: 100-500 ng template DNA, 100 nM primer and 9 µl terminator ready reaction mix. PCR reactions were then performed with the following conditions:

- denaturation : 96°C for 30 sec
- annealing : 46-60 C for 15 sec x 25 cycles
- extension : 60 °C for 4 min

Sequencing reactions were purified by centrifugation at 3000 rpm for 3 min in spin columns (Qiagen DyeEX 2.0 spin Kit) followed by drying in a vacuum centrifuge. Samples were processed by CR-UK Sequencing Services. Briefly, dried DNA was resuspended in loading buffer (deionised formamide, 25 mM EDTA (pH 8), 50 µg/ml blue dextran), mixed and spun. Samples were heated to 90 °C for 2 min to denature the DNA and loaded onto the ABI Prism 377 DNA sequencer (Applied Biosystems). Sequence analysis and alignments were done using Sequence Navigator, DNA Strider or ClustalX.

2.2.2.10 Small and large scale preparation of plasmid DNA (Minipreps and Maxipreps)

High purity small scale or large scale plasmid DNA was prepared using the QIAprep Miniprep Kit or Endo-free Plasmid DNA maxi Kit (Qiagen), respectively following the manufacturer's instructions. Bacteria containing the desired plasmid were grown in 1-5 ml or 100-300 ml LB media containing the appropriate selection drug for minipreps or maxipreps, respectively. Plasmid concentration was measured (as described in 2.2.2.4).

2.2.3 Protein expression and purification

2.2.3.1 Expression of recombinant GST fusion proteins

Expression plasmids were transformed into *E.Coli* strain BL21 pLys and plated on LB-agar plates containing the required antibiotic, which were then incubated at 37 °C O/N. For protein expression, a single colony was grown in LB with ampicillin (100 μg/ml) overnight at 37 °C, shaking at 150 rpm. The next day, the culture was diluted 1:100 into fresh LB and grown at 37 °C until the OD_{600} reached 0.6-0.8. Expression of the desired protein was induced by the addition of 0.2mM IPTG for Synaptotagmin fusion proteins or 1 mM IPTG for other GST fusion proteins. Expression was carried out at 19 °C overnight or 30 °C for 4h for Synaptotagmins or for other GST-fusion proteins, respectively. 1 ml aliquots of the culture were taken before and after induction, and centrifuged at 14,000 rpm for 2 min in a microfuge for analysis. The pellet was resuspended in 200 μl SDS-sample buffer, of which 20 μl was analysed by SDS-PAGE and visualised with Coomassie blue. The remaining bacteria were pelleted by centrifugation at 4000 rpm for 15 min at 4 °C in a JA10 rotor (Beckman centrifuge).

2.2.3.2 Purification of GST fusion proteins

2.2.3.2.1 Purification of GST-fusion proteins on Glutathione beads and thrombin cleavage

Solutions: PBS; lysis buffer (0.1% Triton X-100 + 1xcomplete protease inhibitor cocktail (Roche) in PBS); high salt wash buffer (500 mM KCl in PBS); elution buffer (50 mM Tris-HCl, pH 8); 5 mM glutathione (Sigma); thrombin (Sigma).

The bacterial pellet was resuspended in lysis buffer (20 ml lysis buffer/1 litre culture volume). Lysozyme (1 mg/ml final concentration) was added and cells were lysed by sonication on ice for 5x 10 sec. Insoluble material was eliminated by centrifugation at 10,000 rpm in a Beckman JA20 rotor for 15 min at 4 °C. A column (Biorad) was packed with glutathione-sepharose 4B column (1ml glutathione-sepharose bed volume/500 ml culture volume) and equilibrated with 10 column volumes PBS and 3 column volumes lysis buffer. The soluble material obtained after centrifugation of the sonicated cells was applied onto the column by gravity flow. The column was then washed with 10 column volumes of high salt wash buffer followed by 5 column volumes of PBS. Proteins were then eluted with 10 volumes of elution buffer and 1 ml fractions were collected and analysed by SDS-PAGE. The protein concentration was measured, and the peak fractions were pooled. Glycerol was added to a final concentration of 10%. Finally, the purified proteins were stored at – 80 °C in small aliquots.

For cleavage of the protein from GST, thrombin was added to the fusion protein bound to glutathione sepharose beads. Because the concentration of the protein is not known at that time, for each ml of glutathione sepharose bed volume, 50 µl (1U/µl) of thrombin protease in 950 µl PBS was added to the column with the bound protein and incubated for 2-4 h at RT. The cleaved protein was collected by gravity flow and analysed by

SDS-PAGE. After the protein concentration was determined, the aliquoted protein was stored at – 80 °C in 10 % glycerol.

2.2.3.2.2 Purification of Synaptotagmin proteins by gel filtration and cation-exchange chromatography

Solutions: Gel filtration buffer (0.2 M Sodium Phosphate, pH 6.3, 0.3M NaCl); elution buffer A (20 mM MES, pH 6.3, 10 mM NaCl); elution buffer B (20 mM MES, pH 6.3, 1M NaCl,); water; 20% ethanol. All buffers were filtered through a Millipore GP express membrane, 0.22 μm prior to use.

To eliminate bacterial contaminants (mainly negatively charged), which by binding basic regions of Syts copurify with the fusion proteins, a purification method developed by Ubach et al was used(Ubach et al., 2001). A Superdex 75 (Pharmacia) gel filtration column was connected to an FPLC system (Pharmacia) and pre-washed with water and equilibrated with 1 column volume of gel filtration buffer. The sample (5 ml maximum) was loaded using a superloop, and proteins were separated at a flow rate of 0.2 ml/min. The total column volume was collected in 1 ml fractions and those that contained protein, as measured by OD_{280}, were analysed by SDS-PAGE and coomassie staining. Peak fractions containing the protein were pooled, dialysed in elution buffer A using Snakeskin dialysis membrane (1000 Da MW cut-off (Pierce)) and stored on ice for further purification.

Next, a cation exchange column (5 ml HiTrap SP, Pharmacia) was connected to the Pharmacia FPLC system, washed and equilibrated with at least 5 column volumes elution buffer A, 5 column volumes of elution buffer B and finally with 5 column volumes of elution buffer A. The pooled Peak fractions obtained from the previous purification on the gel filtration column were loaded using a superloop at 0.5 ml/min

flow rate on the HiTrap SP column. The column was then washed with 5 column volumes of buffer A. Proteins were eluted using a linear gradient from 10 mM to 1 M NaCl in 20 column volumes. 1 ml fractions were collected and those containing protein according to OD_{280} were analysed on SDS-PAGE followed by Coomassie staining. Peak fractions containing purified Syts were pooled and concentrated using Centricon plus-20 (Millipore), followed by a determination of the protein concentration. Finally, the purified protein was aliquoted and stored in 10% glycerol at –80 °C.

Proteins were dialysed in the appropriate buffer using Slide-A-Lyser cassettes or Slide-A-Lyser mini dialysis units (10,000 Da MW cut-off (Pierce)) before use.

This sequential purification procedure effectively removed all A_{260} absorbing nucleic acid contaminants as determined by measuring the A_{280}/A_{260} ratio.

2.2.4 Protein biochemistry

2.2.4.1 Determination of protein concentration using Bradford assay

The concentration of purified proteins or proteins in total cell lysates was determined using Bradford method. Serial dilutions of an IgG standard (Biorad) and protein samples were made up in 800 µl water, mixed with 200 µl of Bio-Rad dye solution and incubated for 5-30 min at room temperature. A_{595} was measured using a spectrophotometer and the protein concentration was finally calculated from the IgG standard curve.

2.2.4.2 Precipitation of proteins

2.2.4.2.1 TCA precipitation

Solutions: 100% Trichloroacetic acid (TCA) (w/v); PBS supplemented with 10 µg/ml haemoglobin; ethanol:diethyl-ether (1:1, v/v); unbuffered 1x SDS sample buffer (62.5 mM Tris base (unbuffered), 3% SDS (w/v), 3.3% β-mercaptoethanol (v/v), 10% glycerol, 0.015% bromophenol blue (w/v)).

Protein-containing samples were diluted to 900 µl PBS (or 900 µl PBS + haemoglobin as carrier in samples with low protein concentration) and 100 µl TCA was added. Samples were mixed by vortexing and incubated on ice for 1 hour or overnight at 4 °C. The precipitated proteins were pelleted at 13,000 rpm for 30 min at 4°C in a microcentrifuge. The supernatants were carefully aspirated, washed with 200 µl ethanol:diethyl-ether and centrifuged for 15 min as described above followed by the removal of the supernatant. The pellets were air-dried, resuspended in unbuffered SDS sample buffer and vortexed until completely dissolved. Occasionally, samples appeared yellow (acidic) after resuspension due to residual TCA. In these cases 3 µl of unbuffered 1M Tris base was added.

2.2.4.2.2 Acetone precipitation

Samples were diluted to 1 ml with PBS or PBS + haemoglobin and mixed with 4 ml acetone (-20 °C; 80% (v/v) final concentration) in 5.4 ml cryotubes. Proteins were precipitated overnight at 4 °C followed by centrifugation at 6000 rpm for 15 min, 4 °C in swing bucket centrifuge. Supernatants were aspirated and pellets were air-dried and resuspended in SDS sample buffer.

2.2.4.3 SDS-PAGE electrophoresis

Solutions: 4x lower gel buffer (1.5 M Tris-HCl pH 8.8, 0.4% SDS (w/v)); 4x upper buffer (0.5 M Tris-HCl pH 6.8, 0.4% SDS); protogel (National diagnostics) Bis (30% acrylamide/0.8% bis-acrylamide (w/v)); TEMED; 10% (w/v) Ammonium persulphate (APS); running buffer (190 mM glycine, 25 mM Tris-HCl, 1% SDS (w/v) pH 8.8); 1x SDS-sample buffer (62.5 mM Tris-HCl pH 6.8, 3.3% β-mercaptoethanol (v/v), 3% SDS (w/v), 10% glycerol (w/v), 0.015% bromophenol blue (w/v)); 5x SDS-sample buffer.

SDS-PAGE was performed on 1.5 mm thick Bio-Rad minigels (Mini-Protean II electrophoresis cell) or 20x16 cm Bio-Rad gels (Protean II vertical electrophoresis cell). The tables below show the compositions of separating and stacking gels with different acrylamide percentages, depending on the size of proteins to be resolved. The volumes are sufficient for one mini gel.

Separating gel	7.5%	10%	12%	15%
4xlower buffer	2.25 ml	2.25 ml	2.25 ml	2.25 ml
AA/Bis	2.25 ml	3 ml	3.6 ml	4.5 ml
dH_20	4.45 ml	3.7 ml	3.1 ml	2.2 ml
TEMED	4.5 µl	4.5 µl	4.5 µl	4.5 µl
10% APS	45 µl	45 µl	45 µl	45 µl

Stacking gel	4.5%
4x upper buffer	1 ml
AA/Bis	0.6 ml
dH_20	2.35 ml
TEMED	4 µl
10% APS	45 µl

Samples were resuspended in SDS-sample buffer, boiled for 5 min in a water bath, centrifuged for 1 min in the microcentrifuge at 14000rpm and finally loaded on the gel. Minigels were electrophoresed first at 90 volts for 15 min (stacking) then at 120 volts for 1 hr until the sample buffer dye front had reached the bottom of the resolving gel. Large gels were electrophoresed overnight at 10 mA per gel.

2.2.4.4 Coomassie blue staining of gels

Solutions: Gel staining buffer (50% methanol (v/v), 10% acetic acid (v/v), 1% Coomassie blue R-250 (w/v)); gel destain buffer (20% isopropanol (v/v), 10% acetic acid (v/v)).

After electrophoresis, gels were fixed for 10 min in staining buffer then destained until the background was completely removed. Gels were then placed between wet Whatman 3MM paper and cling film and dried on BioRad vacuum dryer at 80 °C for 2-3 hrs. Alternatively, gels to be used for autoradiography were washed in water for 5 min after destaining, and then incubated for 30 min in 1M sodium salicylate, prior to drying. Finally the dried gels are exposed to Kodak XAR film at –70 °C for a minimum of overnight. Quantitation was performed by densitometry of the autoradiographs using Image J analysis software (NIH).

2.2.4.5 Western blotting

Solutions: Transfer buffer (20 mM Tris-HCl, 150 mM glycine, 20% methanol (v/v), pH 8.3); Ponceau S (Sigma) (2% (w/v)) in 3% TCA (w/v); blocking buffer (5% skimmed milk (w/v), 0.2% Triton-X100 in PBS), wash buffer (0.2% Triton-X100 in PBS).

Transfer of proteins onto nitrocellulose membrane:

After electrophoresis, gels were removed from the glass plate and placed on top of 3 sheets of wet Whatman 3MM paper, cut to size and layered over a fibre pad. A sheet of nitrocellulose membrane (0.2 μM pore size, Schleicher & Schuell), cut to the same size as the gel and soaked in water for 5 min, was placed on the top of the gel. This was covered with another two pieces of wet whatman 3MM paper and finally a fibre pad. Air bubbles were removed using a rubber roller. The cassette in which this gel sandwich was assembled was closed and placed, with the nitrocellulose membrane facing the anode, into a Bio-Rad Mini Trans-Blot transfer cell that contained an ice cooling unit and transfer buffer. The transfer cell unit was placed with a magnetic stirrer and the transfer was performed for 1 hr at 100 volts. After transfer, the membrane was stained in ponceau S for 2 min then destained in dH_20 to check for efficient transfer.

Immunoblotting:

The nitrocellulose membrane was incubated in blocking buffer for 1 hr at room temperature or overnight at 4 °C with gentle shaking. The nitrocellulose membrane was then incubated in the primary ab diluted in blocking buffer for 1-2 hrs at RT or O/N at 4 °C. After four washes for 5 min each in blocking buffer, the membrane was incubated with the HRP-conjugated secondary ab diluted in blocking buffer for 1 hr at RT. The membrane was then washed four times, 5 min each in wash buffer and HRP activity was detected by incubating the membrane in ECL-reagent (Amersham) for 1 min. Finally, the membrane was exposed to Kodak XAR film for various amounts of time. Quantification of the signal was done using Image J anlysis software (NIH).

To reprobe the same membrane, the abs were removed by incubating for 15 min at 50 °C in stripping buffer (Pierce). The membrane was washed for 15 min in wash buffer,

incubated in blocking buffer before adding the new antibody. Membranes were stored at –20 °C.

2.2.4.6 Immunoprecipitation

Direct coupling of the monoclonal anti-HA ab to beads by cross-linking:

Solutions: Protein G-sepharose; 0.2 M sodium borate (pH 9); dimethyl-pimelimidate (DMPD) (20mM final concentration, Sigma), 0.2 M Ethanolamine (pH 8); PBS.

Mouse anti-HA ab was cross-linked to beads as follows: a 1:1 mix of protein G-sepharose (50% slurry, prewashed in PBS) and ab was incubated at RT for 1 h with gentle rocking. Beads were then pelleted at 3000g, 5 min and washed twice with sodium borate, pH 9. The cross-linker, DMPD was added to a final concentration of 20 mM and the mixture was incubated for 30 min at room temperature. Beads were then pelleted as above and the reaction was quenched with Ethanolamine, pH 8 for 2 h. Beads were washed twice in PBS and finally stored in PBS+ 0.01% sodium azide.

Before use, beads were washed twice in immunoprecipitation buffer.

Immunoprecipitation

Solutions: TNTE buffer (20mM Tris-HCl pH 7.5, 150 mM NaCl, 0.3% Triton X-100, 5 mM EDTA); 50% slurry protein G-sepharose (v/v) in TNTE; anti-HA ab cross-linked to protein G-sepharose in TNTE (see above); 1000x CLAPP protease inhibitor cocktail stock (chymostatin 50mg/ml, leupeptin 0.5 mg/ml, antipain 50 mg/ml, pepstatin A 0.5mg/ml, Pefabloc 0.1 mg/ml); Pefabloc 500x stock (250 mg/ml in water); 10 mM Tris-HCl pH 7.5); 5x SDS-sample buffer (see 2.2.4.3).

Cells were scraped in PBS with 1xCLAPP and Pefabloc and washed twice in the same buffer by centrifugation at 1000 rpm for 5 min. Cells were then lysed at 4°C for 15 min in TNTE buffer. To remove nuclei and insoluble material, cells were spun for 10 min at maximum speed in a microfuge at 4 °C and the supernatant carefully transferred to a fresh Eppendorf tube. The supernatant was split equally between the different immunoprecipitation conditions and incubated with the ab for 2 h or overnight at 4°C rotating. For abs other than HA, 60 µl of 50% slurry protein G-sepharose in the appropriate buffer was added and incubated for a further 1-2 h. Alternatively, anti-HA antibody cross-linked to protein G-sepharose (see above) was added directly to the cell lysates and incubated for 1-2 h or overnight at 4°C. The immunoprecipitation reactions were spun at 1000 rpm for 1 min at 4°C in an Eppendorf centrifuge. The supernatants were removed and pellets washed four times with 1 ml in TNTE buffer and once in 1 ml Tris-HCl pH 7.5. For each wash, the mixture-containing tubes were inverted, spun at 1000 rpm for 50 sec in a microfuge and supernatants carefully aspirated with a Pasteur pipette with a reduced opening. Bound proteins were eluted from the beads by adding 10 µl of 5x SDS-sample buffer, vortexed and boiled for 5 min. The bottom of the Eppendorf tube was pierced with a 27 g needle, the tube placed in a fresh Eppendorf and spun briefly in order to separate eluate from beads. The samples were finally subjected to SDS-PAGE and western blotting analysis.

2.2.4.7 GST-pull down assay

Solutions: Binding buffer (25mM Hepes-KOH pH 7.2, 25 mM KCl, 2.5 mM MgOAc, 0.5% Triton X-100; CLAPP (1000x stock); Pefabloc (500x stock); 50% slurry (v/v) glutathione sepharose 4B in binding buffer.

For GST pull down experiments, transfected HEK cells (or a postnuclear supernatant from PC12 cells, prepared as described in 2.2.6.1) were lysed in binding buffer for 15 min at 4°C and spun at 14000 rpm for 10 min to remove insoluble material. Alternatively, bovine adrenal medulla cytosol (BAMC) (prepared as described in 2.2.6.3) was diluted in binding buffer and used for GST-pull down.

To separate membranes from cytosol, a PC12-PNS was centrifuged at 45000 rpm (1 hr at 4°C) in a TLA 45 rotor. The pellet (membrane fraction) was lysed in binding buffer as described above and the cytosol was transferred into a fresh tube and diluted in binding buffer. The cytosol or membranes were used separately in a GST-pull down experiment.

GST-fusion proteins (35 μg) were incubated with 100 μl glutathione sepharose bead and prewashed in binding buffer for 1h at 4°C on a rotating wheel in siliconised safelock Eppendorf tubes. Samples were spun for 1 min at 1000 rpm (4°C) in a microfuge and washed once with binding buffer. The beads were resuspended in HEK cell lysates, PC12 PNS, BAMC, membranes or cytosolic fractions from PC12 PNS (2mg total protein in each condition) and incubated O/N at 4°C on a wheel. Beads were pelleted by centrifugation at 1000 rpm for 1 min in a microfuge and supernatants were removed by aspiration. Beads were washed four times in 1 ml binding buffer and bound proteins were eluted by adding 10 μl 5x SDS-sample buffer. After boiling for 5 min, tubes were pierced with a 27 g needle, placed into a second tube and the eluate was collected by brief centrifugation. Samples were subjected to an SDS-PAGE analysis followed by western blotting.

2.2.5 [^{35}S]-sulphate-labelling of PC12 cells

2.2.5.1 Pulse chase [^{35}S]-sulphate-labelling of PC12 cells

Solutions: Sulphate-free E4 + 4mM glutamine, 0.1% dialysed horse serum and 0.05% dialysed foetal calf serum (both dialysed in PBS); complete E4 + 1.6 mM Na_2SO_4; Tris-buffered saline (TBS) (5.4 mM KCl, 137 mM NaCl, 0.7 mM Na_2HPO_4, 1.6 mM Na_2SO_4, 25 mM Tris-HCl pH 7.4); TBS + PI (TBS, 0.5 mM PMSF, 0.5 mg/ml leupeptin).

In PC12 cells the major sulphated proteins are secretogranin I (SgI) (also called Chromogranin B (CgB)), secretogranin II (SgII), which are both targeted to secretory granules (Rosa et al., 1985), and a heparin sulphate proteoglycan (hsPG), targeted to constitutive secretory granules (Tooze and Huttner, 1990). Therefore, we took advantage of these markers to follow [^{35}S]-sulphate-labelled SgII specifically in immature secretory granules (ISGs) or mature secretory granules (MSGs), which were separated later by subcellular fractionation techniques on sucrose gradients.

To detect ISGs using [^{35}S]-sulphate-labelled SgII, labelling of PC12 cells was performed as follows: a 15 cm dish containing 80% confluent PC12 cells was incubated in sulphate-free E4 for 20 min in a 37 °C, 10% CO_2 incubator in order to deplete cells of endogenous sulphate. The medium was then replaced with 5 ml of sulphate-free medium to which 1mCi/ml [^{35}S]-sulphate was added and cells incubated for 5 min on a rocker in the incubator. In the TGN, modifications such as sulphation of tyrosine residues (Baeuerle and Huttner, 1987) and carbohydrates (Kimura et al., 1984) occur. The medium was then removed and replaced with complete E4 + 1.6 mM Na_2SO_4 and the cells were incubated for a further 15 min to chase the labelled SgII into ISGs. The chase reaction was stopped by placing the dish on ice followed by washing twice with

ice-cold TBS. Cells were then harvested by scraping in 10 ml TBS + PI and centrifuged for 7 min at 800 rpm (4 °C) in a Heraeus centrifuge and further processed to obtain a postnuclear supernatant (see 2.2.6.1).

To detect MSGs, endogenous sulphate was depleted as described above and PC12 cells were grown in a 15 cm dish and incubated in 10 ml sulphate-free E4 supplemented with 0.2 mCi/ml [^{35}S]-sulphate for 6h or overnight without rocking. The medium was later replaced with complete E4 + 1.6 mM Na_2SO_4 and cells were further incubated for 1 h to chase SgII specifically to MSGs. To stop the chase reaction, the procedure was followed exactly as described above.

2.2.5.2 [^{35}S]-sulphate-labelling of PC12 cells for cell-free ISG-ISG fusion assay

3x 500 cm^3 dishes containing PC12 cells were incubated in trypsin for 5 min and the detached cells were collected into a 50 ml tube and centrifuged at 800 rpm (Heraeus megafuge) for 7 min at 4 °C. The pellet was washed once in sulphate-free E4 by centrifugation as described above, resuspended in 10 ml sulphate-free E4 and incubated for 20 min in a 37 °C, 10% CO_2 incubator on a rocker to deplete cells of sulphate. Pellet was obtained by centrifugation at the same speed and rotor as described above, resuspended in 10 ml sulphate-free E4 supplemented with [^{35}S]-sulphate (1mCi/ml) and labelled for 30 min in a 37 °C, 10% CO_2 incubator on a rocker. Labelled cells were pelleted by centrifugation and PNS was prepared as described next (2.2.6.1).

2.2.6 Subcellular fractionation techniques

2.2.6.1 Preparation of a postnuclear supernatant from PC12 cells

Solutions: Trypsin; TBS; TBS + PI; homogenisation buffer (HB) (10 mM Hepes-KOH, pH 7.2, 250 mM sucrose, 1 mM MgOAc, 1 mM EDTA, 5□g/ml leupeptin, 0.5 mM PMSF); trypan blue solution (Sigma).

PC12 cells were washed twice in TBS, scraped into TBS + PI and pelleted by centrifugation at 800 rpm for 7 min in a Heraeus centrifuge. Alternatively, pre-warmed trypsin was added to the cells to detach them from the plates. 5 min later, the cells were collected with a pipette into a Falcon tube, centrifuged as described earlier and the pellet washed in TBS+ PI and re-centrifuged. The cells were resuspended in HB and centrifuged at 1800 rpm for 7 min at 4 °C in a Heraeus centrifuge. To make a single cell suspension, the pellet was resuspended in 1 ml HB and passed 7 times through a 21 g needle. 5 µl of the suspension was mixed with 5 µl of trypan blue solution and analysed using a phase contrast microscope. Typically, 90% were single cells and more than 80% were not broken indicated by exclusion of trypan blue. The single cell suspension was then passed 3-5 times through an ice-cold cell cracker in order to break the cells, which was verified with trypan blue as described above. The breakage was considered optimal when the suspension contained less than 2% of unbroken cells and a minimum of broken nuclei. The cell homogenate was centrifuged at 3200 rpm for 7 min in a Heraeus centrifuge to pellet the nuclei and unbroken cells. The supernatant (PNS) was removed carefully and transferred to a new tube.

2.2.6.2 Preparation of ISGs and MSGs

2.2.6.2.1 Continuous velocity gradient

This method, developed by S.A Tooze (Tooze et al., 1991), obtains fractions enriched in immature secretory granules (ISGs) or mature secretory granules (MSGs).

First, a linear sucrose gradient ranging from a 0.3 M (5.5 ml) and 1.2 M (6 ml) was prepared in a SW40 ultraclear tube (Beckman), placed on a gradient maker (Biocomp), and mixed for 10 min at a 50° angle at 36 rpm, and then 1 min at 80° at 12 rpm. 1.5 ml of the PC12 PNS obtained as described in 1.2.6.1 was then loaded on top of the gradient and centrifugation was carried out for 15 min (time after reaching the set speed) at 25,000 rpm (4 °C) in a SW40 swing-out rotor. 1 ml fractions were collected from top to bottom using the auto densi-flow gradient collector (Labconco). Fractions 1-4 were enriched in ISGs and constitutive secretory vesicles (CSVs), fractions 5-7 were enriched in MSGs whereas fractions 9-11 at the bottom of the gradient contained TGN membranes. For analysis of the gradients using autoradiography or western blotting, 300 µl of each fraction was diluted to 1 ml with PBS + haemoglobin and TCA or acetone precipitated as described in (1.2.4.2). For further purification of vesicles, the separation was carried out as described in the next section.

2.2.6.2.2 Discontinuous equilibrium gradient

Pooled fractions 1-4 or 5-7 from the velocity gradient were loaded onto a discontinuous equilibrium sucrose gradient (top: 0.8 M (1 ml), 1 M (2 ml), 1.2 M (2 ml), 1.4 M (2 ml), 1.6 M (1 ml) bottom) sucrose prepared in ultraclear tubes (Beckman) ISGs or MSGs. If necessary, the volume of the pooled fractions was diluted to 4 mls with HB before loading onto the equilibrium sucrose gradients. The gradients were centrifuged at

25,000 rpm in a Beckman SW40 rotor overnight at 4 °C. 1 ml fractions were collected from top to bottom using the auto densi-flow gradient collector. Fractions 7-9 from the equilibrium gradient, that has been loaded with fractions 1-4 from the velocity gradient, contain ISGs and fractions 9-11 from the equilibrium gradient, that has been loaded with fractions 5-7 from the velocity gradient, contain MSGs.

For autoradiography or western blotting analysis 1 ml fractions were precipitated (as described in 2.2.4.2).

For cell-free assays, ISG-containing fractions 7-9 were pooled, distributed in 1 ml aliquots in cryovials and stored in liquid nitrogen for up to 6 months.

2.2.6.3 Preparation of bovine adrenal medulla cytosol (BAMC)

Bovine adrenal medulla cytosol (BAMC) was prepared by S.Tooze as described in (Austin et al., 2000). Briefly, BAM was dissected from cortical tissue, roughly chopped and homogenised in homogenisation buffer (HB, described in 2.2.6.1) in a Waring blender. The lysate was further homogenised with five strokes in a motor-driven glass/teflon Dounce homogeniser. The homogenate was centrifuged in a Ti70.1 rotor for 30 min at 30,000g at 4 °C. The supernatant was collected and centrifuged for 90 min at 100,000g at 4 °C in the Ti70.1 rotor. The supernatant was collected and dialysed against binding buffer (described in 2.2.4.7) + 10% sucrose, using Snakeskin dialysis tubing (Pierce) with a molecular weight cut off of 3.5 kDa. Typically BAMC concentrations were about 20-30 mg/ml.

2.2.7 Cell-free assays

2.2.7.1 *In vitro* ISG homotypic fusion assay

Solutions: [^{35}S]-sulphate-labelled PC12-PNS (see 2.2.6.1); purified ISGs from PC12/PC2 cells (see 2.2.6.2); 10x fusion buffer (10x FB) (200 mM Hepes-KOH, pH 7.2, 500 mM KOAc, 30 mM $MgCl_2$, 10 mM DTT (1000x stock stored in –20 °C)); 10 mM Hepes-KOH pH 7.2; MES buffer (50 mM MES pH 5.5, 0.3 M sucrose); ATP-regenerating system (Boehringer) (100 mM ATP, pH 7 with NaOH, 800 mM creatine phosphate, 3200 U/ml creatine phosphokinase), which were mixed at equal volumes (30x stock solution) then used immediately; HB (see 1.2.6.1); 5x lysis buffer (500 mM Tris-HCl pH 7.5, 750 mM NaCl, 1.5 % Triton X-100, 25 mM EDTA); Protein G-sepharose (50% slurry in lysis buffer (v/v)).

Aliquots of PC2/PC12 cell ISGs were thawed for 2 min at 37 °C, diluted with 2 volumes of 10 mM Hepes-KOH pH 7.2 and pelleted by centrifugation at 29,000 rpm in a SW55 Beckman rotor for 1 h 5 min at 4 °C. The pellets were resuspended in HB at 50 fold the concentration of the original ISG pool. Each fusion reaction contained: 100 µl of [^{35}S]-sulphate-labelled PC12 PNS (containing the substrate, SgII), 500 µl PC12/PC2 cell purified ISGs (containing the enzyme, PC2; centrifuged and resuspended in 10 µl) 10xFB (final concentration of 20 mM Hepes-KOH pH 7.2, 50 mM KOAc, 3 mM $MgCl_2$, 1 mM DTT) and ATP-regenerating system (30-fold dilution) all in a final volume of 120 µl to 180 µl. At this point, purified proteins or antibodies were added to the fusion reaction to test their effect on ISG-ISG fusion. After vortexing, the reactions were incubated at 37 °C for 30 min to allow fusion to occur and then transferred on to ice. Samples were diluted with MES buffer, pH 5.5 to a final volume of 800 µl, incubated for a further 30 min on ice to equilibrate the pH (in the ISGs) 5.5 and then

transferred to 37 °C for 90 min to allow processing of SgII by PC2 to occur. Reactions were then placed on ice and 200 µl of 5x lysis buffer was added to each sample before shaking for 10 min at RT. The lysed samples were precleared by centrifugation at 14,000 rpm in a microfuge for 10 min at 4 °C. Supernatants were transferred to new tubes to which 90 µl of protein G-sepharose (50 % slurry v/v) and 60 ug of 6β-1 antibody (recognises the SgII processing product of 18 kDa (p18)) was added, and immunoprecipitation of p18 was performed O/N at 4 °C on a rotating wheel. Beads were then pelleted by centrifugation for 1 min at 3000 rpm in an Eppendorf centrifuge and supernatants removed by aspiration. After 4 washes with 1x lysis buffer followed by a final wash in 10 mM Tris-HCl pH 7.5, beads were resuspended in 10 µl 5x sample buffer, vortexed and boiled for 5 min. Tubes were pierced with a 27g needle, placed in a second Eppendorf tube and the eluates were collected by brief centrifugation in a microfuge. Immunoprecipitates were loaded on a 12% SDS-PAGE gel. Gels were Coomassie stained, dried (see 2.2.4.4) and exposed to a Kodak X-AR film at –70 °C. Quantification of p18 signal was done by densitometry using ImageJ analysis software (NIH). The PC2-independent signal (background signal) was subtracted from the signal obtained in the presence of PC12/PC2 ISGs.

2.2.8 SgII processing in PC12/PC2 cells

PC12/PC2 cells grown in 8x32 mm dishes were pulse-labelled with [^{35}S]-sulphate for 5 min (see 2.2.5.1) and either chased for 0 min, 10 min, 20 min, 30 min, 45 min, 60 min, 90 min or 180 min. The chase reaction was stopped on ice, washed in TBS + PI, the cells lysed in 1 ml TNTE buffer. To make heat-stable fractions, lysed cells were collected from the dish into an Eppendorf tube, boiled for 5 min and centrifuged at

maximum speed in a microfuge for 5 min. After the lysed cells are boiled, the granins are in the soluble fraction and are heat stable. After brief centrifugation, the insoluble material is pelleted and the soluble fraction (supernatant) is collected. The soluble fraction will be enriched in granins and devoid of all the insoluble material that aggregated by boiling. The supernatants were transferred into a fresh tube and the heat-stable proteins were acetone-precipitated (see 2.2.4.2), resuspended in SDS-sample buffer and analysed by 12% SDS-PAGE gel followed by autoradiography.

2.2.9 *In vitro* ISG binding assay

Solutions: Purified ISGs (see 2.2.6.2); 10x and 1x FB (see 2.2.7.1); ATP-regenerating system (Boehringer); HB; 1xSDS-sample buffer; trypsin (Sigma); trypsin inhibitor (1 mg/ml, Sigma).

The method to detect the recruitment of exogenous proteins to ISGs was developed by Andrea Dittie (Dittie et al., 1996). Purified proteins or abs were added to 50 µl ISGs with fusion buffer and ATP-regenerating system in a final volume of 250 µl. Samples were mixed and incubated at 37 °C for 30 min. The samples were then diluted with fusion buffer to a total volume of 1 ml and centrifuged at 33,000 rpm in a Ti 50.2 rotor for 1h at 4 °C. The supernatant was removed and the pellets were resuspended in 25 µl 1x SDS-sample buffer. Proteins-bound to ISGs were detected by immunoblotting followed by quantification using ImageJ analysis software (NIH).

In some cases, ISGs were pre-treated with various amounts of trypsin (Sigma) and/ or 1mg/ml soy bean trypsin inhibitor (STI) (Sigma) for 10 min at 37 °C and returned to ice. The amount of protein bound to ISGs membranes was detected as described above.

2.2.10 Cell biology techniques

2.2.10.1 Transient transfection of mammalian cell

Cells were plated onto 6-well dishes or 10 cm dishes one day prior to transfection. Transfection was carried out using Lipofectamine 2000 according to the supplier's instructions (Invitrogen). Briefly, plasmid DNA was mixed with Lipofectamine 2000 in serum and antibiotics-free medium (Optimem, Gibco BRL), and incubated for 20 min at RT before adding the mixture onto the cells. 5 h after transfection, the medium was exchanged for full growth medium. Cells were processed for indirect immunofluorescence or lysed 24h post transfection.

2.2.10.2 Synaptotagmin IV siRNA in PC12 cells

PC12 cells were split a day before transfection 1:3 to obtain 80% confluency in 6-well dishes or 10 cm plates. For transfection, Syt IV siRNA Smart pool (50 nM final concentration) (Dharmacon) (sequence described in 2.2.4) was mixed with Dharmafect 2 transfection reagent (Dharmacon) in serum and antibiotics-free medium (Optimem), and incubated for 20 min at room temperature. The transfection mix was diluted with antibiotics-free medium (supplemented with 10% horse serum and 5% FCS) before being added onto PC12 cells. The medium was exchanged for full growth medium after 24 h transfection. Three days post transfection, the cells were processed for indirect immunofluorescence or lysed for western blotting.

To assess SgII processing in Syt IV-siRNA-treated cells, 2 x 10 cm dishes of PC12/PC2 cells were transfected with Syt IV-siRNA as describe above. 48h post-transfection, cells were trypsinised, pooled and replated onto 8x35 mm dishes. Finally, SgII processing reaction was assayed (as described in 2.2.8).

To confirm that sorting and budding from the TGN was not disrupted, 2x10 cm dishes of PC12 cells were treated with Syt IV-siRNA. 72 h post-transfection cells were pulse-chased with [^{35}S]-sulphate (see 2.2.5.1) and PNS prepared from these cells (see 2.2.6.1) was subjected to velocity and equilibrium sucrose gradient separation (described in 2.2.6).

2.2.10.3 Adenovirus infection of PC12 cells

PC12 cells were infected with adenoviruses expressing HA-Syt IV cytoplasmic domain (obtained from Viraquest) at 500 pfu/cell. Infection was performed by incubating the adenoviruses with PC12 cells overnight in a 37 °C in a 10% CO_2 incubator in full growth medium. Next day, cells were washed twice with medium and processed either for indirect immunofluorescence or electron microscopy.

To check for the presence of acidic compartements in cells infected with HA-Syt IV cytoplasmic domain, infected or non-infected cells were incubated with 30 μM of the acidic granule marker DAMP (Oxford Biomedical Research) for 30 min in the 37 °C incubator. Following a wash with PBS, cells were processed for immuno-EM with monoclonal anti-DNP (1:10) and polyclonal anti-HA abs (1:100) followed by gold conjugated anti-mouse and anti-rabbit secondary abs.

2.2.10.4 Indirect immunofluorescence

Solutions: Poly-D lysine (Sigma) (1mg/ml in dH_2O); 3% paraformaldehyde (PFA) (methanol-free, TAAB, 16% stock diluted in PBS, stored at – 20 °C); PBS; 50 mM NH_4Cl; permeabilisation solution (0.2 % Triton X-100 in PBS); blocking solution (0.2% gelatin in PBS); Moviol prepared as follows: (2.4 g Moviol 4-88 (Calbiochem) were mixed with 6g glycerol and 6 ml of dH_2O for 2h at RT. 12 ml of 200 mM Tris-HCl pH 8.5 was added and the mixture incubated at 53 °C with occasional vortexing until the Moviol was dissolved. The solution was clarified by spinning at 5000g for 15 min in a Heraeus centrifuge, aliquoted and stored at – 20 °C).

Glass coverslips were coated with poly-D-lysine for 10 min at RT and washed twice with dH_2O. Cells were then plated onto the coated coverslips in 35 mm dishes and left to grow O/N. The next day, cells were washed twice with PBS and fixed with 3% PFA for 20 min followed by quenching of the fixative with 50 mM NH_4Cl in PBS for 10 min at RT. After washing twice with PBS, cells were permeabilised for 3-5 min with 0.2% Triton X-100 in PBS followed by washing twice with PBS, then twice again with blocking solution in which cells were incubated for 30 min. The cells were incubated in the primary ab, diluted in blocking solution, for 30 min. Excess antibody was washed away with the blocking solution and cells were incubated again with the secondary ab, diluted as above, for the same duration. Cells were washed twice with blocking solution then twice again with PBS. Finally cover slips were washed in dH_2O and mounted in Moviol on glass slides. Images were acquired by confocal microscopy (Zeiss plan-Apochromat 63x/1.40 NA oil objective lense) using LSM 510 software and processed with Photoshop 7.0.

Alternatively, cells were fixed and permeabilised in cold methanol for 10 min at –20 C°, washed twice with PBS then incubated for 30 min in blocking solution. Cells were

incubated with the primary, then secondary antibodies and processed as described above.

2.2.10.5 FACS-sorting of PC12 cells

Transfected PC12 cells were trypsinised, collected in a Falcon tube and centrifuged for 5 min at 1000 rpm in Heraeus centrifuge. Cells were washed twice in PBS, transferred to an Eppendorf tube, fixed and stained as described previously with slight modifications. The whole procedure was performed in an Eppendorf tube and washings were done by centrifugation at 1000 rpm for 3 min in a microfuge. The ab dilutions were 10x more concentrated than the dilutions used for indirect immunofluorescence. At the end of the procedure, the labelled cells were resuspended in PBS and sorting was performed using the Mo-flo cell sorter (DAKO-cytomation) by the staff of the FACS core laboratory (Cancer Research UK). Sorted cells were pelleted by centrifugation at 1000 rpm for 5 min in a Heraeus centrifuge and the pellet was resuspended in 1x SDS-sample buffer. Samples were loaded on SDS-PAGE gel followed by western blotting analysis.

2.2.10.6 Immunogold-labelling for electron microscopy

Cryo-fixation of cells, specimen preparation and immunogold labelling were performed by Rose Watson in the electron microscopy unit at CR-UK according to standard techniques. Briefly, cells were incubated in DAMP (described in 2.2.10.3) before being processed for immunogold labelling. For immuno-labelling, pelleted cells were fixed in 2% paraformaldehyde/0.2% glutaraldehyde in Sorensens buffer for 2h at RT. After washing, cells were resuspended in 10% gelatine, pelleted and stored in 2.3% sucrose to cryprotect the specimen. After 3h, the specimen was rapidly frozen in liquid nitrogen

followed by the cutting of ultrathin sections. Sections were transferred to a carbon/formvar-coated grids and stored on 2% gelatine at 4 °C.

Prior to labelling, the gelatine on which the grids were placed was heated for 20 min at 37 °C. Samples were then incubated in 0.1% glycine for 3 min followed by 0.1% BSA for 2 min and primary abs diluted in 1% BSA for 30 min. After washing, samples were incubated with protein A gold (5 and 10 mm) diluted 1:50 in 1% BSA. Samples were then washed and post-fixed in 1% glutaraldehyde for 5 min. Negative staining of the sample was done with saturated 2% uranyl acetate for 5 min, followed by washing in water and incubation in 4% methyl cellulose, 0.4% uranyl acetate at 4 °C for 5 min. Finally, sections were embedded in 4% methyl cellulose, 0.4% uranyl acetate and examined. Pictures were taken with JEOL 1010 electron microscope (Japanese Electron Optical Limited).

3 Chapter 3: Synaptotagmin IV is localised on the immature secretory granules and absent from the mature secretory granules in PC12 cells

3.1 Aim

In this chapter, I will present a study aimed at investigating the localisation of Syt IV in the neuroendocrine cell line PC12. The localisation of Syt IV on ISGs, and whether or not it is present on MSGs, is still controversial. It was demonstrated that Syt IV is localised on MSGs in PC12 cells (Ferguson et al., 1999) (Thomas et al., 1999). Later, other studies showed that Syt IV is localised on ISGs and absent from MSGs in the neuroendocrine cell line ATt-20 (Eaton et al., 2000). However, both studies did not examine endogenous Syt IV. A different study looking at the localisation of endogenous Syt IV in PC12 cells using electron microscopy revealed that this isoform is on ISGs and not on MSGs (Fukuda et al., 2003). To confirm these last results, I undertook subcellular fractionation on sucrose gradients, combined with the use of a specific anti-Syt IV ab. This method allows for the efficient separation of ISGs from MSGs, and therefore a potentially more accurate means of determining the localisation of the endogenous Syt IV.

3.2 Generation of antibodies against Synaptotagmin IV

In order to study the localisation of Syt IV in PC12 cells, I generated polyclonal abs against Syt IV. The peptide sequence, KAGSSSDLENVT, corresponding to the amino acids 112 to 121 in the spacer domain of rat Syt IV, was synthesised by the peptide synthesis laboratory, Cancer Research UK. The different isoforms of the Syt family show a high degree of homology, especially within their C2 domains. However, the spacer domain, where the peptide sequence was chosen, is less conserved among members of this family of protein (Figure 3.2.1). This was done to minimise the risk of cross-reactivity of the generated anti-Syt IV ab with other isoforms of the same family. The peptide was crosslinked to *limulus polyphemus* haemocyanin (LPH) and injected into two guinea pigs (MS3 and MS4) by Biogenes (Germany), according to standard procedure. Guinea pig serum MS3 had no detectable titre in an ELISA assay performed by Biogenes, nor did it show any specific signal by indirect immunofluorescence (data not shown). This anti-serum was thus not reactive with Syt IV. The anti-serum MS4 was tested by western blotting of cell lysates from PC12 cells or HEK cells overexpressing the full-length rat T7-Syt IV (Figure 3.2.2). A specific anti-Syt IV ab, provided by Dr Mitsunori Fukuda (Riken Institute, Japan) that recognises both native and overexpressed forms of Syt IV was used as positive control (Ibata et al., 2000).

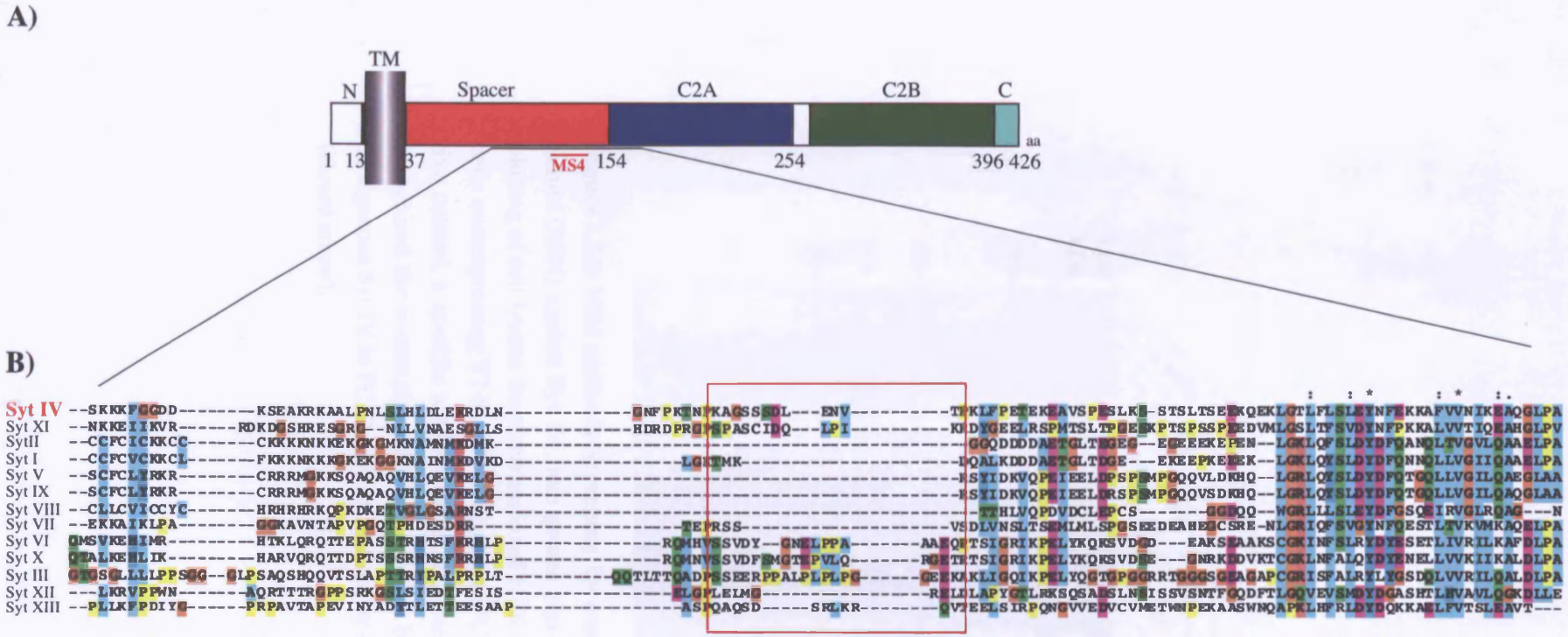

Figure 3.2.1: Anti-Syt IV antibody (MS4) peptide sequence alignment.

A) A schematic representation of Syt IV domain organisation. N is the lumenal N-terminal domain, TM is the transmembrane domain and C is the C-terminal end of the cytoplasmic domain of Syt IV. The red line represents where the MS4 antibody sequence is within the spacer domain . B) The alignement of the MS4 sequence region within the spacer domain of rat Syt IV with rat Syt I-XIII (red box) using ClustalX alignment software.

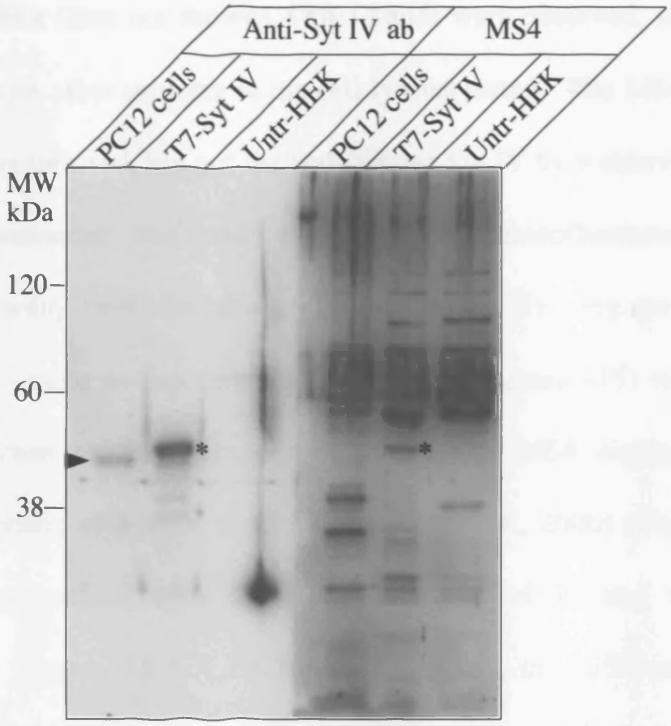

Figure 3.2.2: MS4 antibody Screening by western blotting.
Serum (MS4) against Syt IV from guinea pigs was screened by western blotting of cell lysates from untransfected HEK cells (Untr) (10 μg), HEK cells overexpressing T7-Syt IV (10 μg) and PC12 cells (50 μg). As positive control, a specific anti-Syt IV ab was used (left hand panel). MS4 recognised the overexpressed T7-Syt IV (*) but did not react with the endogenous Syt IV in PC12 cells recognised by the specific anti-Syt IV ab (closed arrow).

In HEK cells, where there is no expression of the endogenous Syt IV, both the MS4 and the control anti-Syt IV ab recognised a ~50 KDa band corresponding to the overexpressed T7-Syt IV. This band was not present in untransfected HEK cell lysates. However, in contrast to the control anti-Syt IV antibody, MS4 did not react with the endogenous Syt IV in PC12 cell lysates. The band was not seen even after longer exposure of the blot (data not shown). Other bands were observed, suggesting that this ab cross-reacts with other proteins in the cell lysates tested. The MS4 is therefore able to detect the overexpressed, but not the endogenous Syt IV by western blotting.

Next, the MS4 antiserum was tested using indirect immunofluorescence. When PC12 cells were fixed using PFA, the MS4 antiserum did not give any specific staining, and the staining was similar to that obtained with the preimmune (PI) serum (Figure 3.2.3 A). However, when methanol fixation was used, the MS4 displayed a perinuclear staining characteristic of Syt IV distribution (Ibata et al., 2000) (Figure 3.2.3 B). The MS4 staining colocalised with the Golgi marker GM130 and with Stx6 in the perinuclear area (Figure 3.2.4 A,B). Most importantly, the MS4 staining colocalised with the specific anti-Syt IV ab provided by Dr M.Fukuda (Figure 3.2.4 C). However, this colocalisation was mostly in the perinuclear area. The granular structures recognised by the specific anti-Syt IV ab in the periphery of the cells were not colabelled with the MS4. To investigate further whether the MS4 staining was specific, PC12 cells overexpressing T7-Syt IV were fixed and labelled with mouse anti-T7 ab and MS4, or with the specific anti-Syt IV ab and MS4. Surprisingly, the MS4 antiserum did not display the same staining as the anti-T7 (Figure 3.2.5 A) or the control anti-Syt IV antibodies (Figure 3.2.5 B), but rather had the same perinuclear staining as seen in untransfected PC12 cells.

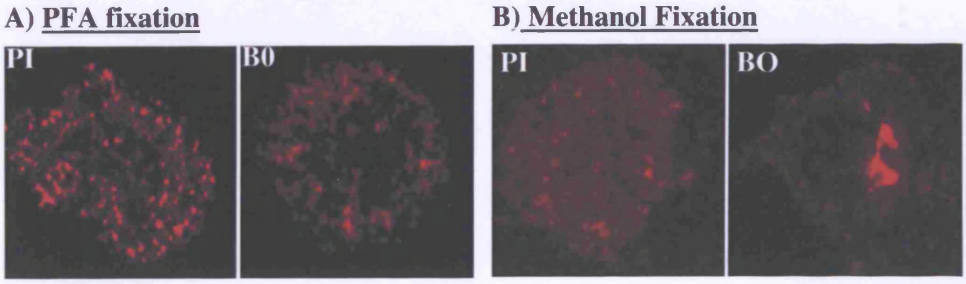

Figure 3.2.3: MS4 antibody screening by indirect immunofluorescence in PC12 cells. PC12 cells were fixed with A) 3% PFA or B) 100% cold methanol then labelled with A,B) MS4 pre-immune (PI) or MS4 bleed-out (BO) at 1:100 dilution. The MS4 was detected with anti-guinea pig-Cy3. Images were acquired with a confocal microscope using LSM 510 software, Zeiss plan-Apochromat 63*/1.40 oil objective lense.

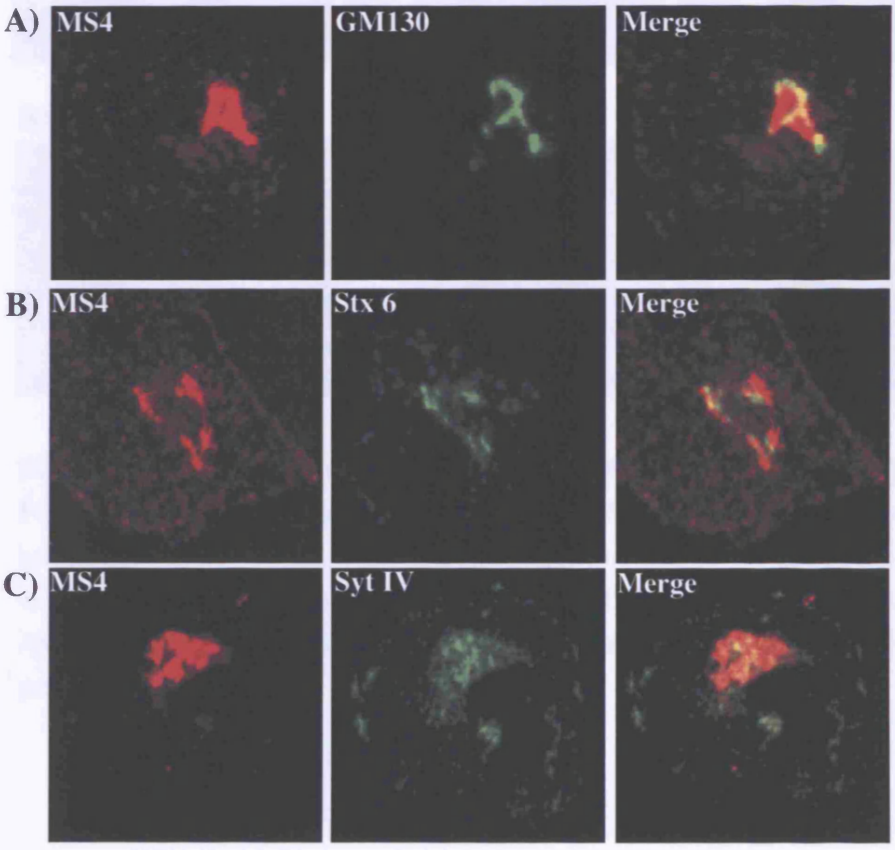

Figure 3.2.4: MS4 serum partially colocalises with Golgi markers by indirect immunofluorescence. PC12 cells were fixed with methanol and labelled with A) MS4 and GM130, B) MS4 and Stx6, C) MS4 and anti-Syt IV ab (provided by M.Fukuda). MS4 was detected with anti-guinea pig -Cy3, monoclonal anti GM130 and anti-Stx 6 ab with anti-mouse Alexa-488 and finally polyclonal anti-Syt IV was detected with anti-rabbit Alexa-488. Images were taken as described above.

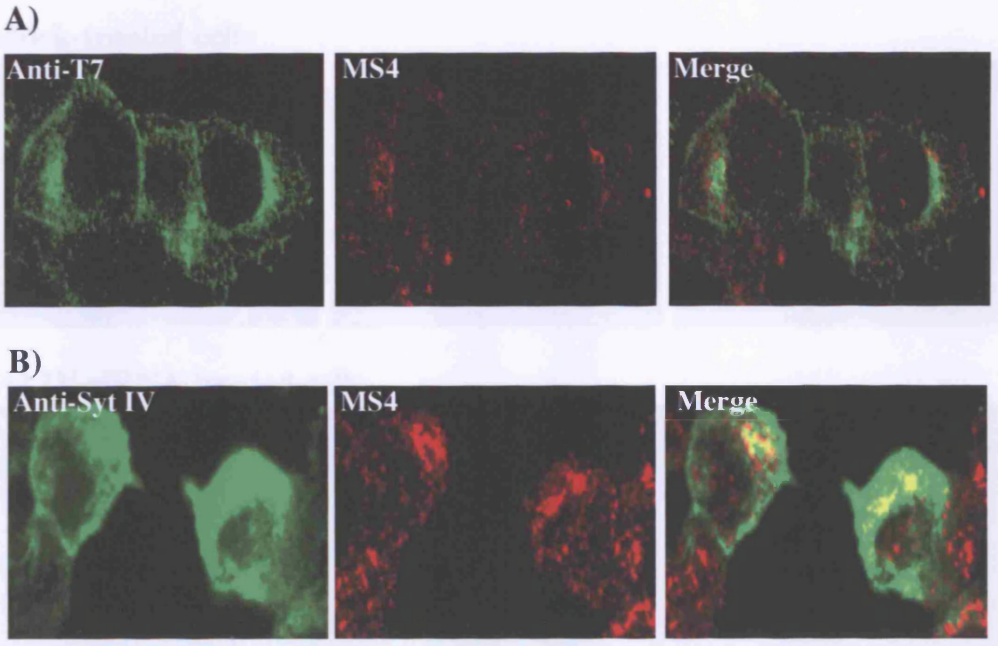

Figure 3.2.5: MS4 serum does not react with the overexpressed T7-Syt IV in PC12 cells. PC12 cells were transfected with T7-Syt IV, fixed with methanol and colabelled with A) MS4 and anti-T7 or B) MS4 and anti-Syt IV (M.Fukuda). MS4 was detected with anti-guinea pig-Cy3, T7 or Syt IV with anti-mouse or anti-rabbit Alexa-488 secondary antibodies, respectively. Images were aquired as described previously.

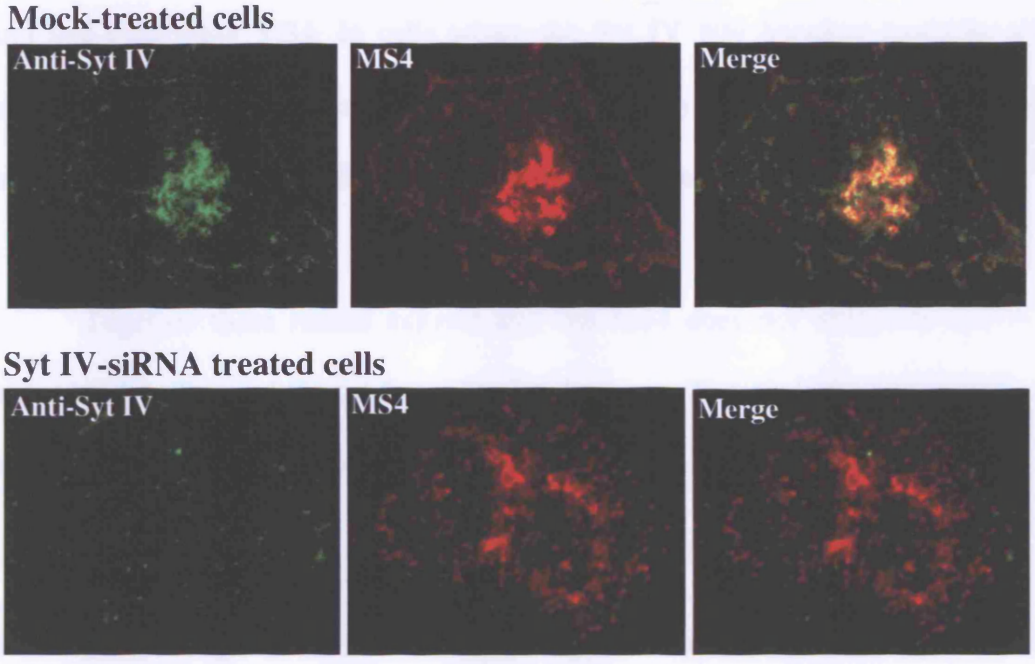

Figure 3.2.6: Indirect immunofluorescence of Syt I siRNA-treated PC12 cells using MS4. PC12 cells were mock treated (top) or treated with Syt IV-siRNA (bottom) as described in Chapter 2. The cells were then fixed with methanol and labelled with MS4 and anti-Syt IV ab (M.Fukuda). MS4 and anti-Syt IV ab were detected with the secondary anti-guinea pig-Cy3 and anti-rabbit Alexa-488 antibodies, respectively. Confocal images were acquired as described previously.

There are two likely explanations for why the MS4 antiserum does not recognise T7-Syt IV. First, the epitope recognised by the MS4 antiserum is masked due to the folding of the overexpressed T7-Syt IV. Second, the MS4 antiserum reacts non-specifically with another Golgi-localised protein. To answer this question, PC12 cells were treated with siRNA against Syt IV, fixed and labelled with the specific anti-rabbit Syt IV antibody and anti-guinea-pig MS4. In cells where the Syt IV was knocked-down by siRNA treatment, shown by the decreased staining of Syt IV by the specific ab, MS4 signal did not disappear but instead still displayed a perinuclear staining (Figure 3.2.6).

Together these results suggest that the MS4 does not recognise Syt IV but instead is labelling a different Golgi-localised protein. Therefore, I concluded that The MS4 antibody was not suitable for use in this study.

3.3 Synaptotagmin IV is localised on ISGs and absent from MSGs in PC12 cells

To study the localisation of endogenous Syt IV in PC12 cells, the specific anti-Syt IV ab provided by Dr M.Fukuda was used. This ab has been tested against all Syt isoforms and was found to recognise only Syt IV (Ibata et al., 2000).

First, I looked at the localisation of Syt IV with different sub-cellular markers by indirect immunofluorescence.

To specifically label MSGs, I used PC12/PC2 cells, a PC12 cell line stably expressing the pro-hormone convertase, PC2 (Dittie and Tooze, 1995). In PC12/PC2 cells, PC2

cleaves SgII at dibasic amino acid cleavage sites and produces a fragment called p18, which accumulates in MSGs. p18 can then be detected using a specific antibody that recognises only p18, and not full length or partially processed SgII (Figure 3.3.1).

PC12/PC2 cells were fixed with PFA, permeabilised and double-labelled with anti-Syt IV ab, with anti-Stx6 ab as perinuclear marker, and anti-Syt I (Perin et al., 1991) and anti-p18 abs as MSG markers. Syt IV showed a strong colocalisation with Stx6 in the perinuclear area (Figure 3.3.2 A). No colocalisation of Syt IV with the MSG markers p18 or Syt I was observed (Figure 3.3.2 B, C).

To see if the endogenous Syt IV is distributed on ISGs, and whether is present or absent from MSGs, I undertook a subcellular fractionation approach. This approach separates ISGs from MSGs on a continuous velocity 0.3M-1.2M sucrose gradient followed by a discontinuous equilibrium 0.8M-1.6M sucrose gradient as described in chapter 3 (Dittie et al., 1996). In PC12 cells, there are three major sulphated proteins, the constitutively secreted heparin sulphated proteoglycan (hsPG) (Gowda et al., 1989) and two secretory granule proteins, secretogranin II (SgII) and chromogranin B (CgB), that follow the regulated secretory pathway (Rosa et al., 1985). After a 5 min labelling with [^{35}S]-sulphate, these three proteins are sulphated in the TGN on tyrosine residues. A 15 min chase will allow the detection of SgII and CgB in ISGs and the hsPG in CSVs. An O/N chase will allow the detection of SgII and CgB in MSGs. PC12 cells were [^{35}S]-sulphate labelled for short periods (5 minutes pulse and chased for 15 minutes), or overnight (1 hour pulse and chased overnight) to label ISGs or MSGs, respectively (Dittie et al., 1996).

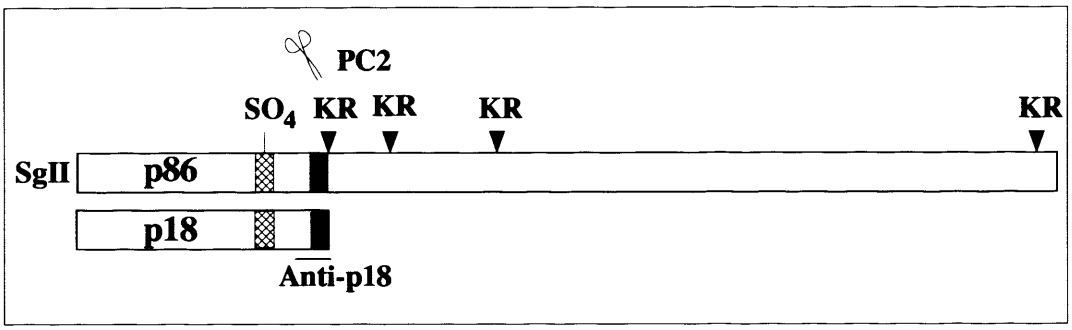

Figure 3.3.1: Schematic representation of SgII and p18. Full length SgII (p86) and its degradation product p18 are represented. the black arrows are dibasic processing sites (Lys-Arg) used by PC2. Many degradation products of SgII are generated by PC2 and the final endoproduct is p18, which accumulates in MSGs. Both SgII and p18 are sulphated on a tyrosine residue (SO_4). Monoclonal anti-p18 ab is directed against the C-terminal end of p18 and is specific for p18.

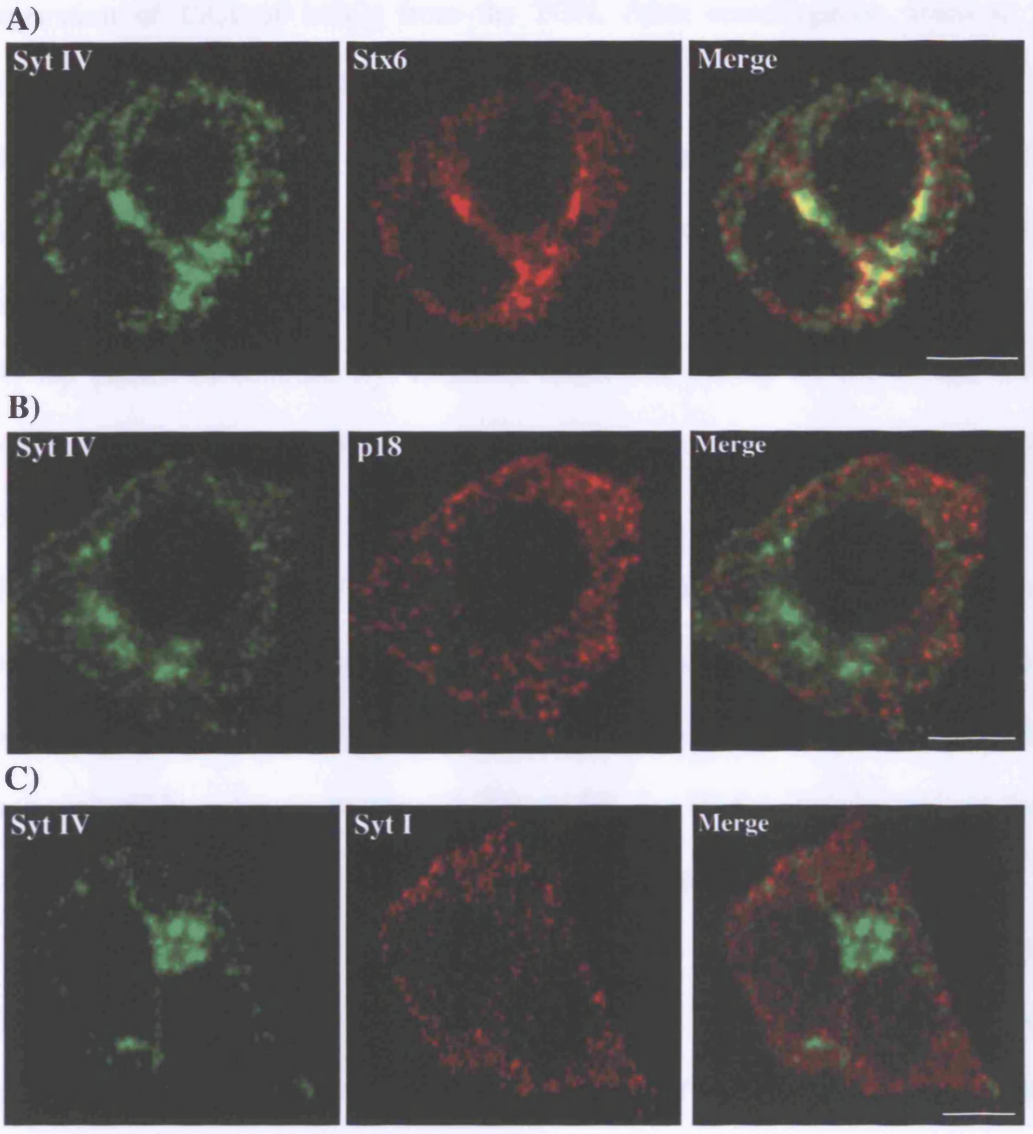

Figure 3.3.2: Localisation of Syt IV in PC12/PC2 cells using indirect immunofluorescence. PC12/PC2 cells were fixed with 3% PFA, permeabilised with 0.2% TX-100 and double labelled with abs against A) Syt IV and Stx 6, B) Syt IV and p18 and C) Syt IV and Syt I. Polyclonal anti-Syt IV abs were detected with secondary anti-rabbit-Alexa 488 and monoclonals anti-Stx 6, anti-p18 and anti-Syt I abs were detected with anti-mouse-Cy3. Images were aquired by confocal microscopy using LSM 510 software, Zeiss plan-Apochromat 63*/1.40 oil objective lense (Bars, 5µm).

The post nuclear supernatant (PNS) from these labelled cells was subjected to a continuous velocity sucrose gradient fractionation. This first gradient will allow the separation of ISGs or MSGs from the TGN. After centrifugation, fractions were collected and then analysed by SDS-PAGE.

Syt IV was found mainly in the light ISG-containing fractions, as well as Golgi-containing fractions at the bottom of the gradients, characteristic of the perinuclear localisation observed by indirect immunofluorescence (Ibata et al., 2000) (Figure 3.3.3 A, top panel). In contrast, Syt I, shown to localise mainly on MSGs and synaptic vesicles (Perin et al., 1991), showed a peak distribution in the slightly heavier MSG-containing fractions (Figure 3.3.3 A, bottom panel).

The light fractions (1-4) and the slightly heavier fractions (5-7) were then loaded on two separate discontinuous equilibrium sucrose gradients. This step will permit further separation of ISGs from CSVs and MSGs. Fractions from both gradients were collected and analysed by autoradiography and SDS-PAGE. Syt IV distributed mainly in the ISG containing fractions (7-9), which contain the [^{35}S]-sulphate-labelled SgII (Figure 3.3.3 B, top panels). In addition, Syt IV displayed the same distribution as Stx6, which was previously found in ISG fractions (Wendler et al., 2001) (Figure 3.3.3 B, bottom panels). In contrast, Syt IV was not found in the MSG fractions (9-11), identified by the [^{35}S]-sulphate-labelled SgII in heavier fractions (Figure 3.3.3 C, top panels), whereas the isoform Syt I distributed in the MSG fractions (Figure 3.3.3 C, bottom panel).

In conclusion, this study confirms that Syt IV is localised on ISGs and is absent from MSGs.

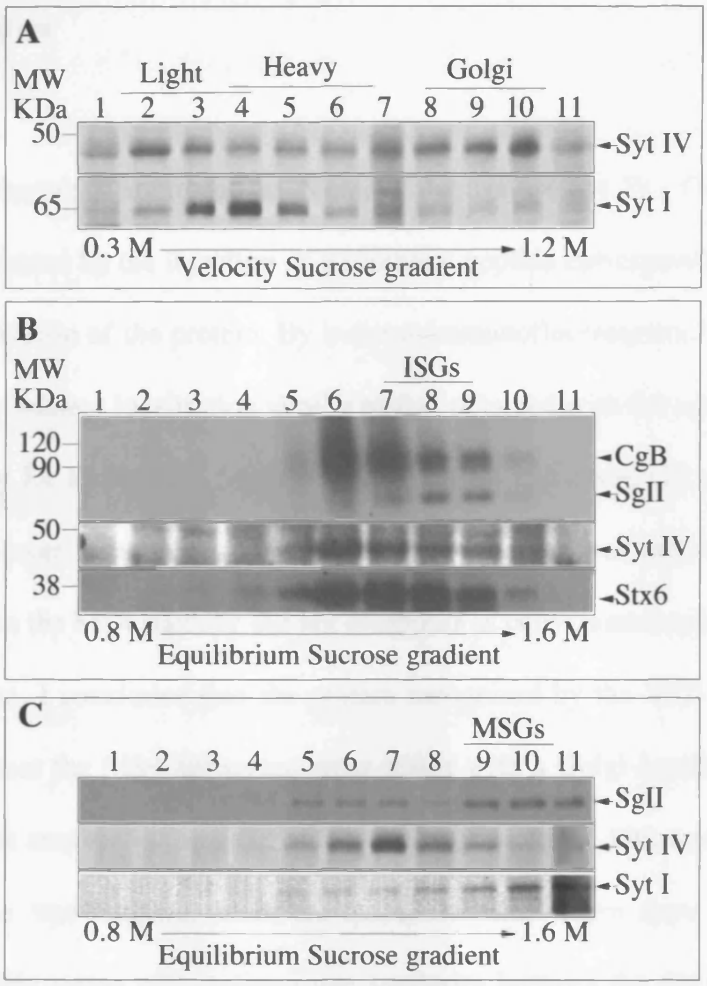

Figure 3.3.3: Distribution of Synaptotagmin IV in PC12 cells by subcellular fractionation. A) PNS from PC12 cells was loaded onto a 0.3 M -1.2 M continuous sucrose gradient, centrifuged and fractions collected. Western blotting was performed using both anti-Syt IV (top panel) and anti-Syt I (bottom panel) abs. Alternatively, PC12 cells were labelled with [^{35}S]-sulphate for B) 5 min and chased for 15 min to label ISGs or C) labelled for 1 h and chased O/N to label MSGs. PNS from these cells was loaded on a continuous velocity sucrose gradient and centrifuged. Fractions B) 1-4 or C) 4-6 from the velocity gradients were further separated on a 0.8-1.6 M discontinuous equilibrium sucrose gradient. Fractions from both gradients were collected and analysed on an SDS-PAGE. Top panels B,C): Autoradiogram showing [^{35}S]-sulphate-labelled CgB and SgII. Bottom panels: western blot analysis using B) anti-Syt IV and anti-Stx 6 abs or C) anti-Syt IV and anti-Syt I abs. The diffuse band between 120 and 90 KDa in a hsPG.

3.4 Discussion

In this chapter, I attempted to generate abs against Syt IV. The anti-Syt IV ab (MS4) was obtained by the injection of a synthetic peptide corresponding to a sequence in the spacer domain of the protein. By indirect immunofluorescence, the MS4 staining displayed a perinuclear localisation similar to that obtained with the specific anti-Syt IV ab provided by Dr M.Fukuda. Surprisingly, the MS4 antiserum did not recognise the overexpressed protein, suggesting that the staining observed was non-specific. This was confirmed when the MS4 staining did not disappear in cells treated with Syt IV siRNA. From these data, I concluded that the protein recognised by the MS4 antiserum is not Syt IV, but rather the MS4 antiserum cross reacts with a Golgi-localised protein. This protein could be another isoform of the Syt family of proteins. Although the sequence of the immunogen was obtained from the spacer domain, where there is less sequence conservation, this region still retains some similarity between the different isoforms of this family of proteins. One candidate could be Syt XI, which is the closest homologue to Syt IV. However, blotting PC12 cell lysates with anti-Syt XI ab did not allow the detection of the protein, suggesting it is not expressed or expressed at very low levels (Tucker et al., 2003). The overexpression of all isoforms and labelling with the MS4 antiserum would reveal whether this ab is cross-reacting with another Syt isoform or a protein that belongs to a different family.

In conclusion, the MS4 antiserum was unsuitable for the purposes of this study. Therefore, for future studies where an ab against Syt IV is required, I used the anti-Syt IV ab provided by M.Fukuda.

An additional aim was to study the localisation of endogenous Syt IV in PC12 cells. At the start of my study, Syt IV localisation was still inconclusive due to the conflicting data from different studies (Ferguson et al., 1999) (Eaton et al., 2000) (Fukuda et al., 2003) (Wang et al., 2001). Initial reports had shown that Syt IV localised to MSGs and colocalised with Syt I in PC12 cells (Ferguson et al., 1999) (Thomas et al., 1999). Because endogenous Syt IV was undetectable in their PC12 cell line, this study was conducted on PC12 cells treated with forskolin, which was known to be one of the stimulants that increases Syt IV expression (Vician et al., 1995). Later, using indirect immunofluorescence, another study demonstrated that Syt IV and Syt I had distinct distributions in PC12 cells (Ibata et al., 2000). Moreover, using electron microscopy, Syt IV was shown to localise on ISGs and not MSGs in wild type PC12 cells (Fukuda et al., 2003). These discrepancies were attributed to the lack of specificity of the anti-Syt IV ab used in the first study. A different analysis conducted in ATt20 cells expressing low levels of Flag-Syt IV showed that the overexpressed protein is on ISGs and not on MSGs (Eaton et al., 2000). However, in AtT20 cells expressing higher levels of Flag-Syt IV, the protein was found on both ISGs and MSGs. Part of the answer to these contradictions came from data that demonstrated that forskolin treatment or overexpression induces the sorting of Syt IV to MSGs (Fukuda and Yamamoto, 2004) (Wang et al., 2003a). Therefore, these earlier data did not identify the true subcellular localisation of the endogenous Syt IV.

In this study, by using the specific anti-Syt IV ab (Ibata et al., 2000) and a subcellular fractionation approach, I found that endogenous Syt IV distributed in the ISG-containing fractions. In contrast to Syt I, Syt IV was not found in MSGs. This was also seen by indirect immunofluorescence, where Syt IV had a distinct staining from that of Syt I and p18.

In the equilibrium sucrose gradients, where ISGs are found in fractions 7-9, Syt IV, as well as Stx 6, were also detected in fraction 6. This fraction contains membranes such as early endosomes and CCVs (Dittie et al., 1999) (Dittie et al., 1996). However, Syt IV did not colocalise with transferrin receptor (Ibata et al., 2000) and EEA1 (data not shown) by immunofluorescence, suggesting it is unlikely that Syt is on early endosomes. The Syt IV found in fraction 6 however could be on clathrin coated vesicles (CCVs). Immuno-EM staining of Stx6 and VAMP4, two proteins removed during ISG maturation (Wendler et al., 2001), revealed that they are localised to CCVs in the proximity of the Golgi (Bock et al., 1997; Steegmaier et al., 1999). Like Stx6 and VAMP4, Syt IV could be removed from the maturing granule via CCVs. It will be interesting to investigate this question. Immuno-EM labelling of Syt IV and Adaptor protein-1 (AP-1) as well as blotting purified CCVs with anti-Syt IV ab will reveal whether this protein is localised on CCVs. Previous studies have shown that VAMP4 is sorted from ISGs via binding to AP-1 (Hinners et al., 2003). It will be of great interest to investigate whther Syt IV displays binding to AP-1, which may suggest a common sorting pathway between proteins removed during granule maturation (The sorting of Syt IV will be further discussed in chapter 7).

In the equilibrium gradient, where MSGs distribute into fractions 9-11, Syt IV was found in fractions 6-8. These fractions contain membranes such as late endosomes and lysosomes (Dittie et al., 1999). To address the question of whether Syt IV localises on late endocytic compartments, a preliminary staining with LAMP-1 was performed (data not shown). Lack of colocalisation with this marker suggests that Syt IV is not on these compartments. However, to further characterise Syt IV localisation, a more thorough analysis should be performed including: costaining with the late endosomal markers,

such as lysobiphosphatidic acid (LPBA) as well as late endosomes subfractionation and subsequent immunoblotting against Syt IV.

An additional explanation to take into consideration is that a small proportion of SgII is also observable in the lighter fractions 6-8, in the MSG gradient, suggesting that a slight contamination of ISG membranes, where Syt IV distributes, is found in this gradient.

In conclusion, I confirm and extend previous findings that Syt IV is found on ISGs, and is removed from these granules during maturation in PC12 cells.

4 Chapter 4: The cytoplasmic domain of Synaptotagmin IV inhibits ISG-ISG homotypic fusion

4.1 Aim

Endocrine, neuroendocrine and exocrine cells are specialised cells that undergo regulated secretion (Arvan and Castle, 1998) (Tooze et al., 2001). In these cells, hormones and peptides to be secreted are packaged into ISGs, which bud from the TGN. After formation, ISGs undergo several changes, which include homotypic fusion (Urbe et al., 1998), membrane remodelling via CCVs (Klumperman et al., 1998) (Kuliawat et al., 1997), and hormone processing subsequent to the acidification of the granule's content (Moore et al., 2002) (Orci et al., 1987). These maturation steps lead to the formation of MSGs, which undergo calcium-dependent exocytosis with the plasma membrane following an external stimuli.

To study one aspect of the maturation of ISGs, an *in vitro* assay that reconstitutes ISG-ISG fusion was developed by S.Urbe (Urbe et al., 1998). This assay revealed an involvement of proteins such NSF and α-SNAP in the regulation of ISG-ISG fusion.

Localisation studies demonstrated that Syt IV, like the SNARE protein Stx6, was present on ISGs and absent from MSGs (Wendler et al., 2001). Moreover, the latter protein was found to be important for ISG homotypic fusion (Wendler et al., 2001).

In Chapter 3, I confirmed that endogenous Syt IV is localised on ISGs and is absent from MSGs in PC12 cells. It is now established, in particular from studies on Syt I, that

the Syt family of proteins are involved in regulating membrane fusion events (Bai and Chapman, 2004).

The similarity in the distribution of Syt IV and Stx6, and the data suggesting that Syts are part of the fusion machinery, have led us to hypothesise that Syt IV might play a role in granule maturation prior to its removal from the maturing granules.

4.2 Purification of the recombinant Synaptotagmin IV cytoplasmic domain

One approach to study the function of Syt IV in granule maturation is to add the purified recombinant Syt IV cytoplasmic domain into the *in vitro* fusion assay, and to ask whether this fragment has an effect on ISG-ISG fusion.

To do this, I generated a GST-Syt IV cytoplasmic domain fusion protein and expressed it in bacteria as described in Chapter 2. This fusion protein was initially purified by affinity chromatography using glutathione-sepahrose beads. The band at ~ 70 kDa represents the purified GST-Syt IV cytoplasmic domain (Figure 4.2.1 A). Two major contaminants appeared to co-purify with the fusion protein. The band at 35 kDa represents a degradation product of the GST-Syt IV cytoplasmic domain. This was demonstrated by blotting with the anti-Syt IV antibody, which reacted with both the GST-Syt IV cytoplasmic domain and the degradation product (data not shown). This degradation product was also reported after bacterial expression of cytoplasmic domains of other Syt isoforms (Tucker et al., 2003).

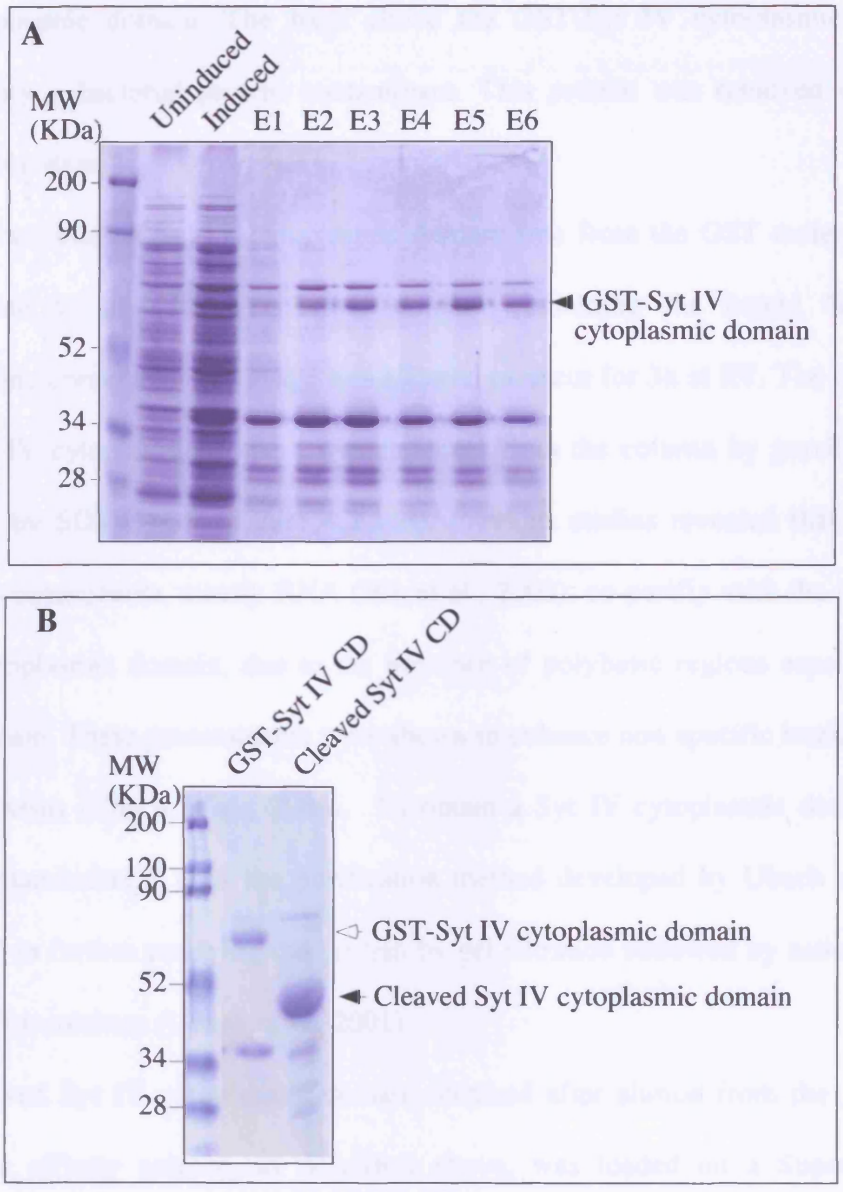

Figure 4.2.1: Purification of the Syt IV cytoplasmic domain.

A) Syt IV cytoplasmic domain was expressed as a GST fusion proteins in *E.coli* and purified by affinity chromatography using glutathione sepahrose beads. Lysates from uninduced or induced bacteria and the proteins eluted with Glutathione (E1-E6) from the column were loaded on an SDS-gel followed by coomassie staining. The arrow shows the position of GST-Syt IV cytoplasmic domain. B) GST-Syt IV cytoplasmic domain (open arrow) was cleaved using thrombin and the Syt IV cytoplasmic domain (closed arrow) was eluted from the column. GST-Syt IV cytoplasmic domain, and Syt IV cytoplasmic domain, was run on an SDS-PAGE and analysed by coomassie blue staining.

The addition of a cocktail of proteases inhibitors did not prevent proteolysis of the Syt IV cytoplasmic domain. The band above the GST-Syt IV cytoplasmic domain is presumably a bacterial protein contaminant. This protein was removed during later purification steps.

In order to obtain a Syt IV cytoplasmic domain free from the GST moiety, thrombin was added to glutathione-sepharose column containing the bound GST-Syt IV cytoplasmic domain, and cleavage was allowed to occur for 3h at RT. The cleaved ~45 kDa Syt IV cytoplasmic domain was collected from the column by gravity flow, and analysed by SDS-PAGE (Figure 4.2.1 B). Previous studies revealed that negatively-charged contaminants, mostly RNA (Wu et al., 2003), co-purifiy with the recombinant Syt I cytoplasmic domain, due to the presence of polybasic regions especially in the C2B domain. These contaminants were shown to enhance non-specific interactions with other proteins (Ubach et al., 2001). To obtain a Syt IV cytoplasmic domain free of these contaminants, I used the purification method developed by Ubach et al, which consisted in further purifying the protein by gel filtration followed by cation exchange purification columns (Ubach et al., 2001).

The cleaved Syt IV cytoplasmic domain obtained after elution from the glutathione-sepharose affinity column, as described above, was loaded on a Superdex-75 gel filtration column (Pharmacia) for separation according to protein size. The eluted peak fractions, as identified by absorbance at 280nm (Figure 4.2.2 A), were analysed by SDS-PAGE. The major peak was found in fractions 51-54, which contained mostly Syt IV cytoplasmic domain (Figure 4.2.2 B). Other fractions contained contaminating proteins, for example the high MW protein, which eluted before the Syt IV cytoplasmic domain.

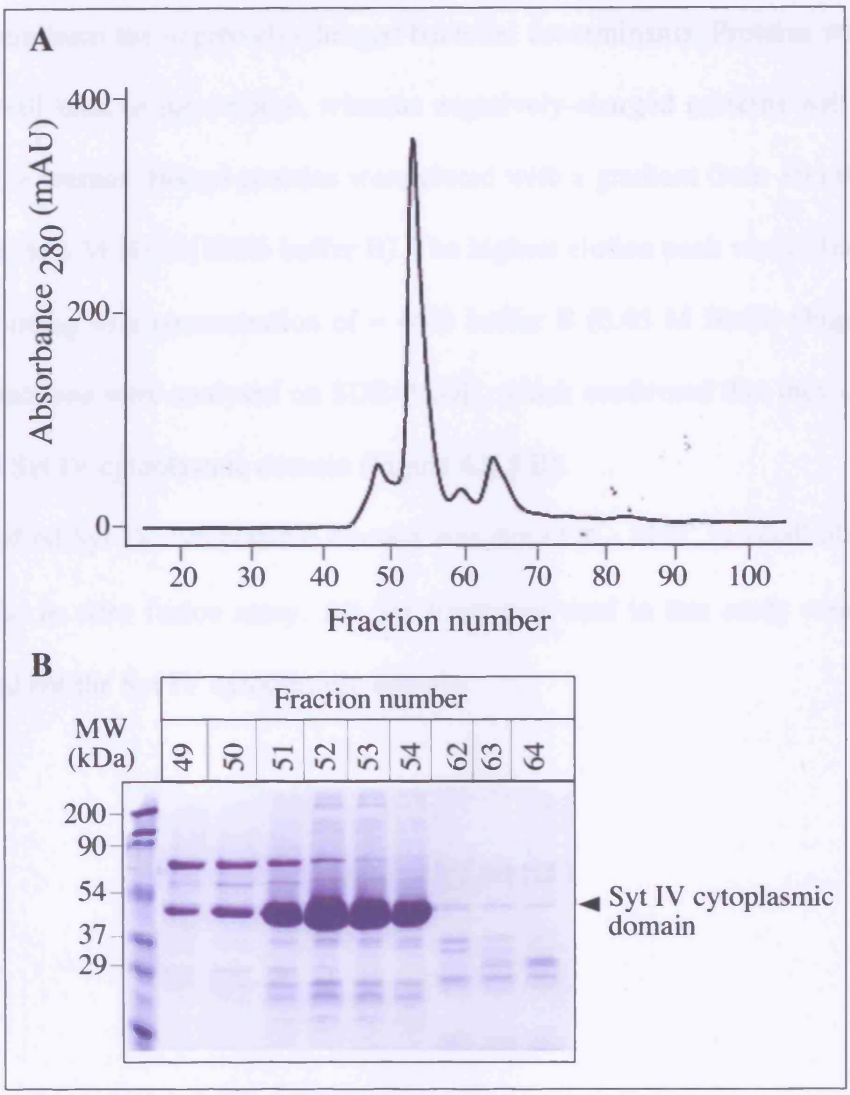

Figure 4.2.2: Syt IV cytoplasmic domain purification by gel filtration. The cleaved Syt IV cytoplasmic domain purified on glutathione beads (shown in figure 4.2.1) was further separated by gel filtration on superdex-75 column. A) Is a chromatogram of the OD_{280} profile from the cleaved Syt IV cytoplasmic domain pool loaded on a superdex 75 size exclusion column. B) Fractions containing peak absorbance were collected and loaded on SDS-gel for analysis. Fractions 51-54 contain Syt IV cytoplasmic domain.

Fractions from the gel filtration column containing the Syt IV cytoplasmic domain were pooled and further purified by cation exchange in the appropriate buffer, which releases the protein from the negatively-charged bacterial contaminants. Proteins with a positive charge will bind to the column, whereas negatively-charged proteins will be removed during the washes. Bound proteins were eluted with a gradient from 10 mM NaCl (0% buffer B) to 1 M NaCl (100% buffer B). The highest elution peak was in fractions 50-60 corresponding to a concentration of ~ 45% buffer B (0.45 M NaCl) (Figure 4.2.3 A). These fractions were analysed on SDS-PAGE, which confirmed that they contained the purified Syt IV cytoplasmic domain (Figure 4.2.3 B).

The purified Syt IV cytoplasmic domain was stored at - 80°C in small aliquots before use in the *in vitro* fusion assay. All Syt fragments used in this study were purified as described for the Syt IV cytoplasmic domain.

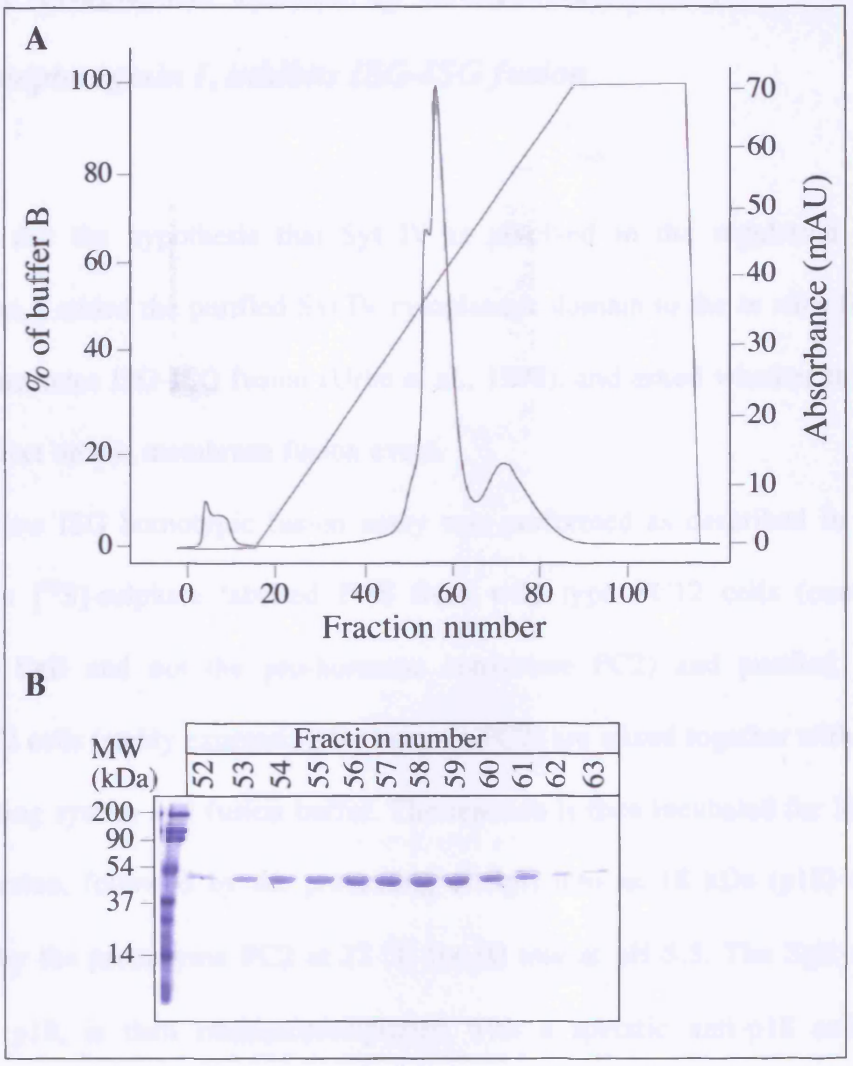

Figure 4.2.3: Syt IV cytoplasmic domain purification on cation exchange column. Peak fractions containing Syt IV cytoplasmic domain separated on the gel purification column (shown in figure 4.2.2) were pooled and further purified on a cation exchange, Hi-Trap SP column. Syt IV cytoplasmic domain elution with a NaCl gradient from 10 mM (0% buffer B) to 1M (100% buffer B) from the cation exchange column. A) is a chromatogram of the OD_{280} profile and the % of buffer B. B) Peack fractions were collected and loaded on an SDS-PAGE gel for analysis. The purified Syt IV cytoplasmic domain is eluted mostly in fractions 54-59 at ~ 45% of buffer B.

4.3 The cytoplasmic domain of Synaptotagmin IV, but not that of Synaptotagmin I, inhibits ISG-ISG fusion

To test the hypothesis that Syt IV is involved in the regulation of granule maturation, I added the purified Syt IV cytoplasmic domain to the *in vitro* fusion assay that reconstitutes ISG-ISG fusion (Urbe et al., 1998), and asked whether this fragment has an effect on this membrane fusion event.

The *in vitro* ISG homotypic fusion assay was performed as described in Chapter 2. Briefly, a [^{35}S]-sulphate labelled PNS from wild type PC12 cells (containing the substrate SgII and not the pro-hormone convertase PC2) and purified ISGs from PC12/PC2 cells (stably expressing the enzyme PC2) are mixed together with ATP, ATP regenerating system and fusion buffer. The reaction is then incubated for 30 min at 37 °C for fusion, followed by the processing of SgII into an 18 kDa (p18) degradation product by the proenzyme PC2 at 37 °C for 90 min at pH 5.5. The SgII degradation product, p18, is then immunoprecipitated with a specific anti-p18 antibody. The immunoprecipitates are finally solubilised in SDS-sample buffer, and the proteins are separated on a SDS-PAGE gel followed by autoradiography and quantification of the p18 signal (see figure 4.3.1 for illustration).

To test the effect of Syt IV on ISG fusion, I added an increasing amount of the purified recombinant Syt IV cytoplasmic domain into the complete fusion reaction mixture. This resulted in a dose-dependent inhibition of ISG homotypic fusion to a maximum of ~ 40% (Figure 4.3.2 circle). In contrast, the addition of the denatured Syt IV cytoplasmic domain into the complete reaction did not have any effect on the ISG-ISG fusion

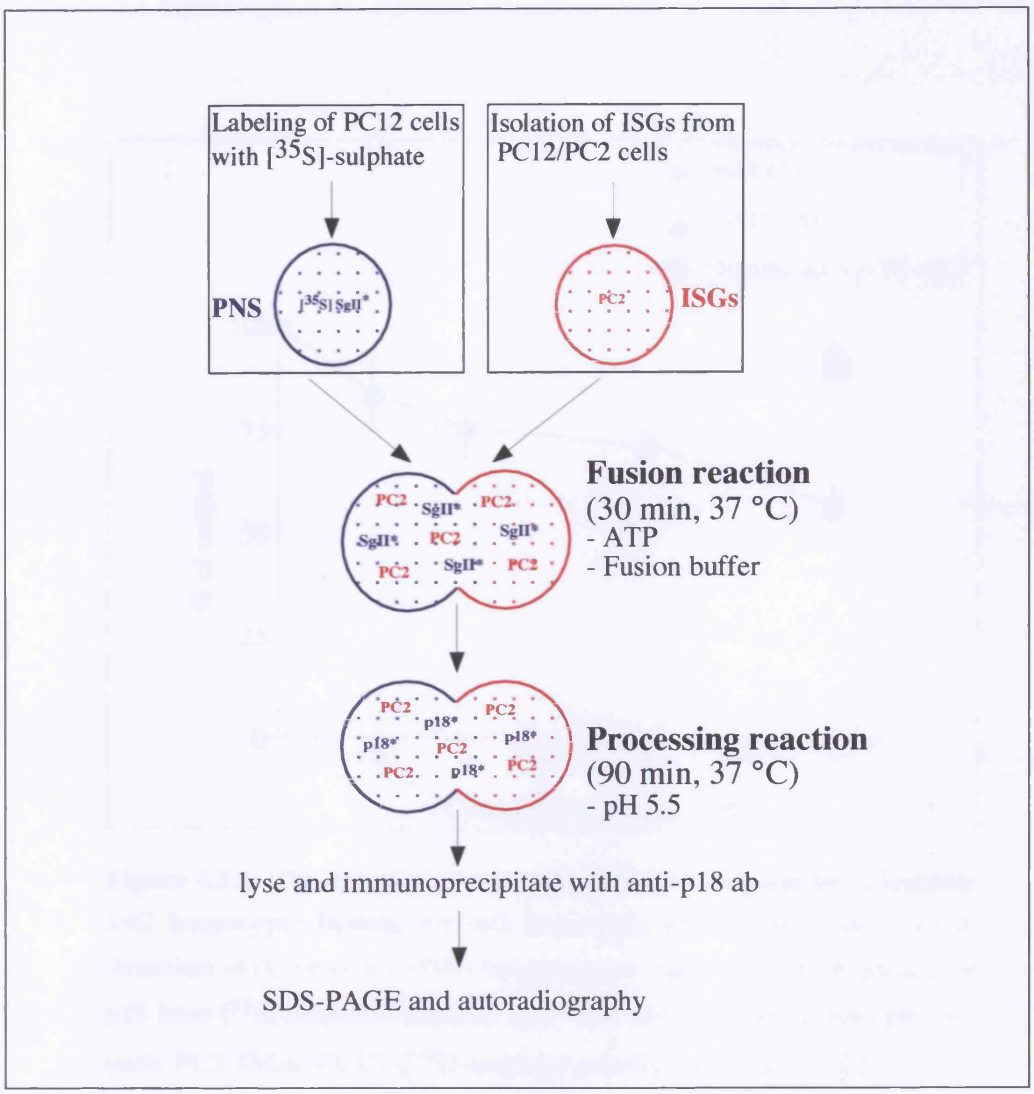

Figure 4.3.1: ISG-ISG *in vitro* assay scheme.

[^{35}S]-sulphate labelled PNS (containing the substrate, SgII) are mixed with Purified ISGs from PC12/PC2 cells (containing the enzyme PC2) in the presence of ATP, ATP regenerating system and fusion buffer. The complete reaction is incubated at 37 °C for 30 min for fusion to occur. The processing of SgII by PC2 into the 18 kDa degradation product, p18, is then done at 37 °C for 90 min at pH 5.5. The p18 is then immunoprecipitated using the specific anti-p18 ab. Immunoprecipitates are solubilised and subjected to SDS-PAGE gel analysis followed by autoradiography. Quantification of p18 signals is done using ImageJ analysis software.

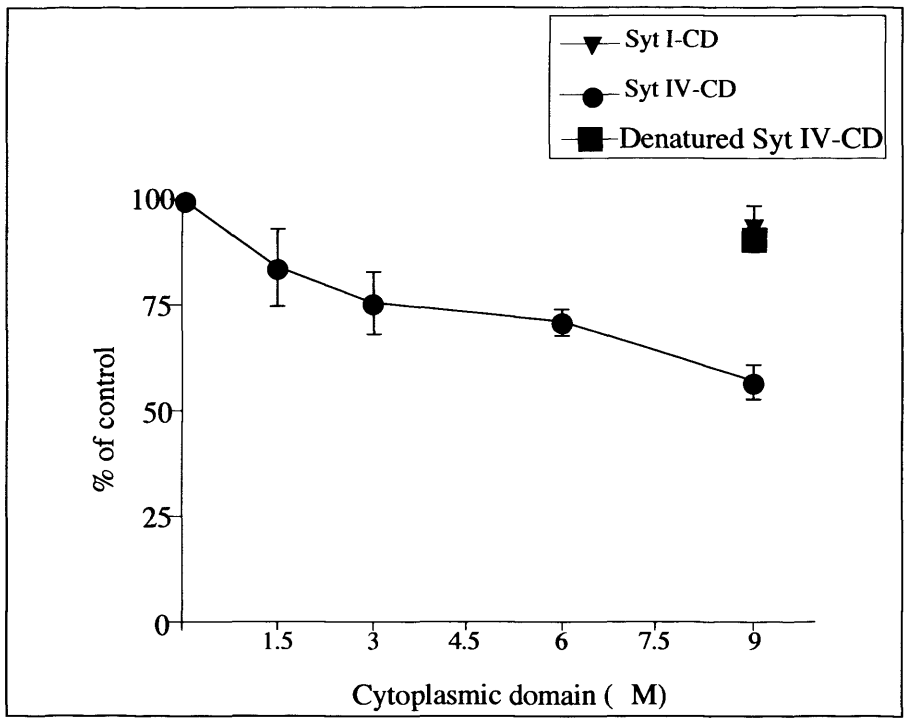

Figure 4.3.2: The cytoplasmic domain of Syt IV, but not Syt I inhibits ISG homotypic fusion. An ISG homotypic fusion was performed as described in (Urbe et al., 1998) and measures fusion by the production of p18 from [^{35}S]-sulphate- labelled SgII. The complete fusion reaction contains PC2 ISGs, PC12 [^{35}S]-sulphate-labelled PNS and ATP. Syt IV (circle), denatured Syt IV (square) or Syt I (triangle) cytoplasmic domains were added at the indicated concentrations on ice, and fusion assay was performed. After subtraction of the background from PC2-ISG minus reactions, the fusion was assayed by quantifying the amount of p18 produced using ImageJ software and is presented as a percent of the complete fusion reaction (n=3 experiments in duplicates, error is SEM). The addition of more Syt IV cytoplasmic domain did not increase the inhibition further than 50% (data not shown).

(Figure 4.3.2 square). In PC12 cells, Syt I, IV and IX are the most abundant Syt isoforms, while Syt IV is expressed at lower levels compared to Syt I and IX (Zhang et al., 2002). I asked whether ISG homotypic fusion could be regulated by another Syt isoform. The addition of the purified Syt I cytoplasmic domain, previously shown to inhibit exocytosis (Earles et al., 2001), into the complete fusion reaction, had no effect on ISG-ISG fusion (Figure 4.3.2 triangle). This suggests that the inhibition of ISG homotypic fusion is specific to the Syt IV cytoplasmic domain, and does not involve Syt I.

In conclusion, the ISG-localised Syt IV is a component important for ISG homotypic fusion.

4.4 The Syt IV cytoplasmic domain and anti-Stx6 ab have an additive inhibitory effect on ISG homotypic fusion

Previous data showed that the ISG-localised SNARE protein Stx6 is also involved in ISG homotypic fusion (Wendler et al., 2001). This effect was shown by the addition of anti-Stx6 ab to the *in vitro* fusion assay, resulting in the inhibition of ISG homotypic fusion.

Because both Syt IV and Stx6 are involved in the regulation of ISG fusion, I asked what effect the combined inhibitory reagents would have. The addition of Syt IV cytoplasmic domain or anti-Stx6 ab separately into the fusion reaction resulted in inhibition of ISG-ISG fusion to a maximum of ~ 40% (Figure 4.4.1 A), confirming the previous data that both proteins are involved in ISG homotypic fusion. Surprisingly, the addition of Syt IV cytoplasmic domain together with anti-Stx6 ab into the fusion assay resulted in an

additive inhibitory effect on ISG homotypic fusion (Figure 4.4.1 A). To ensure that this effect is specific, the Syt IV cytoplasmic domain was combined with the anti-Stx1 ab, shown previously to have no effect on ISG fusion (Wendler et al., 2001), and the anti-Stx6 ab was combined with Syt I cytoplasmic domain, which did also not have an inhibitory effect on ISG homotypic fusion. The combined reagents were added in the complete fusion reaction (Figure 4.4.1B). In contrast to the combination of anti-Stx 6 ab with Syt IV cytoplasmic domain, anti-Stx1 ab with Syt IV cytoplasmic domain or anti-Stx6 ab with Syt I cytoplasmic domain combinations did not increase the inhibition of ISG-ISG fusion (Figure 4.4.1 B). This demonstrates that the additive inhibitory effect is specific to the combination of Syt IV and Stx 6.

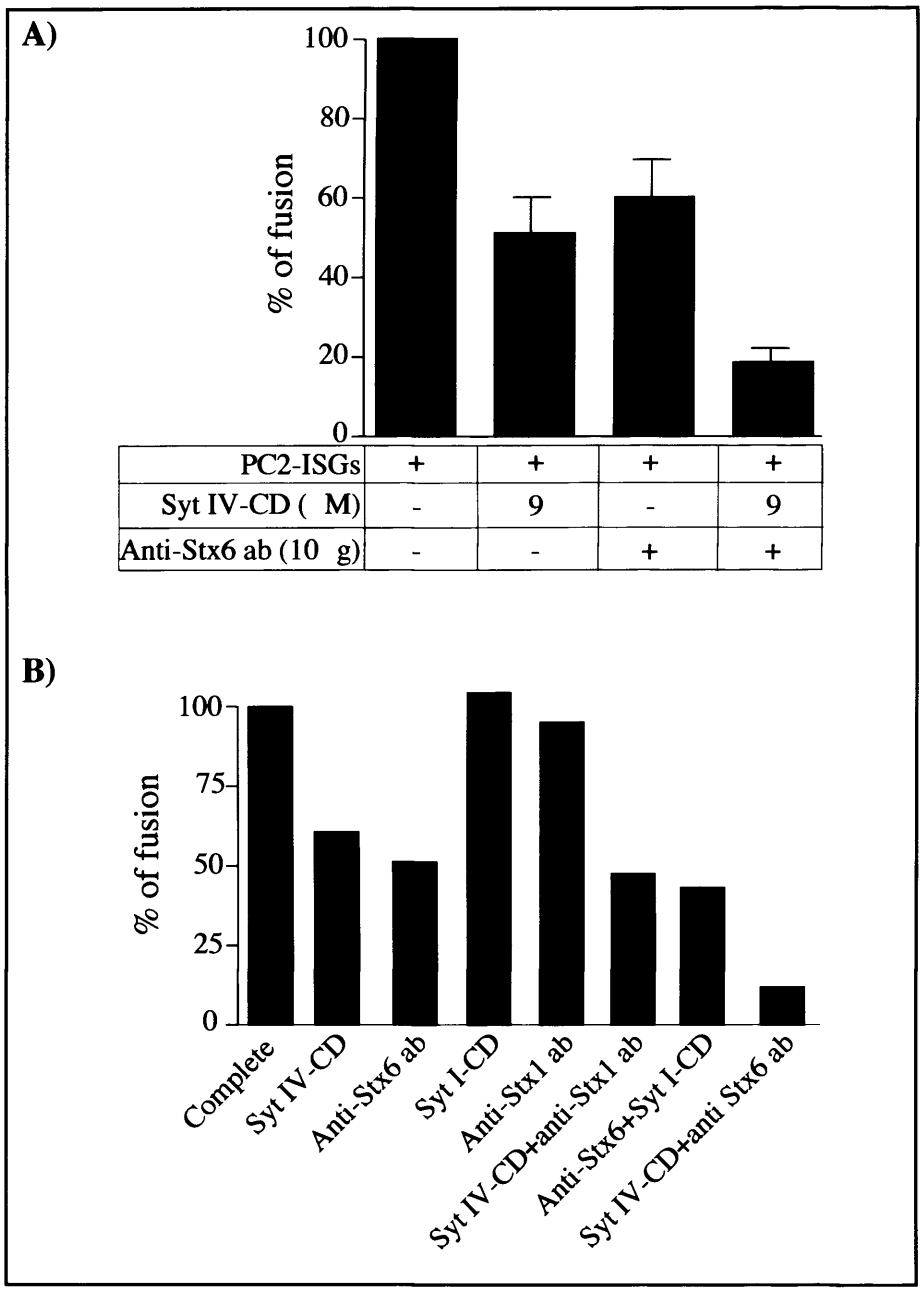

Figure 4.4.1: Syt IV cytoplasmic domain and anti-Stx6 antibody have an additive inhibitory effect on ISG-ISG fusion.

A) A complete fusion reaction was incubated with 9 M Syt IV-CD, 10 g anti-Stx6 ab, or Syt IV-CD combined with anti-Stx6 ab (n=3 in duplicates, error is SEM). B) As control, complete fusion reaction was incubated with 9 M Syt IV-CD, 10 g anti-Stx6 ab, 9 M Syt I-CD, 10 g anti-Stx1 ab, 9 M Syt IV-CD combined with 10 g anti-Stx1 or anti-Stx6 ab and 10 g anti-Stx 6 combined with 9 M Syt I-CD. A and B) Fusion reactions were performed at 37 °C for 30 min followed by substrate processing for 90 min as described in Chapter 2. p18 was immunoprecipitated and the signal quantified using ImageJ analysis software. The background signal measured in the absence of PC2 signal was subtracted.

4.5 BAPTA inhibits ISG homotypic fusion

Many membrane fusion events, such as yeast homotypic vacuole fusion (Peters and Mayer, 1998), early endosome-early endosome fusion (Mills et al., 1999), and fusion of granules with the plasma membrane (Heinemann et al., 1994), are known to be calcium-dependent.

Syt family of proteins are characterised by the presence of the C2A and C2B domains in their cytoplasmic tail. Some, but not all Syts, are able to bind calcium ions. For example, Syt I binds a total of five calcium ions via its C2 domain, and functions as the calcium sensor for exocytosis. It is established that Syt IV is not able to bind calcium via its C2A domain due to an amino acid substitution in one of the calcium-binding sites (von Poser et al., 1997). However, it was assumed that rat Syt IV could bind calcium via its C2B domain because it retains all the calcium binding sites found in Syt I (Wang et al., 2003a). A recent crystal structure of rat Syt IV revealed that changes in the orientation of the calcium ligands within the C2B region render this domain unable to form full calcium-binding sites (Dai et al., 2004), making Syt IV a non-calcium binding isoform.

The finding that Syt IV is involved in ISG homotypic fusion, and the recent data showing that rat Syt IV does not bind calcium raised the question of whether this fusion event is dependent on calcium. To investigate whether or not ISG-ISG fusion is dependent on calcium, an increasing amount of BAPTA was added to the complete fusion reaction. This resulted in a dose-dependent inhibition of ISG homotypic fusion of up to ~ 90% (Figure 4.5.1 A). Addition of BAPTA after the fusion reaction had no effect on ISG-ISG fusion. Preliminary results showed that the addition of the same

concentrations of EGTA into the fusion assay did not have an inhibitory effect on ISG fusion (Figure 4.5.1 B). A slight stimulation of ISG-ISG fusion is observed upon addition of EGTA. However, this stimulation was not significantly higher with increasing concentrations of EGTA compared to that of control (no EGTA). Although this result needs to be verified, I think that this effect is not significant.

Yeast vacuole fusion and early endosome homotypic fusion events were also found to be inhibited by BAPTA and not EGTA (Peters and Mayer, 1998) (Mills et al., 1999). This is presumably due to the fact that calcium is released at the final step of fusion (Peters and Mayer, 1998). Therefore a fast calcium-chelator, such as BAPTA, is required to abolish the calcium effect. It was not possible to determine whether the calcium involved in ISG homotypic fusion is released from the lumen of ISGs, as is the case for yeast vacuole fusion (Peters and Mayer, 1998), since in our *in vitro* fusion assay the substrate donor compartment is obtained from a postnuclear supernatant.

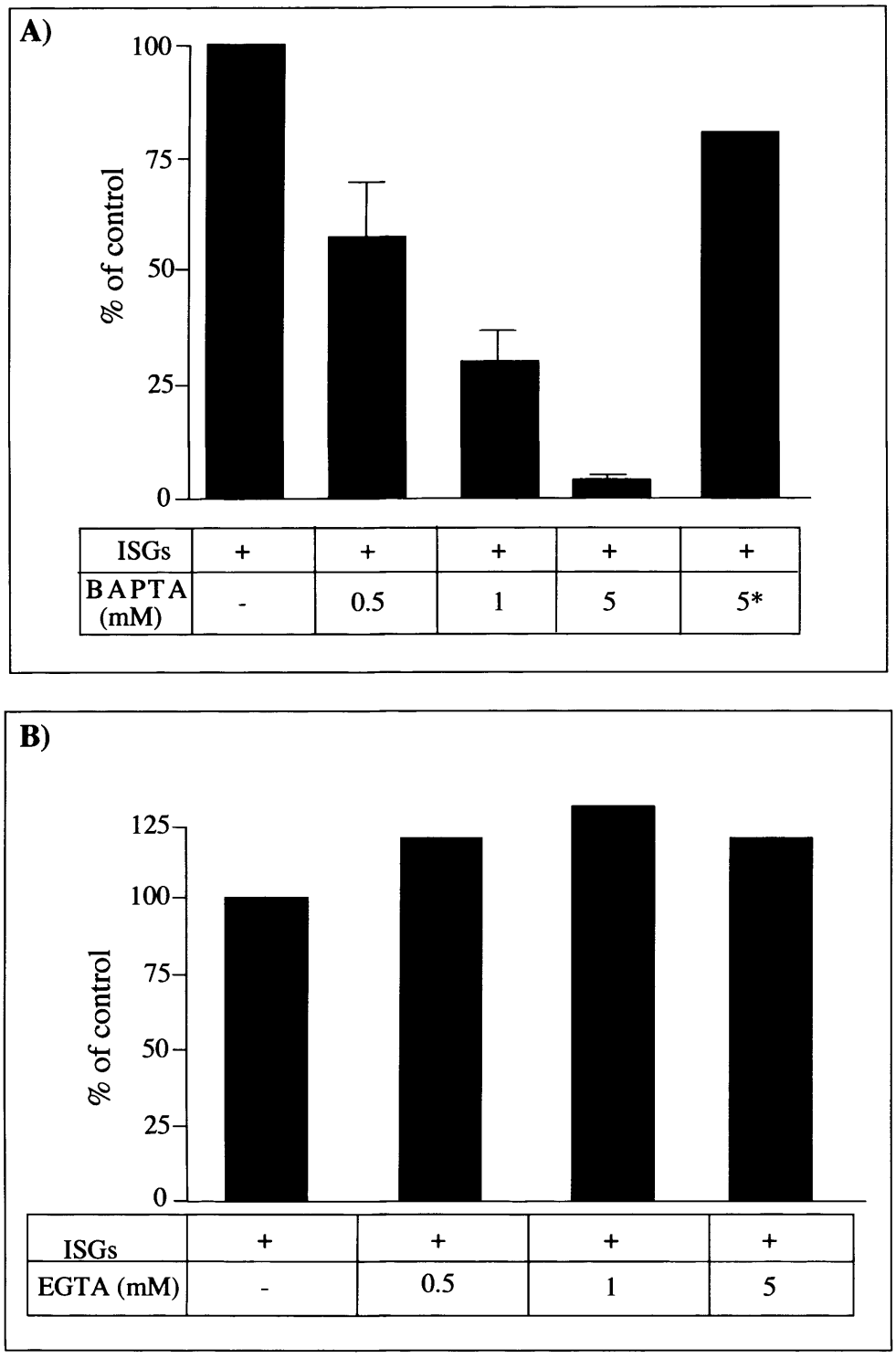

Figure 4.5.1: BAPTA, but not EGTA inhibits ISG homotypic fusion.

A) Complete fusion reactions containing [^{35}S]-sulphate-labelled PNS from PC12 cells, PC2-ISGs, ATP and fusion buffer, were pre-incubated with or without increasing amounts of BAPTA or 5mM BAPTA* added after the fusion incubation, (n=3 in duplicates, error is SEM). B) Complete fusion reactions were pre-incubated with increasing amounts of EGTA. The fusion assay and the quantification of p18 signal was carried as described in Chapter 2.

4.6 Discussion

Syt IV is involved in ISG-ISG fusion

I have confirmed that endogenous Syt IV is localised on ISGs and not MSGs in PC12 cells (Chapter 3). This protein was of particular interest because of its similar localisation to Stx6 and VAMP4, two SNARE proteins involved in ISG maturation (Wendler et al., 2001) (Hinners et al., 2003). Moreover, Syts represent a large family of proteins with a role as regulators of membrane fusion (Bai and Chapman, 2004).

In this study, I used the *in vitro* ISG-ISG fusion assay to test the hypothesis of whether Syt IV is involved in ISG-ISG fusion. I showed that the addition of increasing amounts of purified recombinant Syt IV cytoplasmic domain into the complete fusion assay inhibited ISG homotypic fusion in a dose-dependent manner. These findings revealed a novel role for the endogenous Syt IV in the regulation of granule maturation in PC12 cells.

Most studies looking at the function of Syt IV were conducted with the overexpressed protein, where it is sorted to MSGs (Wang et al., 2003a). The overexpressed Syt IV is involved in exocytosis and, in particular, kiss-and-run fusion (Wang et al., 2003a). It is unlikely that endogenous Syt IV participates in kiss-and-run fusion events of ISGs because upon fusion ISGs increase in size, suggesting that they undergo full fusion (Tooze et al., 1991).

The removal of endogenous Syt IV during granule maturation (Eaton et al., 2000) (Fukuda et al., 2003) suggests that it is not involved in exocytosis, in contrast to the overexpressed protein. In confirmation, several studies have investigated whether the

endogenous Syt IV is involved in vesicle fusion with the plasma membrane. Firstly, in an N-terminal antibody-uptake experiment, abs against the luminal domain of Syt IV were added to the extracellular medium of K^+-depolarised PC12 cells. If the MSGs undergoing exocytosis contain Syt IV, the N-terminus of Syt IV would be accessible on the outer surface of the cell membrane, and therefore it should be recognised by anti-Syt IV ab in the culture medium. In these conditions, there was no uptake of the N-terminal anti-Syt IV abs by the wild type PC12 cells, suggesting that endogenous Syt IV is not present on MSGs undergoing exocytosis (Fukuda et al., 2003). A second study showed that catecholamine release from "cracked" PC12 cells was not affected by the addition of recombinant Syt IV cytoplasmic domain, whereas an inhibition of release was observed when recombinant Syt I was added (Tucker et al., 2003). Together, these studies demonstrate that endogenous Syt IV is not a regulator of exocytosis in neuroendocrine cells.

In PC12 cells, Syt I, IX and IV are the most highly expressed Syt isoforms (Zhang et al., 2002). Syt I and IX are both found on MSGs and are involved in exocytosis (Fukuda et al., 2002) (Tucker et al., 2003). Because it was found that the addition of recombinant cytoplasmic domains of both Syt I and Syt IX inhibits secretion from PC12 cells, possibly through hetero-oligomerisation of both isoforms (Tucker et al., 2003), I tested whether an isoform other than Syt IV was involved in ISG homotypic fusion.

Consequently, I added the purified recombinant Syt I cytoplasmic domain into the *in vitro* fusion assay. In contrast to Syt IV, Syt I cytoplasmic domain did not inhibit ISG homotypic fusion, suggesting that Syt I is not involved in this membrane fusion event. It was suggested previously that endogenous Syt I and IV have different functions in PC12 cells. First, Syt IV and I display different distributions (Ibata et al., 2000), and

second, the two isoforms do not have the ability to hetero-oligomerise (Fukuda and Mikoshiba, 2000a) (Osborne et al., 1999).

It is also unlikely that Syt IX is involved in ISG homotypic fusion. Syt IX also displays a different distribution than Syt IV (Fukuda, 2004), and both isoforms do not oligomerise (Fukuda and Mikoshiba, 2000a). Moreover, Syt IX, like Syt I, regulates exocytosis from PC12 cells (Tucker et al., 2003). Although it needs to be verified, I think a role of Syt IX in ISG homotypic fusion is unlikely because these data suggest that Syt IX possesses a more similar role to Syt I, which does not inhibit ISG-ISG fusion.

Syt IV cytoplasmic domain and Stx6 ab have an additive inhibitory effect on ISG homotypic fusion.

Both Stx6 and Syt IV are involved in ISG homotypic fusion. In an attempt to increase our understanding of how these two proteins regulate this membrane fusion event, I asked what effect the addition of inhibitory reagents for both proteins would affect ISG homotypic fusion.

The combined addition of the anti-Stx6 ab and Syt IV cytoplasmic domain resulted in an unexpected additive inhibitory effect on ISG-ISG fusion. This result suggested that the binding on ISGs, as well as the function of an individual reagent, was not affected by their combined addition. Indeed, I verified and confirmed that the binding of both Syt IV cytoplasmic domain and anti-Stx6 ab on ISG membranes was not affected by the addition of the other reagent (Chapter 5, Figure 5.4.2).

The additive effect on ISG homotypic fusion obtained by the combination of anti-Stx6 ab and Syt IV cytoplamsic domain is difficult to interpret. One reason is that we do not

have a substantial understanding of how ISG homotypic fusion occurs. In addition, we do not know how these inhibitory reagents act on their effectors.

However, I speculate that there are two possible explanations:

First, the additive inhibitory effect is due to the fact that Stx6 and Syt IV act in parallel pathways, meaning that there are some vesicles that lack Stx6 and/or Syt IV. This scenario requires that ISGs be of a heterogeneous nature. I think that this is unlikely, because we have no indication that ISGs have different SNAREs or Syt components. In fact, immunoisolation experiments using the anti-Stx6 ab showed that close to 100% of the ISG-localised SgII was recovered (Wendler et al., 2001), suggesting that all ISGs have Stx6.

Second, and the likeliest explanation, is that the additive effect could be attributable to the Syt IV cytoplasmic domain and anti-Stx6 ab inhibiting different stages during ISG homotypic fusion. Because when isolated ISGs at different stages of fusion (Urbe et al., 1998), it is therefore possible that ISGs are susceptible to specific inhibition by either anti-Stx6 ab or by the Syt IV cytoplasmic domain.

In conclusion, although the experiments presented in Figure 4.4.1 confirmed that both Syt IV and Stx6 are indeed needed for ISG homotypic fusion, they did not reveal at which specific stage of fusion Syt IV and Stx6 are involved.

It will be interesting to understand how these two reagents inhibit ISG fusion. An important question to answer is at what stage of fusion, whether tethering, docking or fusion, do Syt IV and Stx6 act. Adding individual reagents during the time course of fusion, and observing whether the susceptibility to the inhibitory reagent is lost at the beginning or end of fusion, will help answer this question.

Calcium is required for ISG-ISG fusion

It is established that calcium is required for many membrane fusion events. For example, exocytosis, yeast vacuole-vacuole fusion, early endosome homotypic fusion, and endosome-lysosome fusion were all shown to depend on the presence of calcium (Burgoyne and Clague, 2003). In addition, calcium is required at the last step of membrane fusion, and subsequent to SNARE assembly, as was shown for yeast vacuole homotypic fusion (Peters and Mayer, 1998).

Some proteins, such as Syts, which possess the ability to sense calcium and to bind to the fusion machinery, were shown to be involved in membrane fusion. Indeed, Syt I is able to bind calcium through its C2 domain. In the presence of calcium, Syt I displays high-affinity interactions with phospholipids as well as with the SNARE machinery involved in exocytosis (Bai and Chapman, 2004).

Syt IV differs from Syt I in that it is not able to bind calcium (Dai et al., 2004). This led to the question of whether calcium sensing is accomplished by another protein, or whether ISG fusion is calcium independent and possibly requires a non-calcium binding Syt isoform. The addition of BAPTA to the in *vitro fusion* assay inhibited ISG-ISG fusion, demonstrating that ISG homotypic fusion is in fact calcium-dependent. This suggested that a calcium-binding protein, as yet to be identified, is required for ISG fusion. Two hypotheses emanate from these observations:

The first hypothesis is that a second Syt isoform, which localises on ISGs, could play a role in sensing calcium during ISG membrane fusion. This role could be either dependent or independent of Syt IV function in ISG homotypic fusion. Indeed, the putative calcium sensing Syt isoform will act at a different stage of fusion than that Syt

IV. In support of this, studies on Syt I showed that it is involved in multiple stages of fusion, docking (Chieregatti et al., 2002), fusion pore opening (Wang et al., 2001) and membrane recycling (Nicholson-Tomishima and Ryan, 2004). It would then be likely that Syt IV acts at a stage prior to the one involving the calcium sensing Syt isoform.

However, the putative calcium sensor protein activity could be dependent on hetero-oligomer formation with Syt IV. Indeed, many Syts were shown to form hetero-oligomers *in vitro* in a calcium-dependent manner (Fukuda and Mikoshiba, 2000a) (Osborne et al., 1999). The hetero-oligomerisation of different isoforms with different calcium affinities is thought to modulate calcium sensitivity of membrane fusion.

In both cases, this isoform has to be identified and the hypothesis verified. Because I did not find an involvement of Syt I in ISG homotypic fusion, it is unlikely that it is the calcium sensor involved in this fusion event. At present there are no other identified Syt isoform that display the same localisation as Syt IV in PC12 cells, i.e. present on ISGs and not MSGs. Moreover, Syt IV did not show any calcium-dependent hetero-oligomerisation activity *in vitro* with Syt I (Fukuda and Mikoshiba, 2000a).

The identification of other Syt isoforms which bind calcium, and display an ISG localisation, and testing their effect on ISG fusion, will be a first step towards addressing this hypothesis.

The second hypothesis is that another calcium-binding protein, such as calmodulin, could be involved in ISG homotypic fusion. Calmodulin is an EF-hand calcium-binding protein, and was identified as a calcium sensor for many membrane fusion events. Indeed, in yeast, calmodulin antagonists such as W7, as well as anti-calmodulin abs, inhibit vacuole homotypic fusion (Peters and Mayer, 1998). Moreover, the requirement for calcium/calmodulin was found to be downstream of the completed docking reaction, suggesting they act at the final step of fusion (Peters and Mayer, 1998). Calmodulin was

suggested to act in the final stage of vacuole fusion by interacting with the V0 sector of the V-ATPase, which through an association on opposite membranes forms the fusion pore (Bayer et al., 2003).

Other intracellular membrane fusion events, such as early endosome homotypic fusion, are regulated by calmodulin in a calcium-dependent manner (Colombo et al., 1997). Interestingly, calmodulin was found to interact with Stx13 and EEA1, two proteins shown to be involved in early endosome homotypic fusion (Mills et al., 2001). This data suggested that EEA1 and Stx13 could serve to localise calmodulin to the site of fusion. To address this second hypothesis, addition of calmodulin antagonists into the *in vitro* assay might reveal whether calmodulin is involved in the regulation of ISG homotypic fusion.

In conclusion, I showed in this chapter that the ISG-localised Syt IV is involved in ISG homotypic fusion. This fusion event was specific to Syt IV, as the MSG-localised Syt I, shown to be involved in exocytosis, had no effect. The calcium-dependence of ISG-ISG fusion, and the fact that Syt IV does not bind calcium, raises the possibility that another protein, possibly another calcium sensor as yet to be discovered, could be involved in regulating the calcium-dependence step of ISG homotypic fusion.

5 Chapter 5: Syt IV cytoplasmic domain is recruited to ISG membranes and binds to the SNARE protein Stx6

5.1 Aim

The findings I presented in chapter 4 showed that Syt IV cytoplasmic domain inhibited ISG-ISG fusion, suggesting that this isoform is an important component in the regulation of granule maturation. Because the cytoplasmic domain of Syt IV was able to inhibit ISG homotypic fusion, I asked whether the target of this domain resides on these membranes, and specifically if its recruitment was via protein components on ISG membranes. Syts, via their C2 domains, can bind SNARE proteins, and this binding is thought to be an important requirement in the regulation of membrane fusion events (Bai and Chapman, 2004). I therefore tested whether Syt IV interacts with the SNARE protein, Stx6, which resides on ISG membranes and, like Syt IV, is involved in the regulation of ISG homotypic fusion.

5.2 Synaptotagmin IV cytoplasmic domain is recruited to ISG membranes

In an attempt to answer the question of whether the Syt IV cytoplasmic domain is recruited to ISG membranes, I used an *in vitro* ISG binding assay, which reconstitutes

binding of exogenous proteins to purified ISG membranes. This assay was previously used to demonstrate ARF-1 (Austin et al., 2000) and AP-1 binding to ISGs (Dittie et al., 1996).

Increasing amounts of the purified Syt IV cytoplasmic domain were incubated with a constant amount (50 µl) of purified PC12 ISGs in fusion buffer and ATP at 37 °C for 30 min. Membranes were subsequently collected by centrifugation and the bound Syt IV cytoplasmic domain was detected using anti-Syt IV ab (Figure 5.2.1A).

The Syt IV cytoplasmic domain was recruited to ISG membranes in a dose-dependent manner. This demonstrates that ISGs contain saturable binding sites for Syt IV, and further suggests that the inhibitory effect of the Syt IV cytoplasmic domain on ISG homotypic fusion is on these membranes. No recombinant protein was detected in the pellet in the absence of ISGs (Figure 5.2.1B), demonstrating that the binding is not a result of non-specific aggregation of the protein.

Having shown that Syt IV cytoplasmic domain is recruited to ISG membranes, I asked whether this recruitment is via protein or lipid components in the ISGs. Using liposome-binding assays, it was demonstrated that Syts such as Syt I and IX are able to bind phospholipids via their C2 domains in a calcium-dependent manner (Hui et al., 2005). In contrast, there are several reports that Syt IV does not bind phospholipids (Bai et al., 2002) (Dai et al., 2004) (Hui et al., 2005), except one study, which showed that Syt IV was in fact able to bind liposomes containing only negatively-charged phospholipids

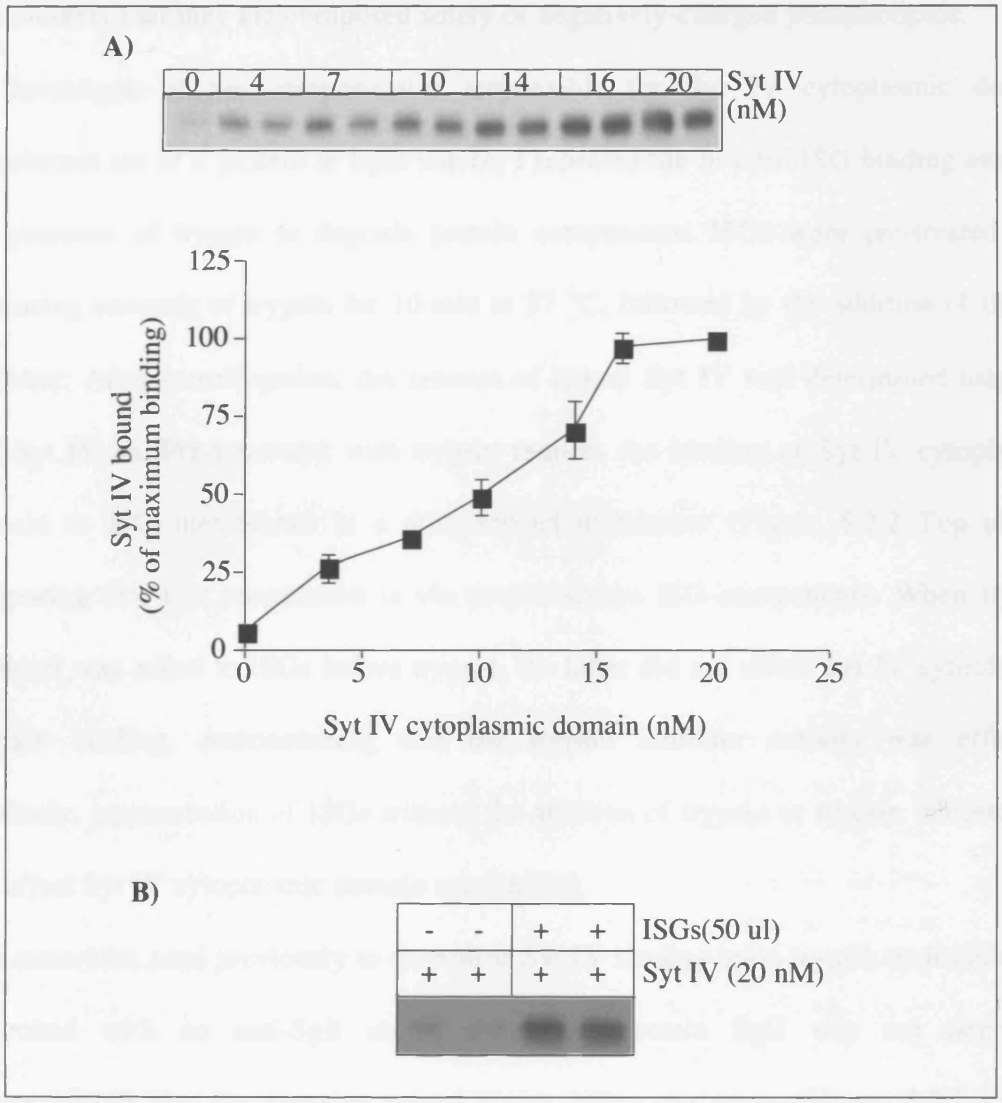

Figure 5.2.1: The cytoplasmic domain of Syt IV is recruited to ISG membranes. A) Increasing amounts of Syt IV cytoplasmic domain were incubated with purified PC12-ISGs (50 µl) in fusion buffer and ATP for 30 min at 37°C followed by centrifugation to pellet the membranes. The amount of Syt IV bound to ISG membranes was determined by immunoblotting with anti-Syt IV ab and quantified using ImageJ software (n=3 in duplicates, error is SEM). B) 20 nM of Syt IV cytoplasmic domain were incubated without or with PC12-ISGs (50 µl) as described above and bound Syt IV was detected with anti-Syt IV ab.

(Fukuda et al., 1996). Although the lipid composition of ISG membranes is not known, it is unlikely that they are composed solely of negatively-charged phospholipids.

To investigate if the component(s) responsible for Syt IV cytoplasmic domain recruitment are of a protein or lipid nature, I repeated the *in vitro* ISG binding assay in the presence of trypsin to degrade protein components. ISGs were pre-treated with increasing amounts of trypsin for 10 min at 37 °C, followed by the addition of trypsin inhibitor. After centrifugation, the amount of bound Syt IV was determined using an anti-Syt IV ab. Pre-treatment with trypsin reduces the binding of Syt IV cytoplasmic domain to ISG membranes in a dose-dependent manner (Figure 5.2.2 Top panel), suggesting that this recruitment is via proteinaceous ISG-components. When trypsin inhibitor was added to ISGs before trypsin, the latter did not affect Syt IV cytoplasmic domain binding, demonstrating that the trypsin inhibitor activity was efficient. Similarly, preincubation of ISGs without the addition of trypsin or trypsin inhibitor did not affect Syt IV cytoplasmic domain recruitment.

The same blot, used previously to determine Syt IV binding upon trypsin treatment, was re-probed with an anti-SgII ab. The luminal protein SgII was not degraded, demonstrating that the granules stayed intact during the assay (Figure 5.2.2 bottom panel). While it cannot be excluded that phospholipases could be activated by trypsin, which could alter the lipid composition of membranes, these results are in agreement with several reports demonstrating that Syt IV is unable to bind phospholipids (Dai et al., 2004) (Hui et al., 2005).

In conclusion, these data suggest that protein components on ISG membranes are necessary for the recruitment of the Syt IV cytoplasmic domain.

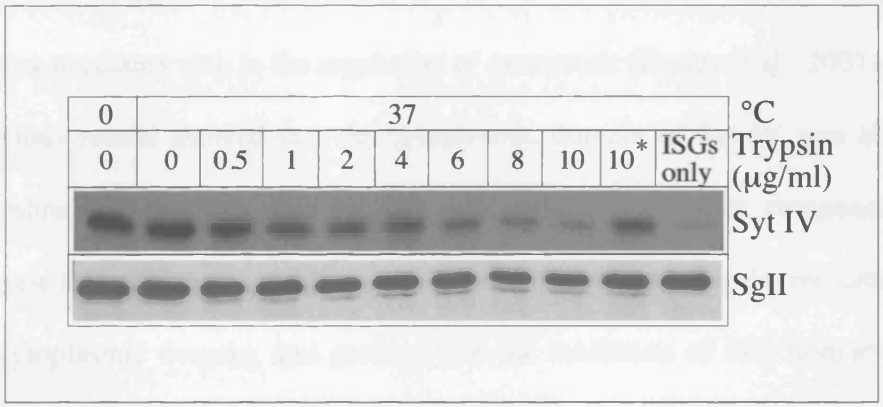

Figure 5.2.2: The Syt IV cytoplasmic domain recruitment to ISG membranes is sensitive to trypsin-treatment. ISGs (50μl) were pre-incubated with increasing amounts of trypsin for 10 min at 37 °C. Trypsin inhibitor (STI) was added before (*) or after the pre-incubation. Binding reactions including 10 nM Syt IV cytoplasmic domain were performed as described previously. Syt IV bound to ISGs was detected with anti-Syt IV ab. The same blot was stripped and reprobed with anti-SgII ab, SgII is not degraded, suggesting that the vesicles were intact during the assay (bottom panel).

5.3 Synaptotagmin IV interacts with The SNARE protein, Syntaxin 6

It is now established that Syts are part of the machinery that regulate membrane fusion events (Tucker and Chapman, 2002). Syt I, for example, was found to bind the t-SNAREs Stx1 (Chapman et al., 1995) and SNAP-25 (Schiavo et al., 1997), and this binding is a necessary step in the regulation of exocytosis (Earles et al., 2001).

The previous results showed that the cytoplasmic domain of Syt IV was able to bind ISG membranes. Moreover, this binding was mainly via protein components. These data suggest that protein(s) on ISG membranes are responsible for the recruitment of the Syt IV cytoplasmic domain, and perhaps that the inhibition of ISG homotypic fusion observed after the addition of this domain is accomplished via this interaction.

Because Stx6 is the only ISG SNARE protein found so far to regulate ISG-ISG fusion (Wendler et al., 2001), I hypothesised that Syt IV may be part of a complex that includes Stx6. I therefore looked for interaction between Stx6 and Syt IV.

To address this question, I first performed a GST pull-down assay with GST-Syt IV cytoplasmic domain. This was obtained with the same purification method used for the cleaved Syt IV cytoplasmic domain, as described in Chapter 4 (data not shown). This method eliminates the possibility that bacterial contaminants might interfere with the binding properties of Syt IV, which was a problem for recombinant Syt I (Ubach et al., 2001). Purified GST-Syt IV cytoplasmic domain as well as GST bound to glutathione-sepharose beads were incubated with Triton –X 100-extracted lysates from HEK cells over-expressing myc-full length Stx6. The bound proteins were subjected to SDS-PAGE, followed by immunoblotting with anti-myc ab. GST-Syt IV interacted with

myc-stx6 in a dose-dependent manner (Figure 5.3.1). No binding of myc-Stx6 to GST alone was detected, indicating that the Syt IV-Stx6 interaction is specific.

Next, to reinforce the GST-pull down data, I tested whether Syt IV interacted with Stx6 using co-immunoprecipitation. HA-Syt IV cytoplasmic domain and myc-Stx6 were co-transfected into HEK cells. Cells were then lysed in Triton X-100-containing buffer, and lysates subjected to immunoprecipitation with either anti-HA or anti-myc ab bound to protein G beads, or beads alone. Myc-Stx6 was immunoprecipitated with anti-HA ab (Figure 5.3.2 A), as was HA-Syt IV cytoplasmic domain when using anti-myc ab for immunoprecipitation (Figure 5.3.2 B). No proteins were immunoprecipitated with beads alone, suggesting that Syt IV interaction with Stx6 is specific. The unavailability of a suitable anti-Syt IV ab for immunoprecipitation did not allow me look for interactions with the endogenous proteins.

These data demonstrate that Syt IV and Stx6 interact, and further imply that both proteins are part of the same protein complex.

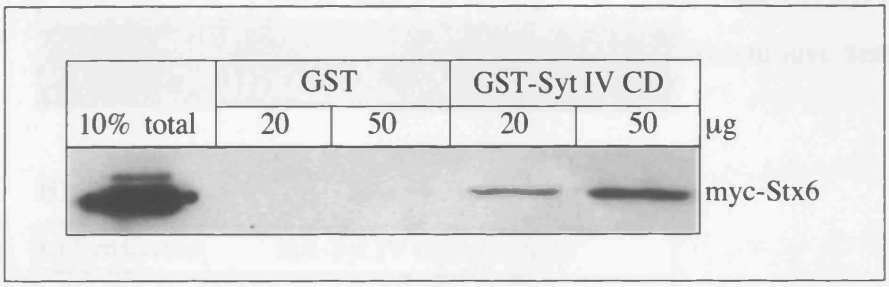

Figure 5.3.1: Syt IV interacts with Stx6 in GST pulldown assays.
GST-Syt IV cytoplasmic domain, or GST alone were bound to glutathione beads then incubated with Triton X-100 lysates from HEK cells overexpressing myc-Stx6. Bound proteins as well as 10% of the total used for each sample were subjected to SDS-PAGE followed by western blotting with anti-myc ab.

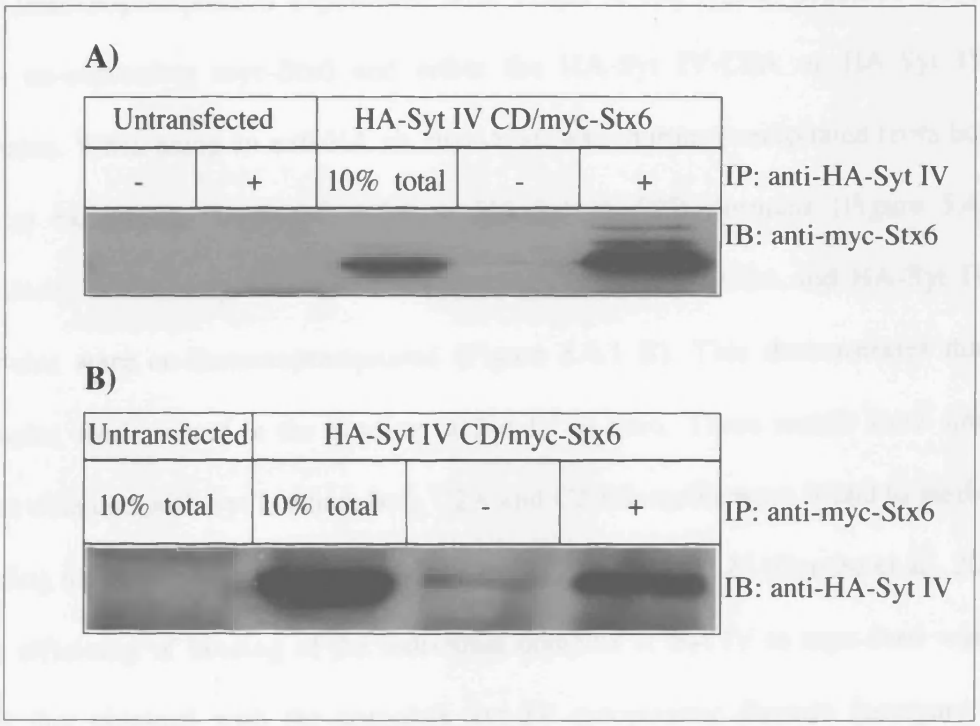

Figure 5.3.2: HA-Syt IV cytoplasmic domain interacts with myc-Stx6.
HEK cells were cotransfected with HA-Syt IV cytoplasmic domain and myc-Stx6. Triton X-100 lysates from A) untransfected and A,B) transfected cells were used for immunoprecipitation with anti- A) HA (+) or beads alone (-) and B) with anti-myc antibody (+) or beads alone (-). Immunoprecipitates as well as 10% of total input were subjected to SDS-PAGE and analysed with A) anti-myc or B) anti-HA antibodies.

5.4 Both Syt IV-C2A and C2B domains display binding to Stx6

To investigate which Syt IV domain is required for binding to Stx6, I performed a co-immunoprecipitation experiment with Triton X-100 lysates prepared from HEK cells co-expressing myc-Stx6 and either the HA-Syt IV-C2A or HA-Syt IV-C2B domains. When using an anti-HA ab, myc-Stx6 was immunoprecipitated from both cell lysates expressing HA-Syt IV-C2A or HA-Syt IV-C2B domains (Figure 5.4.1 A). Similarly, when using anti-myc antibody, both HA-Syt IV-C2A and HA-Syt IV-C2B domains were co-immunoprecipitated (Figure 5.4.1 B). This demonstrates that both domains are involved in the binding of Syt IV to Stx6. These results were similar to those obtained with Syt I, where both C2A and C2B domains were found to mediate the binding to the plasma membrane t-SNAREs Stx1 and SNAP-25 (Gerona et al., 2000).

The efficiency of binding of the individual domains of Syt IV to myc-Stx6 was lower than that obtained with the complete Syt IV cytoplasmic domain (compare Figure 5.3.2A and 5.4.1B). This observation suggests that the C2A and C2B domains of Syt IV can cooperate to mediate binding to Stx6, as is the case for Syt I binding to plasma membrane SNAREs (Earles et al., 2001) (Bai et al., 2004b).

Next, I attempted to look at which region of Stx6 binds Syt IV. Although Stx6 is classified as a Qc-SNARE, it harbours a great similarity to the Qa-SNAREs, such as Stx1, due to the presence of the Habc domain at the N-terminus of the protein (Bock et al., 2001) (Misura et al., 2002), lacking in the Qc SNAREs. Previous results in the lab have shown that, in contrast to the anti-Stx6 ab, the recombinant Stx6 cytoplasmic domain does not inhibit ISG homotypic fusion and is unable to bind SNARE proteins,

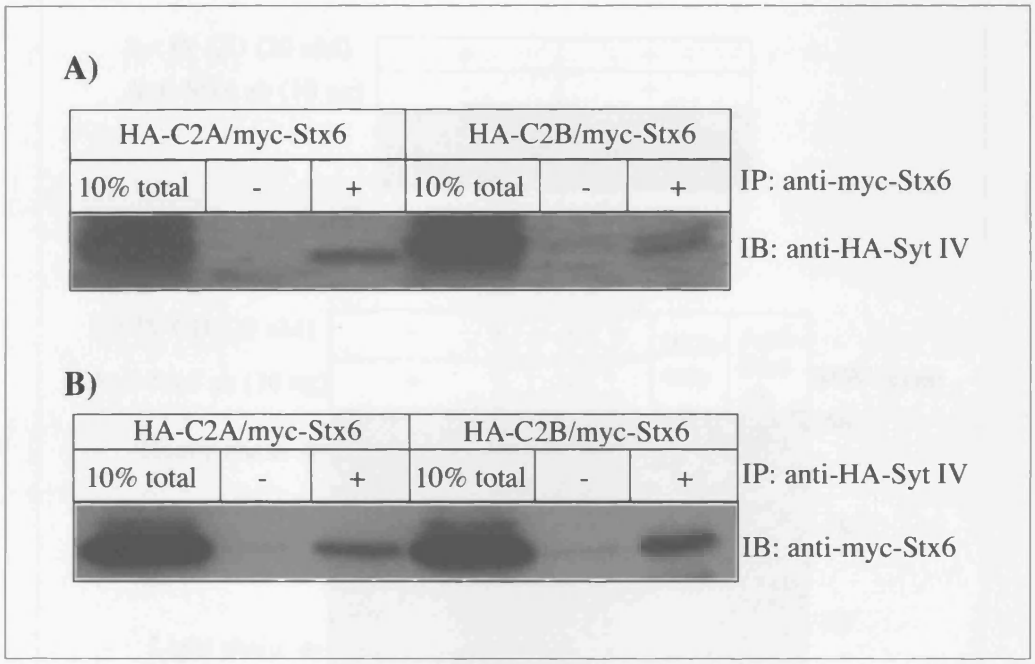

Figure 5.4.1: HA-Syt IV binds to myc-Stx6 via both C2A and C2B domains.
HEK cells were cotransfected with myc-Stx6 and HA-C2A domain or myc-Stx6 and HA-C2B domain. Triton X-100 lysates from HEK cells were subjected to immunoprecipitation with A) anti-myc (+) or beads alone (-) and B) anti-HA (+) or beads alone (-). 10% of the input for each sample and the immunoprecipitates were analysed with A) anti-HA and B) anti-myc abs.

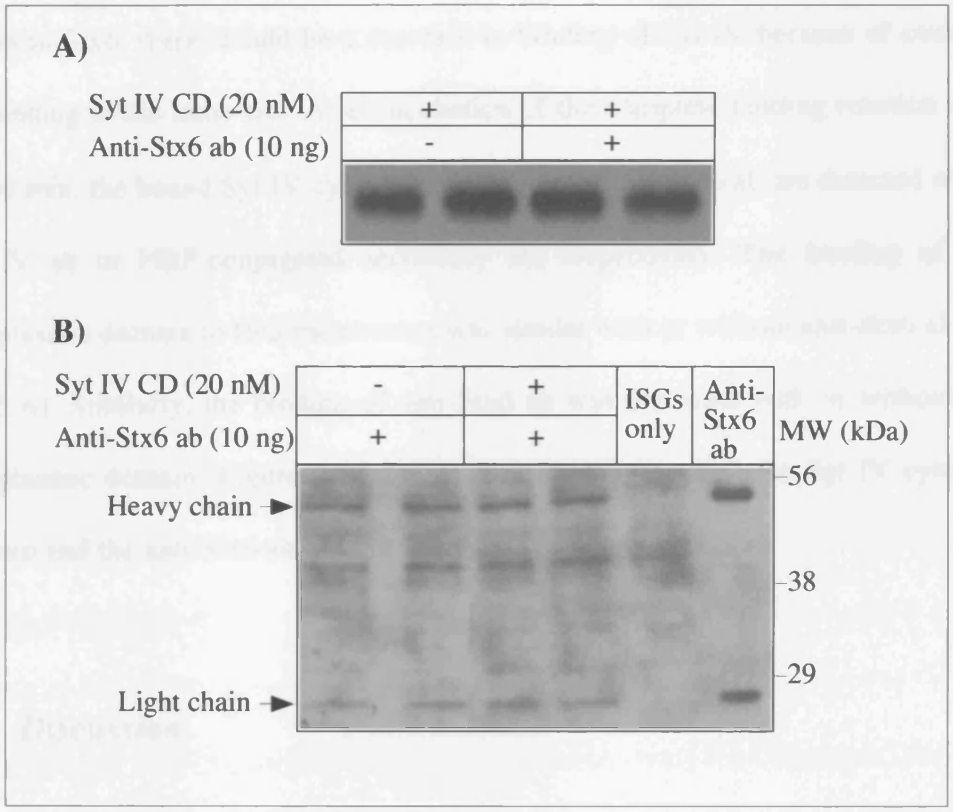

Figure 5.4.2: Syt IV cytoplasmic domain and anti-stx6 ab bind to a different region within Stx6. Complete *in vitro* ISG binding reactions containing 50 µl ISGs, ATP and A) 20 nM Syt IV cytoplasmic domain, with or without 10 ng anti-Stx6 ab or B) 10 ng anti-Stx6 ab with or without 20 nM Syt IV cytoplasmic domain were incubated for 30 min at 37 °C. Bound A) Syt IV cytoplasmic domain was detected using anti-Syt IV ab and B) anti-stx6 ab using anti-mouse secondary ab-HRP conjugated.

such as VAMP4, suggesting that the bacterially-expressed Stx6 cytoplasmic domain is inactive (Wendler et al., 2001) (Wendler F, unpublished observations). Therefore, I performed an *in vitro* ISG binding assay with both the anti-Stx6 ab, which binds to Stx6 Habc domain (Otto G and Wendler F, unpublished observation), and the Syt IV cytoplasmic domain. If Syt IV cytoplasmic domain and anti-Stx6 ab bind to the same region in Stx6, there should be a decrease in binding of Syt IV because of competition for binding to the same site. After incubation of the complete binding reaction at 37 °C for 30 min, the bound Syt IV cytoplasmic domain or anti-Stx6 ab are detected with anti-Syt IV ab or HRP-conjugated secondary ab, respectively. The binding of Syt IV cytoplasmic domain to ISG membranes was similar with or without anti-Stx6 ab (Figure 5.4.2 A). Similarly, the binding of anti-Stx6 ab was the same with or without Syt IV cytoplasmic domain (Figure 5.4.2 B). This result suggests that the Syt IV cytoplamsic domain and the anti-Stx6 ab bind to a different region within Stx6.

5.5 Discussion

Possible mode of inhibition of ISG homotypic fusion by the cytoplasmic domain of Syt IV.

The cytoplasmic domain of Syt IV was able to inhibit ISG-ISG fusion, and could be recruited to ISG membranes. This result suggests that the target of Syt IV cytoplasmic domain inhibition resides on these membranes. This binding is mediated strictly by protein components, as the recruitment of Syt IV cytoplasmic domain was reduced after the pre-treatment of ISG membranes with trypsin. This confirms reports

showing that Syt IV, in contrast to Syt I, is not a phospholipid-binding isoform (Dai et al., 2004).

The Syt family of proteins are components of the fusion machinery, and were found to bind to SNARE proteins. Syt I, for example, forms a complex with Stx1 and SNAP-25 (Chapman et al., 1995; Gerona et al., 2000). Although the mechanism of Syt function in regulating membrane fusion events is not fully understood, the ability of the cytoplasmic domain of Syts to inhibit secretion is clearly based on their ability to disrupt endogenous Syt-effector interactions that are critical for membrane fusion to occur (Bai and Chapman, 2004).

A scenario has been proposed by which the Syt I cytoplasmic domain could inhibit exocytosis through binding to the endogenous SNAP-25 and Stx1, therefore inhibiting the formation of the functional complex formed by endogenous Syt I-SNAP-25-Stx1. Indeed, mutations in SNAP-25 that affect interactions with Syt I reduce exocytosis (Zhang et al., 2002). In addition, selective disruption of the ability of Syt I to engage SNAP-25 and Stx1, by lengthening the linker that connects the C2A and C2B domains, inhibited exocytosis (Bai et al., 2004b). These studies suggest that the Syt-SNARE interaction is an essential step in regulating membrane fusion.

Based on these data, the finding that Syt IV interacts with the ISG-SNARE Stx6 could suggest that Syt IV is part of a protein complex which includes Stx6 that regulates ISG-ISG fusion. It is therefore conceivable that, in the same way observed for Syt I cytoplasmic domain, the exogenous Syt IV cytoplasmic domain might bind to an ISG SNARE(s), possibly Stx6, thereby inhibiting the formation of a functional endogenous Syt IV-ISG-SNARE complex, and leading to inhibition of ISG homotypic fusion.

Previous studies have shown that Syt IV is also able to bind Stx1 and SNAP-25, and that this binding is thought to regulate exocytosis, a function of the overexpressed Syt IV, which localises to MSGs (Wang et al., 2003a). It is therefore possible that Syt IV forms a complex with SNAP-25 and Stx1 on ISG membranes. SNAP-25 and Stx1 are not thought to function on ISGs, but rather that the presence of these two proteins on these membranes is a result of their transport to the plasma membrane. It is unlikely that the formation of a Syt IV-Stx1-SNAP-25 complex is functional in ISG homotypic fusion. Indeed, the addition of botulinum neurotoxin A and C, which cleave SNAP-25 and Stx1, as well as anti-SNAP 25 and anti-Stx1 abs into the *in vitro* reaction did not inhibit ISG-ISG fusion (Wendler et al., 2001), suggesting that the complex including SNAP-25 and Stx1 at least is not functional during ISG-ISG fusion (Wendler et al., 2001).

At present, we do not know the nature of the full ISG-SNARE complex involved in homotypic fusion. Stx6 has been found in two different SNARE complexes, one containing SNAP-25, SNAP-29 and VAMP4 (Wendler et al., 2001) and another containing Stx16, Vti1a and VAMP4 (Kreykenbohm et al., 2002) (Mallard et al., 2002). Also, an involvement of these other SNAREs in ISG homotypic fusion has not been determined. It will be interesting to investigate whether Syt IV interacts with any of these proteins.

The identification of the full SNARE complex involved in ISG-ISG fusion will help resolve this issue. This could be done by proteomic analysis of the ISG protein components. Inhibitory reagents for likely candidates from this analysis could be added to the *in vitro* fusion reaction to determine an involvement of specific proteins in the regulation of ISG homotypic fusion. Alternatively, immunoprecipitation of solubilised ISG membranes using anti-Stx6 or a suitable anti-Syt IV ab, followed by mass-

spectroscopy analysis, would reveal unknown binding partners of Stx6, to which reagents could be developed and tested in the fusion assay. The lack of an anti-Syt IV ab to use in immunoprecipitation experiments did not allow me to look for interaction with endogenous Stx6.

It is unlikely that the Stx6 and Syt IV complex are on early endosomes. The immunostaining of PC12 cells with an anti-Stx6 and anti-Syt IV ab showed they colocalise mainly in the perinuclear area (Chapter 3, Figure 3.3.1), where ISGs localise. In addition, unlike Stx6 (Bock et al., 1997) (Simonsen et al., 1999), Syt IV is not found on endosomes (Ibata et al., 2000). However, it is still possible that the Stx6-Syt IV complex is also on other membranes.

Mode of interaction of Syt IV with Stx6

Binding studies with the Syt IV-C2A or Syt IV-C2B domains revealed that both domains are involved in the interaction with Stx6. The binding of the full Syt IV cytoplasmic domain to Stx6 was, however, greater than that obtained with the individual domains, suggesting that both domains cooperate to mediate binding to Stx6. In studies performed with Syt I, it was also found that binding affinity to SNAP-25 and Stx1 was higher with the full Syt I cytoplasmic domain than with the individual C2A or C2B domains (Gerona et al., 2000) (Rickman and Davletov, 2003) (Zhang et al., 2002). Moreover, both Syt I domains were found to cooperate to regulate exocytosis (Earles et al., 2001) (Wang et al., 2003b). The binding of both Syt IV-C2A and C2B domains to Stx6 suggests that, like Syt I binding to t-SNAREs, both Syt IV domains are required for high-affinity binding to Stx6, and that this binding is required for ISG homotypic fusion.

It would be interesting to investigate whether either or both domains of Syt IV are required for ISG homotypic fusion. Unfortunately, due to the insolubility of the GST-C2A and GST-C2B domains, I could not investigate this question using recombinant proteins.

Next, I attempted to identify the Stx6 domain responsible for Syt IV binding. Previous studies mapped the Syt I binding domain to the SNARE motif of both Stx1 or SNAP-25 (Kee and Scheller, 1996) (Gerona et al., 2000). I therefore asked whether Syt IV interacts with the SNARE domain of Stx6. To do this, I performed a GST-pull down experiment using GST-Stx6-Habc domain and GST-Stx6 cytoplasmic domain. After several attempts, using Triton X-100 extracts of PC12 or HEK-cells overexpressing HA-Syt IV cytoplasmic domain as a starting material, I could not detect binding of Syt IV to either the GST-Stx6-Habc or cytoplasmic domain (data not shown). Work in the lab has identified specific binding partners, other than SNAREs, of the Stx6-Habc domain (G. Otto, unpublished observations), suggesting that the recombinant Habc domain is folded properly and is functional. However, several attempts to co-immunoprecipitate other SNARE proteins, such as VAMP4, using the Stx6 cytoplasmic domain were never successful (F. Wendler, unpublished observation), whereas co-immunoprecipitation of VAMP4 with full length Stx6 was possible (Wendler et al., 2001). This indicates that the cytoplasmic portion of Stx6 is not folded properly, and is not fully functional when expressed without the transmembrane domain. This could be due to the fact that the SNARE motif, close to the C-terminal membrane spanning of the protein, requires the trans-membrane domain for its proper folding and/or interactions with its SNARE partners. Therefore, I could not investigate which domain of Stx6 mediates the binding with Syt IV.

As an alternative strategy, and to have an indication of the Stx6 domain responsible for Syt IV binding, I combined both anti-Stx6 ab and Syt IV cytoplasmic domain in the binding assay. This combination did not affect the binding of either reagent, suggesting that the Stx6 ab and the Syt IV cytoplasmic domain interact with separate sites in Stx6. The anti-stx6 ab binding site was mapped to the Habc domain of Stx6 (G. Otto, unpublished observations), suggesting that the Syt IV cytoplasmic domain binds to Stx6 somewhere other than the Habc domain.

In conclusion, in this chapter I found that the Syt IV cytoplasmic domain inhibited ISG homotypic fusion and that it is recruited to ISG membranes strictly via protein components on these membranes. The finding that Syt IV interacts with Stx6 via both C2A and C2B domains suggests that these proteins are part of the same complex involved in ISG homotypic fusion.

6 Chapter 6: Syt IV cytoplasmic domain and siRNA-mediated knockdown of Syt IV inhibit granule maturation *in vivo*

6.1 Aim

In neuroendocrine and endocrine cells, granins and prohormones are processed by prohormone convertases (PCs) during granule maturation. This processing is dependent on the acidification of the granule lumen, which is required for PC activation, and therefore function.

In Chapter 4, I presented data showing that the Syt IV cytoplasmic domain inhibits ISG-ISG fusion *in vitro*. In this chapter, I will study the effect of this domain, as well as siRNA specific for Syt IV, on granule maturation *in vivo*. I will specifically look at whether these reagents have an effect on Secretogranin II (SgII) processing, which occurs during ISG maturation and can be used as a measure of granule maturation.

6.2 Syt IV cytoplasmic domain inhibits SgII processing

In PC12/PC2 cells, SgII processing by PC2 starts in the TGN and continues in the MSG (Urbe et al., 1997). The final degradation product, which accumulates in MSGs is an 18 kDa peptide (p18) detectable with a specific anti-p18 ab, which does not

recognise full length SgII. I investigated the effect of the Syt IV cytoplasmic domain on ISG maturation *in vivo*, by specifically using SgII processing as a read-out for maturation. A key point for my studies is the use of wild type PC12 cells transiently transfected with PC2 rather than the PC12/PC2 cell line, which are PC12 cells stably expressing PC2 (Dittie and Tooze, 1995). Use of this double transfection protocol was necessary because of the background signal of p18 in PC12/PC2 cells where a storage pool in MSGs existed before the addition of Syt IV cytoplasmic domain. Therefore, wild type PC12 cells will be transfected with the Syt IV cytoplasmic domain, together with PC2, in order to investigate whether the appearance and accumulation of p18 is affected. Wild type PC12 cells were transfected with HA-Syt IV cytoplasmic domain and PC2, GFP and PC2 or PC2 alone. Cells were fixed, permeabilised and labelled with rat-anti-HA, rabbit-anti-PC2 and mouse-anti-p18 abs (Figure 6.2.1 A). Transfection of HA-Syt IV cytoplasmic domain together with PC2 resulted in an inhibition of p18 accumulation, whereas transfection of GFP with PC2 or PC2 alone, did not have any effect on p18 appearance and accumulation. In addition, transfection of HA-avidin with PC2 also had no effect, showing that the HA tag does not interfere with SgII processing (data not shown). Quantification of the intensity of the p18 signal in an equivalent number of cells co-transfected with HA-Syt IV cytoplasmic domain and PC2 revealed a three-fold decrease compared to the intensity of p18 in cells expressing GFP and PC2 or PC2 alone (Figure 6.2.1 B).

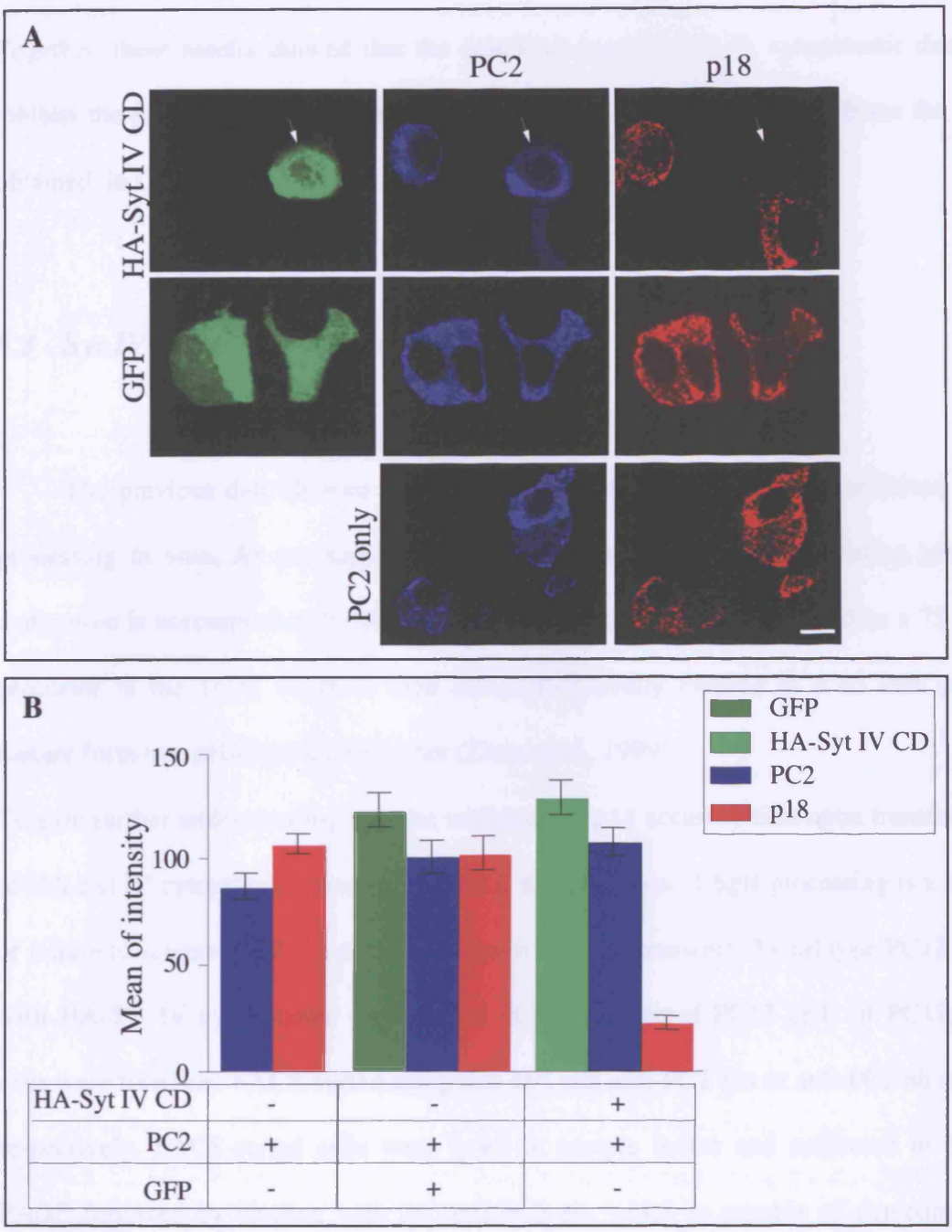

Figure 6.2.1: HA-Syt IV cytoplasmic domain inhibits SgII processing.

A) PC12 cells were cotransfected with HA-Syt IV cytoplasmic domain and PC2, GFP and PC2, or PC2 alone. The cells were fixed and labelled with rat anti-HA (green), rabbit anti-PC2 (blue) and mouse anti-p18 abs (red). Images were taken with identical acquisition parameters using a Zeiss LSM 510 confocal microscope (bar, 5 μM). B) Transfected cells were individually selected and the mean of intensity of each channel was measured using Photoshop 7.0 software. Columns represent the average of the mean of intensity of each channel, error is the SEM, where n=44 cells for all conditions.

Together, these results showed that the dominant negative Syt IV cytoplasmic domain inhibits the processing of SgII into its degradation product p18. This confirms the data obtained in Chapter 4 that Syt IV is involved in the maturation of ISGs.

6.3 Syt IV cytoplasmic domain inhibits PC2 maturation

The previous data showed that the cytoplasmic domain of Syt IV inhibited SgII processing *in vivo*. As previously mentioned, the processing of SgII during granule maturation is accomplished by the protease activity of PC2. PC2 is found as a 75 kDa precursor in the TGN, which is then autoproteolytically cleaved to a 65 kDa active mature form in a pH-dependent manner (Zhou et al., 1999).

To gain further understanding into the inhibition of p18 accumulation upon transfection of HA-Syt IV cytoplasmic domain, I asked if the inhibition of SgII processing is a result of failure to activate PC2. To answer this question, I co-transfected wild type PC12 cells with HA-Syt IV cytoplasmic domain and PC2. Transfected PC12 cells or PC12/PC2 cells were fixed and FACS-sorted using anti-HA and anti-PC2 abs or anti-PC2 ab alone, respectively. FACS-sorted cells were lysed in sample buffer and subjected to SDS-PAGE followed by blotting with the anti-PC2 ab, which is capable of detecting the precursor 75 kDa and the mature/processed 65 kDa form of PC2 (Figure 6.3.1 A). In the cells transfected with the dominant negative HA-Syt IV cytoplasmic domain, there was a higher ratio of pro-PC2 to PC2 than in PC12/PC2 cells. As a positive control for PC2 activity, I used stably transfected PC12/PC2 cells, because of the low transfection

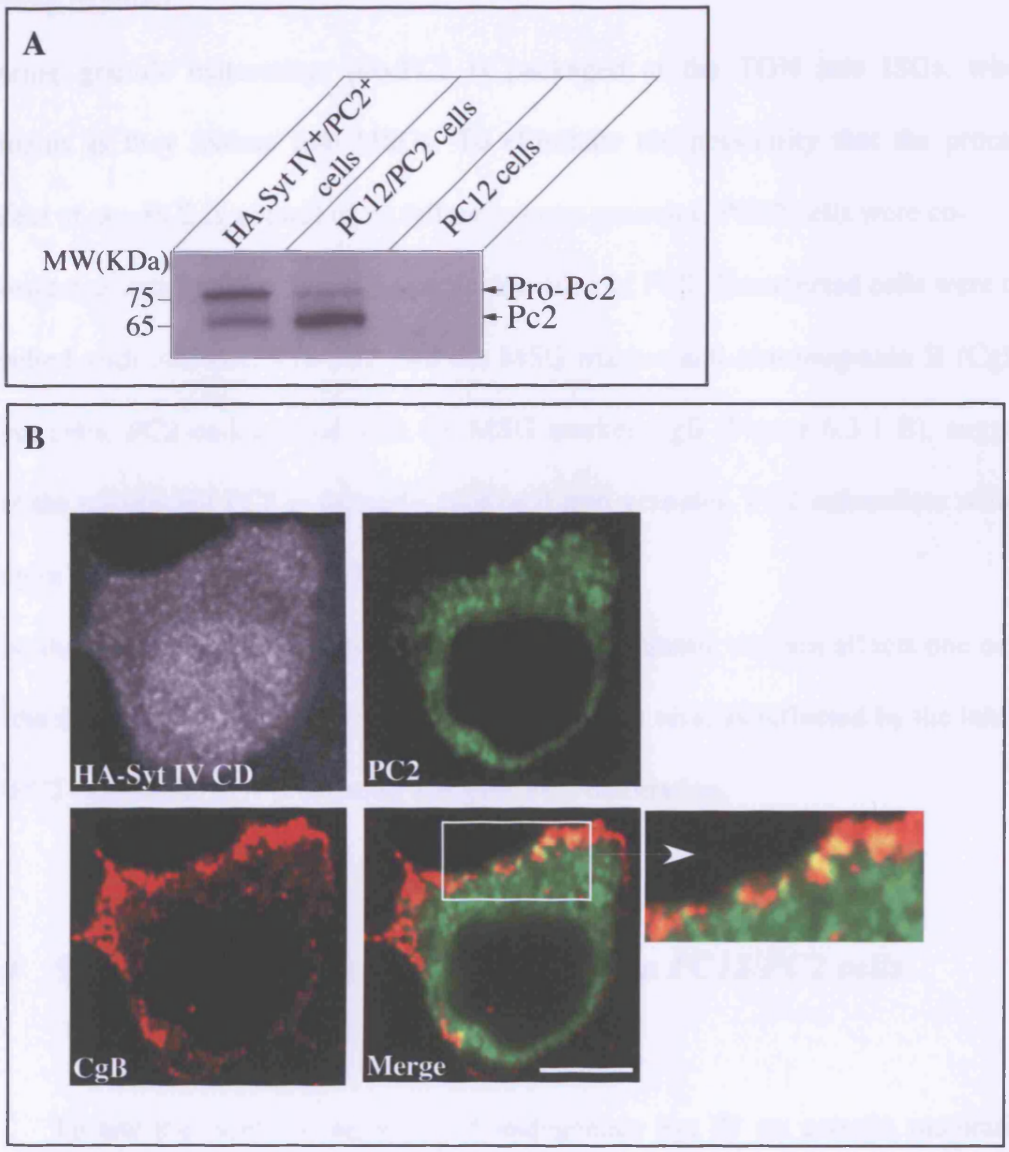

Figure 6.3.1: PC2 is found mainly in the proform in cells expressing the HA-Syt IV cytoplasmic domain. PC12 cells were cotransfected with HA-Syt IV cytoplasmic domain and PC2. A) Cells positive for both HA-Syt IV and PC2 were FACS sorted by labelling with anti-HA (Alexa 488) and anti-PC2 (Alexa 647) abs. As control PC12/PC2 cells labelled with anti-PC2 ab were FACS sorted using identical conditions. 150,000 HA-Syt IV$^+$/PC2$^+$ cells and 300,000 PC12/PC2 cells were loaded on an SDS-PAGE gel and blotted with the anti-PC2 ab. 5 µg of a PC12 cells lysate was used as a negative control for the PC2 ab. B) HA-Syt IV cytoplasmic domain and PC2 cotransfected PC12 cells were fixed and labelled with anti-HA (white) anti-PC2 (green) and CgB abs (red). Images were taken using confocal microscopy and LSM 510 software (bar 10 µM).

efficiency obtained with transient transfection combined with the extended FACS sorting required.

During granule maturation, pro-PC2 is packaged at the TGN into ISGs, where it remains as they mature into MSGs. To eliminate the possibility that the processing defect of pro-PC2 is a result of its failure to enter granules, PC12 cells were co-transfected with HA-Syt IV cytoplasmic domain and PC2. Transfected cells were triple-labelled with anti-HA, anti-PC2 and the MSG marker anti-chromogranin B (CgB). In these cells, PC2 co-localised with the MSG marker CgB (Figure 6.3.1 B), suggesting that the transfected PC2 is properly packaged into granules. PC2 colocalises with CgB only in the newly formed MSGs.

Together, these results suggest that the Syt IV cytoplasmic domain affects one or more of the steps leading to secretory granule maturation *in vivo,* as reflected by the inhibition of PC2-dependent SgII processing and pro- PC2 maturation.

6.4 Syt IV siRNA reduces SgII processing in PC12/PC2 cells

To test the effect of depletion of endogenous Syt IV on granule maturation *in vivo,* and to confirm my previous results obtained with the Syt IV cytoplasmic domain, I treated PC12/PC2 cells with siRNA directed against Syt IV, and asked whether this affects SgII processing.

PC12/PC2 cells were transfected with a smart pool of 4 siRNA duplexes directed against rat Syt IV (Dharmacon), or mock-transfected using Dharmacon transfection reagents (described in Chapter 2). Three days post-transfection cells were fixed, permeabilised and labelled with anti-Syt IV and anti-Syt I abs for immunofluorescence.

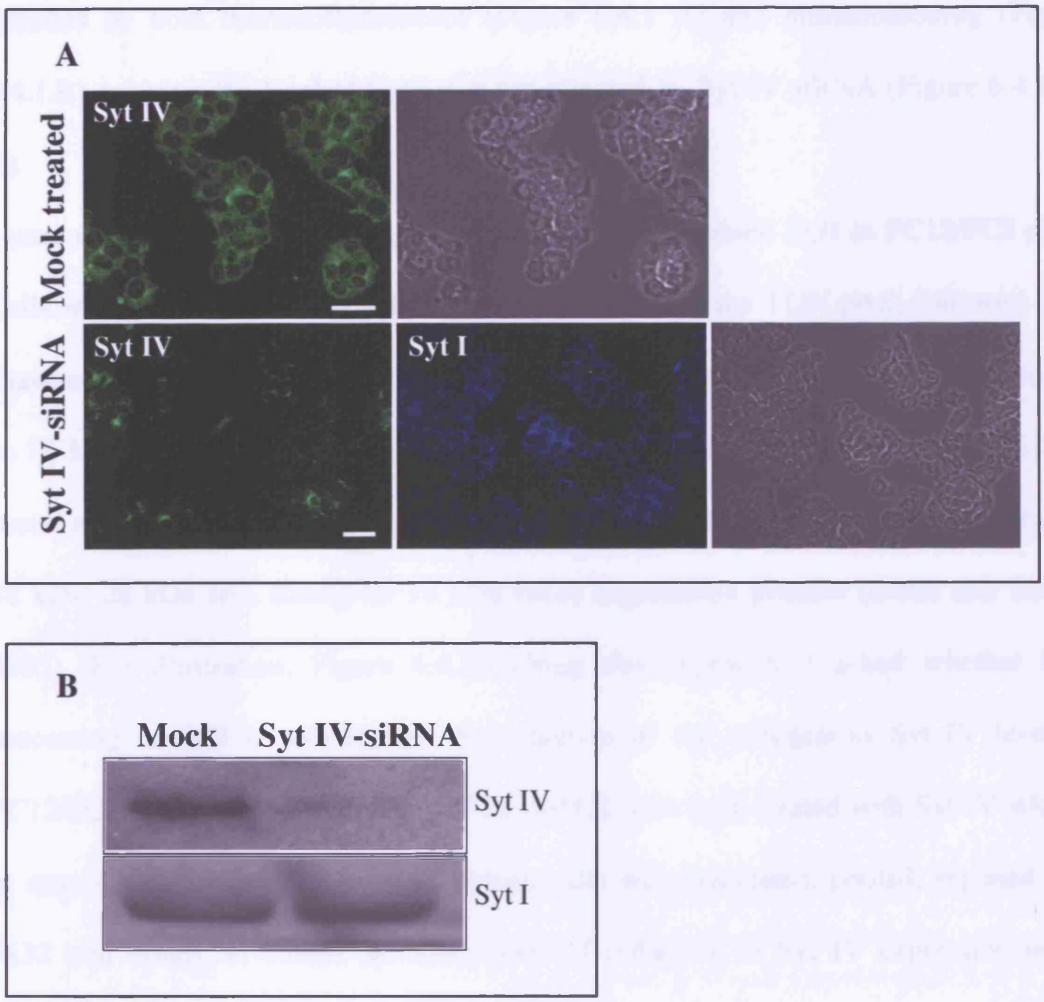

Figure 6.4.1: Syt IV-siRNA in PC12 cells. PC12 cells were treated with 50 nM Syt IV-siRNA or mock treated using Dharmacon transfection reagents. A) 72 h post treatement, cells were fixed, permeabilised and labelled with anti-Syt IV (green) and anti-Syt I abs (Blue). Images were acquired using confocal microscopy and LSM 510 software (bar, 20 μM). B) Alternatively, cells were lysed in sample buffer and subjected to an SDS-PAGE followed by western blotting with anti-Syt IV and anti-Syt I abs.

Alternatively, cells were lysed and subjected to SDS-PAGE, followed by blotting with anti-Syt IV and anti-Syt I abs (Figure 6.4.1). Depending on the experiment, a reduction of between 45% and 80% in Syt IV levels in siRNA-treated PC12/PC2 cells was detected by both immunofluoresence (Figure 6.4.1 A) and immunoblotting (Figure 6.4.1.B), whereas the level of Syt I was not affected by Syt IV siRNA (Figure 6.4.1 A, B).

I used a pulse-chase protocol to follow the newly-synthesised SgII in PC12/PC2 cells. Cells were pulsed for 5 min with [^{35}S]-sulphate to label the TGN pool, followed by a chase with excess sulphate. In the TGN, the newly sulphate-labelled SgII is detected as an 86 kDa precursor. After its exit from the TGN, and during the chase, when SgII is found in ISGs then MSGs, it is processed at several dibasic sites by PC2 to generate a 38 kDa, 28 kDa and, finally an 18 kDa (p18) degradation product (Dittie and Tooze, 1995) (For illustration, Figure 6.4.2). Using this approach, I asked whether PC2 processing of SgII is affected by the reduction of the endogenous Syt IV level in PC12/PC2 cells. Two 15 cm dishes of PC12/PC2 cells were treated with Syt IV siRNA or mock-treated. Two days post-treatment, cells were harvested, pooled, replated into 7x32 mm dishes, to ensure the same level of reduction in Syt IV expression in all samples, and incubated for a further 24h. All dishes were then pulse-labelled with [^{35}S]-sulphate for 5 min then chased for 0, 10,20,30,60,90 and 180 min to follow SgII processing. The chase reaction was stopped by transferring the dishes onto ice, followed by cell lysis in a Triton X-100-containing buffer. Heat-stable fractions, which allow an enrichment of granins, were prepared, and the heat-stable proteins were precipitated and subjected to SDS-PAGE and autoradiography (Figure 6.4.3). In cells treated with Syt IV siRNA, the processing of full length SgII to the degradation products p38, p28 and finally p18 was lower compared to that in mock-treated cells (Figure 6.4.3 A).

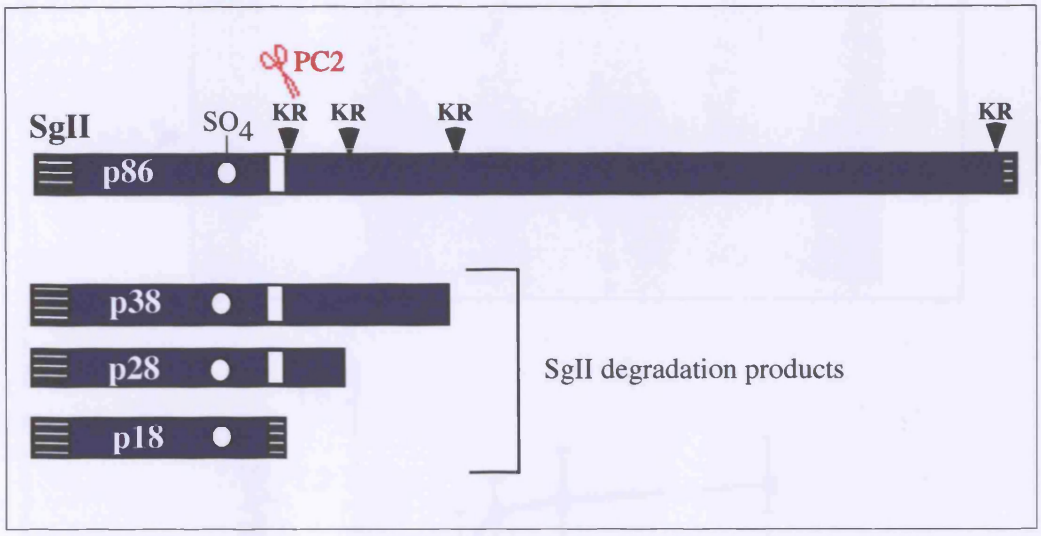

Figure 6.4.2: Schematic representation of SgII and its processing products.
p86 is the full length SgII (MW=86 kDa). p 38, p28, p18 are the SgII-degradation products (MW=38, 24, 18 kDa, respectively). Arrows represent dibasic cleavage sites (Lys-Arg) utilised by PC2. SgII and its degradation products are sulphated on Tyr 126 (SO_4).

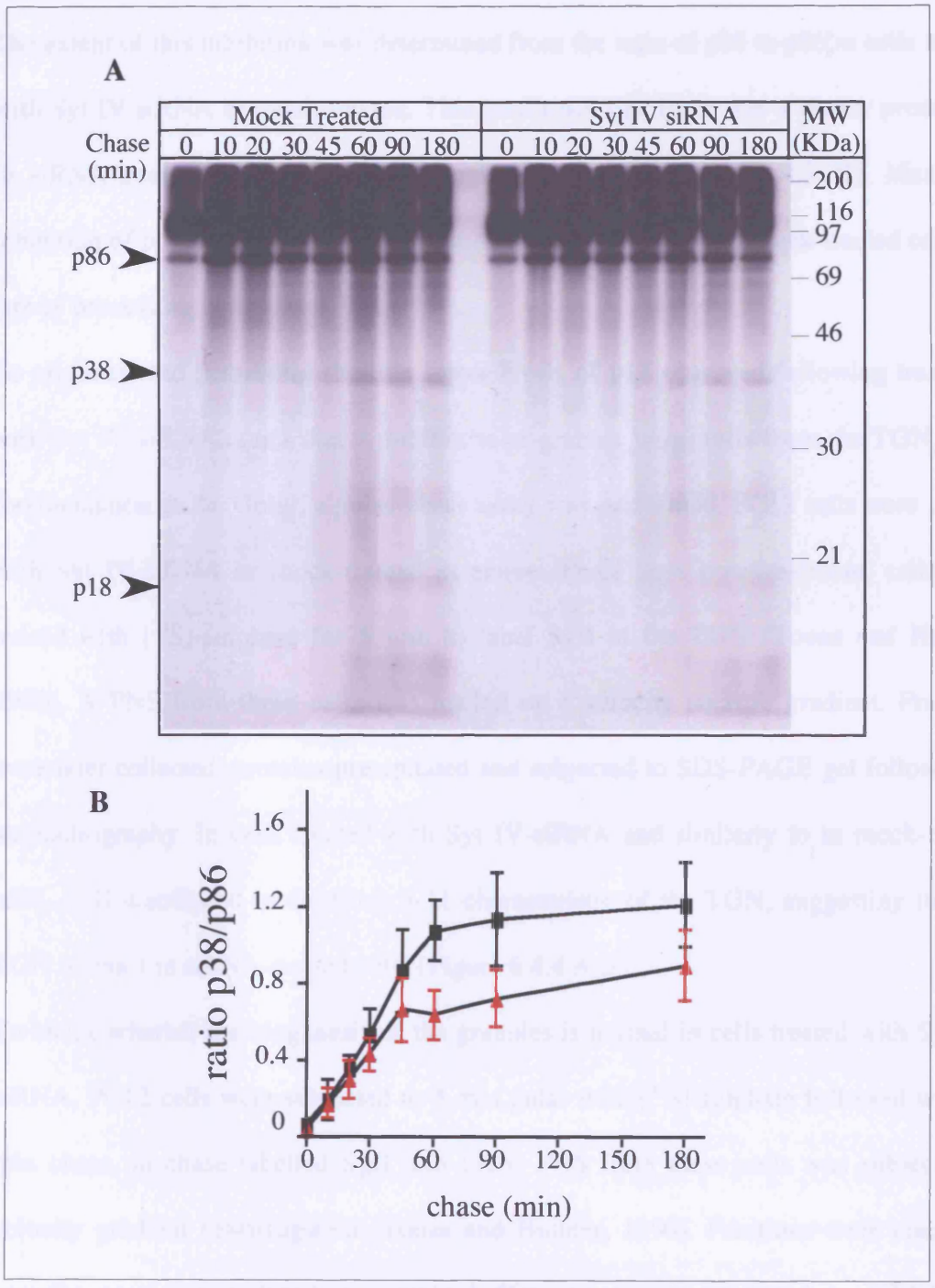

Figure 6.4.3: Syt IV-siRNA reduces SgII processing in PC12/PC2 cells.

A) PC12/PC2 cells were treated with Syt IV-siRNA or mock treated with transfection reagents alone as described previously. 72 h post-treatment, cells were pulse labelled with [^{35}S]-sulphate for 5 min and chased for the indicated length of time. Cells were lysed in TNTE buffer, a heat-stable fraction was prepared, and analysed by SDS-PAGE gel and autoradiography. Arrows indicate the position of the SgII-processing products p38 and p18. B) Quantification of the ratio of p38/p86 using ImageJ software. Three separate experiments were analysed and the average is shown. Error is SEM, P= 0.0159, paired t-test.

The extent of this inhibition was determined from the ratio of p38 to p86 in cells treated with Syt IV siRNA or mock-treated. This confirmed that there was a slower processing in siRNA-treated compared to the mock-treated cells (figure 6.4.3 B). Maximum inhibition of processing occurs after 45 min of chase, when in the mock-treated cells the rate of processing is maximal.

To eliminate the possibility that the lower levels of p18 observed following treatment with Syt IV-siRNA is not due to inhibition of granule biogenesis from the TGN, or to fragmentation of the Golgi, a pulse-chase assay was performed. PC12 cells were treated with Syt IV-siRNA or mock-treated as above. Three days post-treatment, cells were pulsed with [^{35}S]-sulphate for 5 min to label SgII in the TGN (Tooze and Huttner, 1990). A PNS from these cells was loaded on a velocity sucrose gradient. Fractions were later collected, proteins precipitated and subjected to SDS-PAGE gel followed by autoradiography. In cells treated with Syt IV-siRNA and similarly to in mock-treated cells, SgII distributed in fractions 9-11 characteristic of the TGN, suggesting that the TGN is intact in siRNA-treated cells (Figure 6.4.4 A,B).

To check whether the biogenesis of the granules is normal in cells treated with Syt IV-siRNA, PC12 cells were subjected to 5 min pulse with [^{35}S]-sulphate followed with 15 min chase, to chase labelled SgII into ISGs. PNS from these cells was subjected to velocity gradient centrifugation (Tooze and Huttner, 1990). Fractions were collected, proteins precipitated, lysed in sample buffer and finally subjected to SDS-PAGE followed by autoradiography. Similarly to mock-treated cells, in Syt IV-siRNA cells SgII distributed in fractions 1-4 in the velocity gradient (Figure 6.4.5 A,B), the distribution characteristic of ISGs. This demonstrates that secretory granule formation occurred normally in the absence of Syt IV.

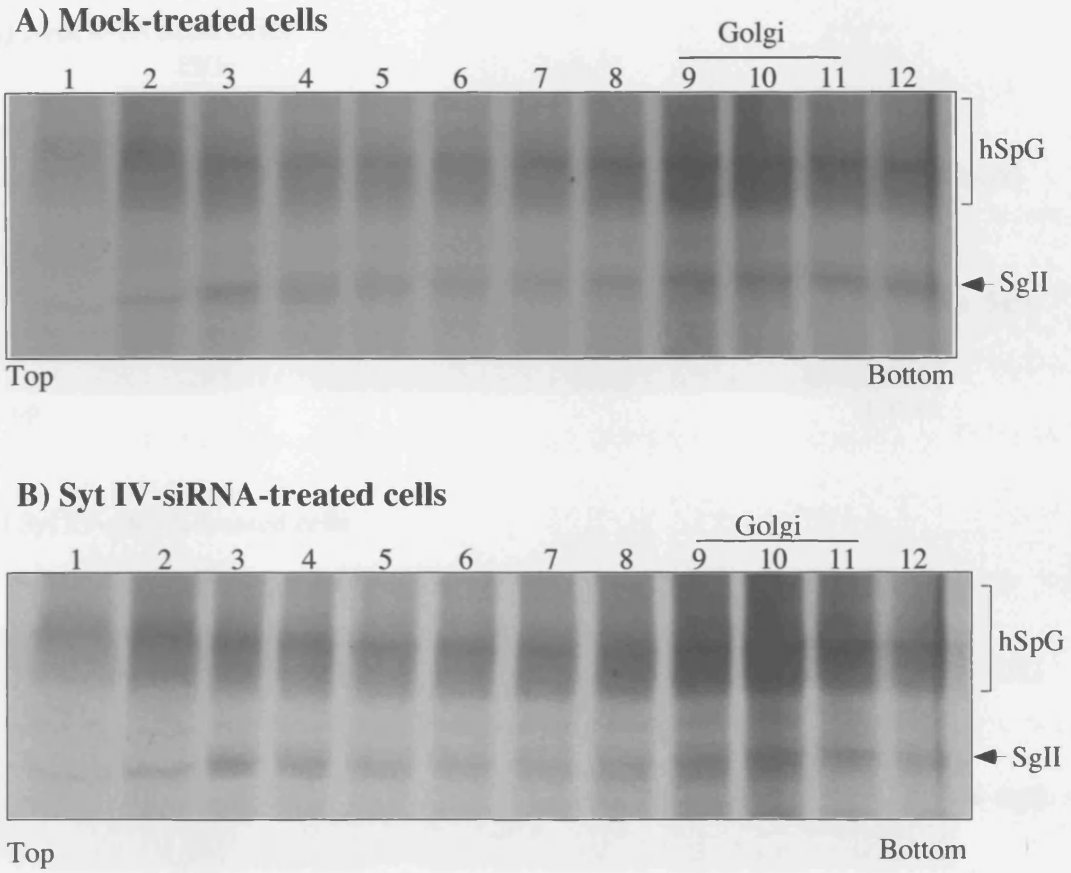

Figure 6.4.4: The Golgi is not fragmented in cells treated with Syt IV-siRNA. PC12 cells were mock treated (A) or treated with Syt IV-siRNA (B) as described previously. 72 h post-treatement, cells were pulse labelled with [^{35}S]-sulphate for 5 min. A PNS from these cells was prepared and separated by velocity gradient centrifugation. Fractions were collected and analysed by SDS-PAGE and autoradiography.

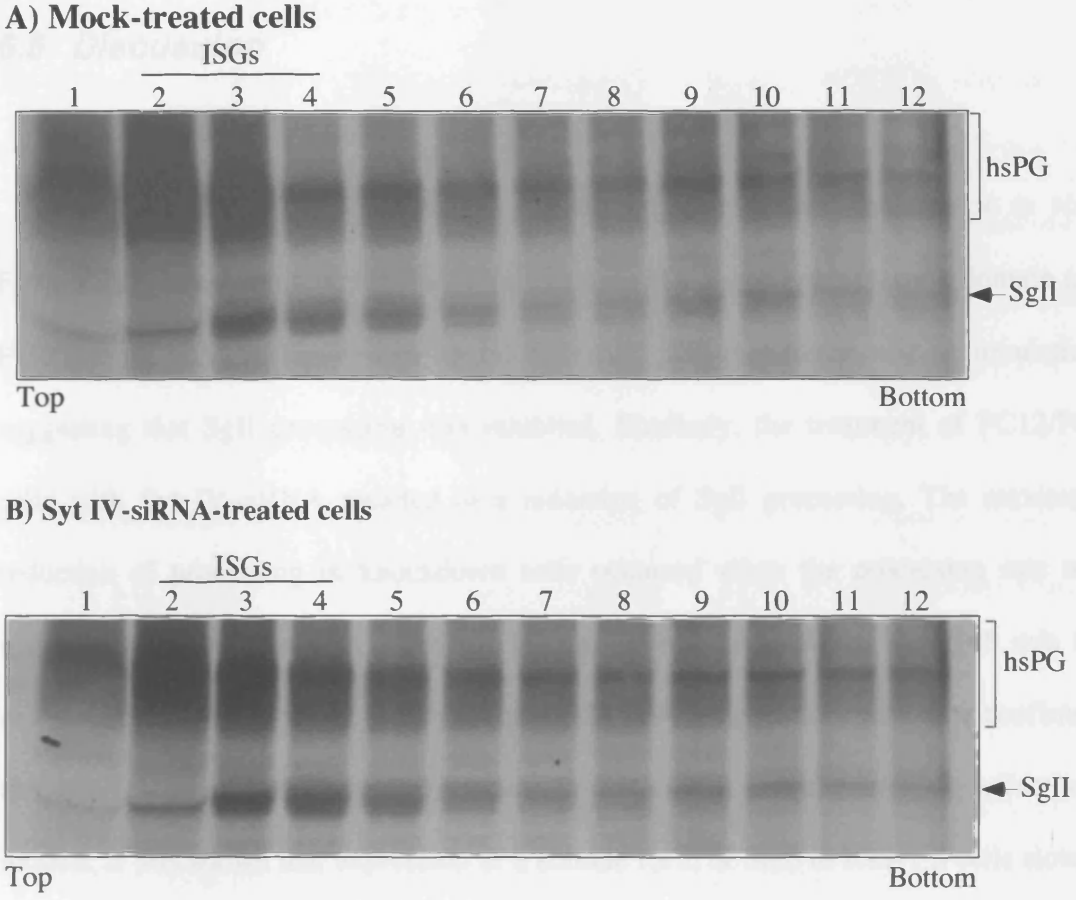

Figure 6.4.5: Secretory granule biogenesis is normal in Syt IV-siRNA treated cells. PC12 cells were mock treated (A) or treated with Syt IV-siRNA (B). Cells were then labelled with [^{35}S]-sulphate for 5 min followed by 15 min chase to label ISGs. PNS from these cells was prepared and subjected to velocity gradient centrifugation. Fractions were later collected and precipitated proteins were separated on an SDS-PAGE gel followed by autoradiography.

Together, these results demonstrate that reducing the levels of endogenous Syt IV affects SgII processing, further confirming that this protein is important for granule maturation.

6.5 Discussion

In this chapter, I demonstrated a role of Syt IV in granule maturation *in vivo*. First, the co-transfection of the dominant negative HA-Syt IV cytoplasmic domain and PC2 into PC12 cells resulted in an inhibition of p18 appearance and accumulation, suggesting that SgII processing was inhibited. Similarly, the treatment of PC12/PC2 cells with Syt IV-siRNA resulted in a reduction of SgII processing. The maximum reduction of processing in knockdown cells occurred when the processing rate was maximal in control cells, at 45 min. This correlates well with the $t_{1/2}$ of 45 min for maturation of ISGs in PC12 cells (Tooze et al., 1991). Together, these data confirmed that Syt IV is required for granule maturation. Recently, and although the effect was modest, it was shown that expression of a soluble form of Stx6 in INS-1 β cells slowed proinsulin processing (Kuliawat et al., 2004). This is an interesting observation, because Stx6, like Syt IV, is involved in ISG maturation in PC12 cells (Wendler et al., 2001).

I speculate that the inhibition of SgII processing is probably a result of an inability to activate PC2 during ISG maturation. Indeed, in cells transfected with the dominant negative Syt IV cytoplasmic domain, PC2 was found mainly in the unprocessed form, whereas in PC12/PC2 cells, PC2 was mainly in mature/processed form. We have been unable to test for PC2 activation after siRNA treatment because of the lower than usual

transfection efficiency after siRNA treatment, which precludes expressing PC2 in the Syt IV-deficient wild-type PC12 cells.

PC2 autocatalytic activation was found to be dependent on the acidification of granules (Lamango et al., 1999), which occurs during the maturation from ISGs to MSGs. Indeed, the pH of ISGs was found to be 6.3, which acidifies to 5.5 in the MSGs, where the catalytic activity of PC2 is at its maximum (Urbe et al., 1997). The findings that PC2 is mainly in the unprocessed form in transfected HA-Syt IV cells, and that PC2 activation is pH-dependent (Urbe et al., 1997), led me to speculate that the reduction in pro-PC2 processing was due to a failure of ISG acidification. Although the mechanism of secretory granule acidification is not known, it has been proposed to occur following an increase in the membrane density of the vacuolar H^+-ATPase, as well as a decrease in H^+-permeability (Wu et al., 2001). Interestingly, perturbation of the vacuolar H^+-ATPase has also been shown to reduce processing in *Xenopus* intermediate pituitary cells (Schoonderwoert et al., 2000).

The inhibitory effect on SgII processing observed with the dominant negative Syt IV cytoplasmic domain or Syt IV-siRNA could be explained by the following hypothesis: Addition of these inhibitory reagents could lead to the inhibition of homotypic fusion of ISGs, which would also limit membrane remodelling. This will lead to the retention of normally removed proteins, such as other ATPases, for example the Na^+/K^+ ATPAse, that may compete with the V-ATPase for ATP. Additionally, removal of H^+ channels responsible for H^+ leaks into ISGs, as well as an increase in density of the V-ATPase, might also be inhibited. This would lead to the subsequent inhibition of granule acidification, which is necessary for the activity of PC2 and therefore SgII processing.

I attempted to investigate whether the granule pH in cells transfected with the dominant negative Syt IV cytoplasmic domain was perturbed. I chose to use DAMP (3-(2,4

dinitroanilino)-3'-amino-N-methyldipropylamine) as a tool to visualise acidic granules. DAMP accumulates in acidic organelles, where it can be visualised using electron microscopy (EM), after fixation and labelling with anti-DNP abs (Anderson et al., 1984) (Anderson and Orci, 1988). DAMP has previously been used to label the maturing granules in endocrine and neuro-endocrine cells (Orci, 1986) (Tooze and Tooze, 1986). To do this, I infected PC12 cells with an adenovirus expressing the HA-Syt IV cytoplasmic domain. To facilitate the detection of transfected cells during EM analysis, viral infection was used to obtain a maximal transfection efficiency (Figure 6.5.1), as transfection of PC12 cells using Lipofectamine 2000 (Invitrogen) usually gives only 5% transfection efficiency. Infected and non-infected PC12 cells were incubated with DAMP, followed by immunolabelling with anti-HA and anti-DNP abs using electron-microscopy (EM) techniques. From the analysis so far, no major differences in the staining of DAMP were observed (Figure 6.5.2). Furthermore, ~ 70% of the 220 granules counted in cells infected with adenovirus-HA-Syt IV cytoplasmic domain, with similar results obtained in uninfected cells, were DAMP-positive. Therefore, these results were inconclusive. The difficulty in such an analysis comes from the fact that these cells contain many "old" granules, making it impossible to distinguish the "new" granules from the "old". Another drawback is that determining the pH from the DAMP accumulation is not a very sensitive technique.

The development of more sensitive techniques is required for an accurate analysis of pH, such as using the pH-sensitive GFP protein, ratiometric pHluorin, fused to the granule marker, phogrin (Yuste et al., 2000). This will allow for the specific detection of newly made granules, and has the advantage of accurate quantification of the pH changes during the maturation of ISGs. A small difference in the pH of MSGs, between cells overexpressing the dominant negative HA-Syt IV cytoplasmic domain or Syt IV-

siRNA, and normal cells, will be detectable by a change in the measured fluorescence of the ratiometric pHluorin-phogrin.

In conclusion, I demonstrated in this chapter that the transfection of Syt IV cytoplasmic domain and reduction of expression levels of endogenous Syt IV using siRNA, affected granule maturation *in vivo,* measured by SgII processing.

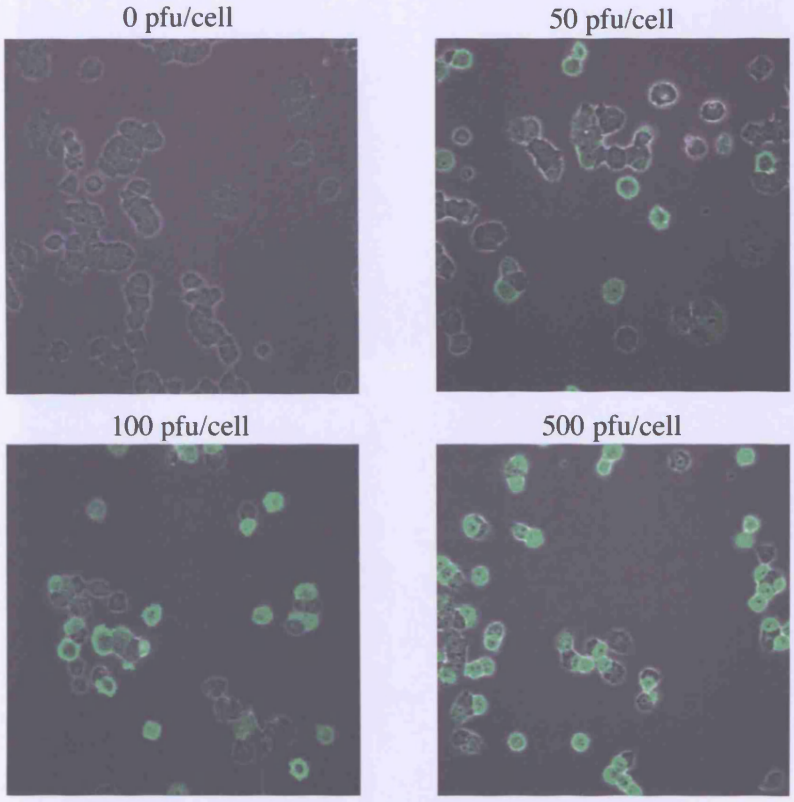

Figure 6.5.1: Optimisation of the adenovirus expressing HA-Syt IV cytoplasmic domain in PC12 cells. PC12 cells were infected with adenovirus expressing HA-Syt IV cytoplasmic domain at 50, 100 or 500 pfu/cell. Infection was performed by incubating the adenovirus with PC12 cells O/N at 37 °C in full growth medium. Infected cells were washed, fixed, permeabilised and labelled with anti-HA ab. Images were acquired using confocal microscopy and LSM 510 software.

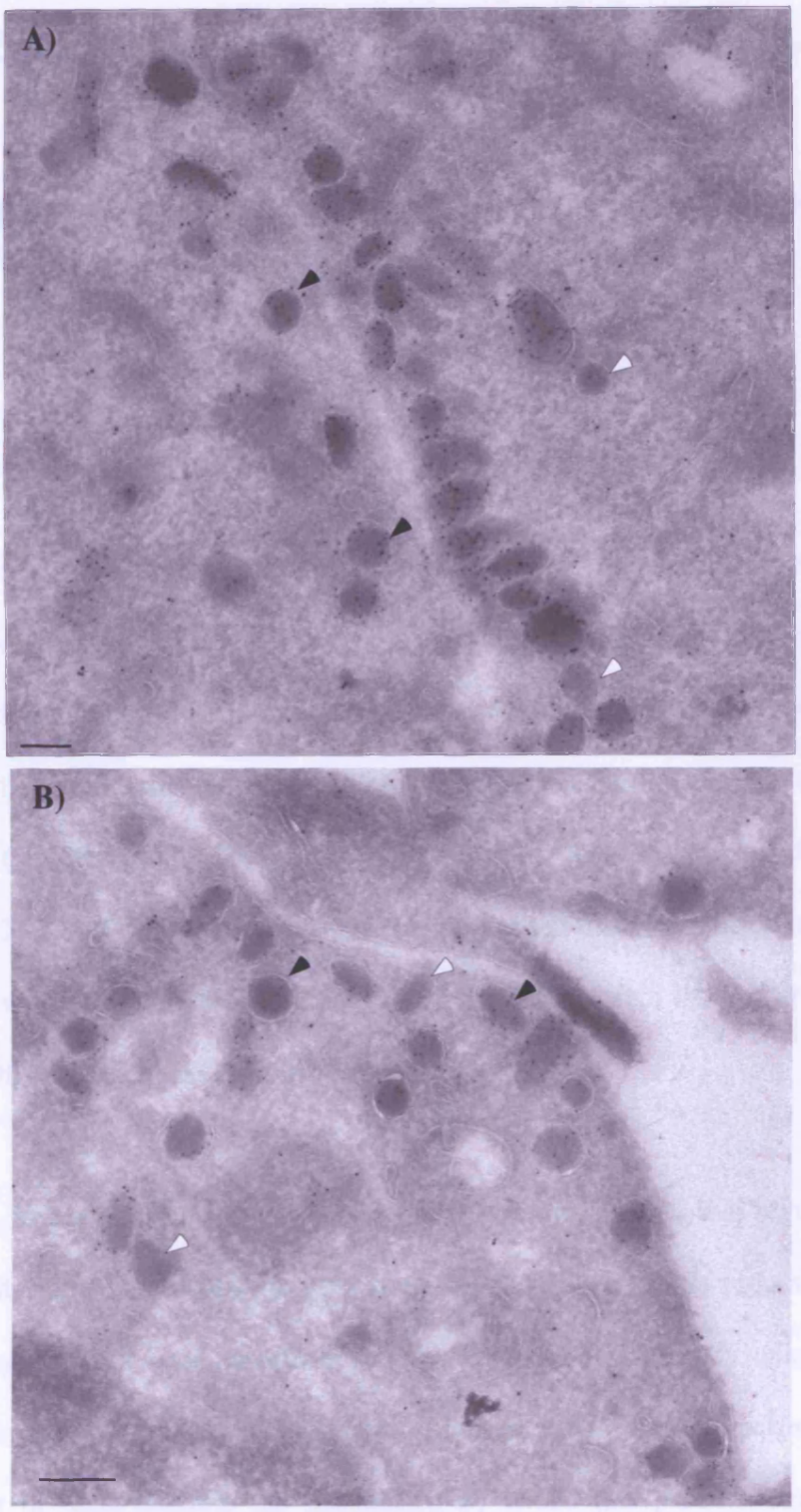

Figure 6.5.2: Identification of pH changes in cells expressing HA-Syt IV cytoplasmic domain. PC12 cells were infected with HA-Syt IV cytoplasmic domain. 24 h later, infected or non-infected PC12 cells were incubated with DAMP for 30 min at 37 °C. Later cells were prepared and sectioned for immunogold labelling. A) Ultra-thin sections of infected PC12 cells were labelled with rabbit anti-HA and mouse anti-DNP abs followed by 10 nM anti-rabbit-protein A-gold and 5nM anti-mouse protein A-gold. B) Non-infected cells were labelled with mouse anti-DNP ab followed by 5 nM protein A-gold. Black arrows show dense core granules, where DAMP accumulated characterised with anti-DNP ab labelling and white arrows show granules that did not have any DAMP accumulation (bar 0.2 μM).

7 Chapter 7: Synaptotagmin IV interacts with the adaptor protein-1 (AP-1)

7.1 Aim

In Chapter 3, I presented data showing that Syt IV is localised on ISGs and is absent from MSGs. This result suggested that Syt IV is removed from secretory granules during their maturation. Previous work in the lab has demonstrated that removal of proteins, such as M6PR (Dittie et al., 1999), Furin (Dittie et al., 1997) and VAMP-4 (Hinners et al., 2003), from ISGs was via AP-1-containing clathrin-coated vesicles (CCVs). Based on these studies, I hypothesised that the removal of Syt IV from the maturing granules could occur in the same way; therefore, I looked for interaction of Syt IV with AP-1 using a GST pull-down assay.

Next, because of our limited knowledge of the mechanisms that regulate ISG-ISG fusion and, more specifically, protein complexes involved in this process, Syt IV and Stx6 being the only ones identified so far, I attempted to identify unknown binding partners for Syt IV. Moreover, the identification of Syt IV binding partners will direct us further in understanding the mechanism by which this protein regulates granule maturation. In an attempt to identify unknown Syt IV binding partners, I undertook a tandem affinity purification (TAP) approach (Puig et al., 2001).

7.2 Syt IV interacts with AP-1 in a GST-pull-down assays

The maturation of secretory granules includes removal of proteins, which are thought not to be needed for later steps, via CCVs in an AP-1-dependent pathway. It was demonstrated that the cytosolic domains of components on ISGs, such as VAMP4, M6PR and furin, are able to recruit AP-1, and that their sorting from the maturing granules depends on this interaction (Dittie et al., 1999) (Dittie et al., 1997) (Hinners et al., 2003). As Syt IV is not found on MSGs, I asked whether the sorting of this protein during granule maturation was via an AP-1 dependent pathway.

First, I used immunofluorescence to look at whether Syt IV colocalises with AP-1. PC12 cells were fixed, permeabilised and double-labelled with polyclonal anti-Syt IV and monoclonal anti-γ-adaptin (AP-1) ab. Syt IV displayed a good colocalisation with AP-1 near the Golgi area (Figure 7.2.1). Next, in order to determine whether Syt IV and AP-1 interact, I performed a GST pull-down assay. Recombinant GST-Syt IV or GST-VAMP-4 cytoplasmic domains, or GST alone, were bound to glutathione-sepharose beads for 2h at 4 °C. GST fusion proteins bound to beads were then incubated with total PNS prepared from PC12 cells (described in Chapter 2) O/N at 4 °C. After several washes, proteins bound to beads, as well as 10% of total input for each sample, were subjected to SDS-PAGE followed by immunoblotting with anti- γ-adaptin ab (Figure 7.2.2). Syt IV interacted with AP-1 in a dose-dependent manner. Similarly, VAMP-4 interacted with AP-1, as shown previously (Peden et al., 2001) (Hinners et al., 2003). No binding to GST alone was detected, demonstrating that this binding was not a result of a non-specific interaction with the GST moiety.

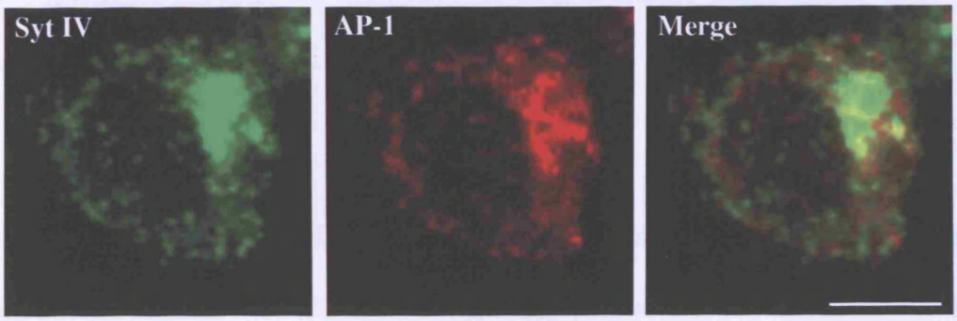

Figure 7.2.1: Syt IV colocalises with AP-1 in the perinuclear region of PC12 cells. PC12 cells were fixed with 3% PFA, permeabilised and double labelled with anti-Syt IV and AP-1 abs. Polyclonal anti-Syt IV and monoclonal anti-AP-1 abs were detected with secondary anti-rabbit Alexa-488 and anti-mouse-Cy3 abs, respectively. Images were acquired by confocal microscopy using LSM 510 software, Zeiss plan-Apochromat 63*/1.40 oil objective lense (bar 5 μM).

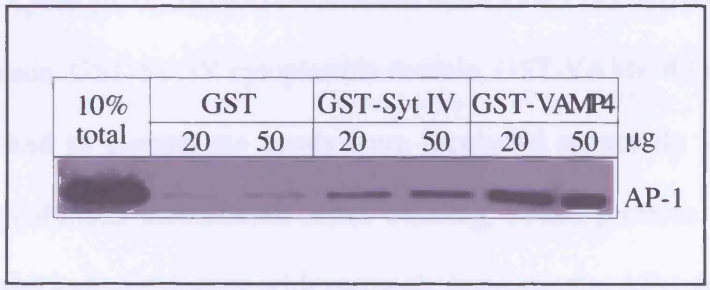

Figure 7.2.2: Syt IV interacts with AP-1 in a GST pull down assay. GST-Syt IV, GST-VAMP4 cytoplasmic domains and GST (20, 50 μg)-bound to glutathione beads were incubated with total PC12 PNS. After washing, bound proteins were lysed in sample buffer and subjected to an SDS-PAGE followed by western blotting with anti-γ-adaptin ab (AP-1).

7.3 Synaptotagmin IV displays a preferential binding to membrane-bound AP-1

Previous work in the lab has demonstrated binding of VAMP-4 to cytosolic AP-1 using bovine adrenal medulla cytosol (BAMC) (Hinners et al., 2003). Similarly to the previous experiment, GST-Syt IV or GST-VAMP-4 cytoplasmic domains, as well as GST alone, were bound to glutathione beads. Proteins bound to beads were further incubated with BAMC, washed and bound proteins were subjected to SDS-PAGE analysis, followed by blotting with anti-Ap-1 ab. Surprisingly, GST-Syt IV did not bind AP-1 very efficiently in these conditions, whereas VAMP-4 binding was robust (Figure 7.3.1). In the previous experiment (Figure 7.2.2), a total PNS containing both cytosolic and membrane-bound AP-1 was used. To confirm differential binding of Syt IV to AP-1, I prepared cytosolic or membranes fraction from total PNS derived from PC12 cells by centrifugation. GST-Syt IV cytoplasmic domain, GST-VAMP-4 cytoplasmic domain and GST bound to glutathione beads were incubated separately with the cytosolic fraction or solubilised membranes. After washing, bound proteins were subjected to SDS-PAGE and immunoblotting with anti-γ-ab. Interestingly, AP-1 from the membrane fraction bound strongly to Syt IV (Figure 7.3.2 A). In contrast, a lower binding of cytosolic AP-1 to Syt IV was observed (Figure 7.3.2 B). VAMP-4 displayed the same degree of binding regardless of the source of AP-1 used. Together, these results demonstrate that Syt IV, in contrast to VAMP-4, binds more efficiently to the

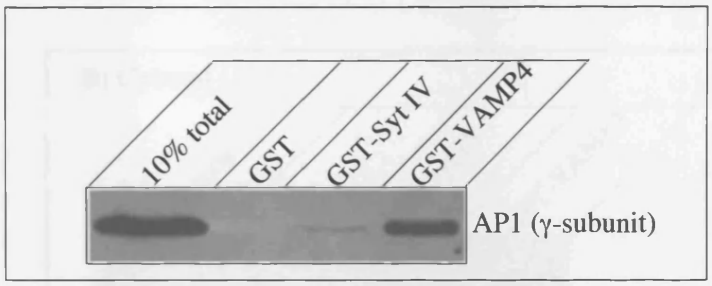

Figure 7.3.1: Syt IV does not bind efficiently to AP-1 from bovine adrenal medulla cytosol (BAMC). GST, GST-Syt IV and GST-Vamp4 cytoplasmic domains (30 μg) bound to glutathione beads were incubated with BAMC. bound proteins were lysed in sample buffer and subjected to SDS-PAGE and blotting with anti-γ-adaptin ab.

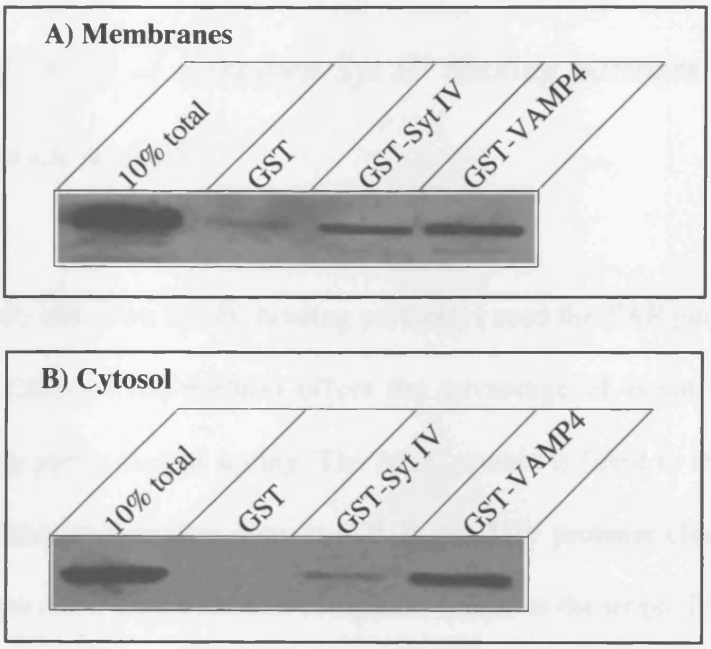

Figure 7.3.2: Syt IV binds preferentially to the membrane-bound AP-1. Total PNS from PC12 cells was subjected to ultracentrifugation to separate cytosol from membrane fractions. The solubilised membranes (A) and cytosolic fractions (B) were later incubated with GST, GST-Syt IV and GST-Vamp4 cytoplasmic domains (30 μg). After washing, bound proteins were lysed in sample buffer and subjected to an SDS-PAGE and blotting with anti-γ-adaptin ab.

membrane-bound than to the cytosolic AP-1. These findings further suggest that Syt IV possesses a different AP-1-binding mechanism than that of VAMP-4.

While I have not determined how this binding occurs, the possibilities as to why Syt IV displays this preferential binding towards AP-1 on membranes will be discussed below.

7.4 *Identification of unknown Syt IV binding partners using the TAP purification method.*

To identify unknown Syt IV binding partners, I used the TAP purification approach (Puig et al., 2001). This method offers the advantage of isolating whole protein complexes in a physiological setting. The target protein is fused to the TAP tag, which contains a calmodulin-binding domain (CBD), the TEV protease cleavage site, and the protein A domain. To purify protein complexes bound to the target TAP-tagged protein, lysates from cells overexpressing the fusion protein are first passed over an IgG column. The tagged protein and its interactors will bind to the IgG beads via the protein A domain. After several washes, the fusion protein is subjected to cleavage with the tobacco etch virus (TEV) protease, which will release the tagged protein and interactors from the IgG column. This eluate is then subjected to a second purification step on a calmodulin column (CBD), where the tagged protein will bind via the CBD domain in a calcium-containing buffer. The tagged protein and its binding partners are finally released from the CBD column with an EGTA-containing buffer. Protein in the eluate is precipitated and subjected to SDS-PAGE, followed by analysis using mass-spectrometry to identify the unknown binding proteins (For illustration, Figure 7.4.1).

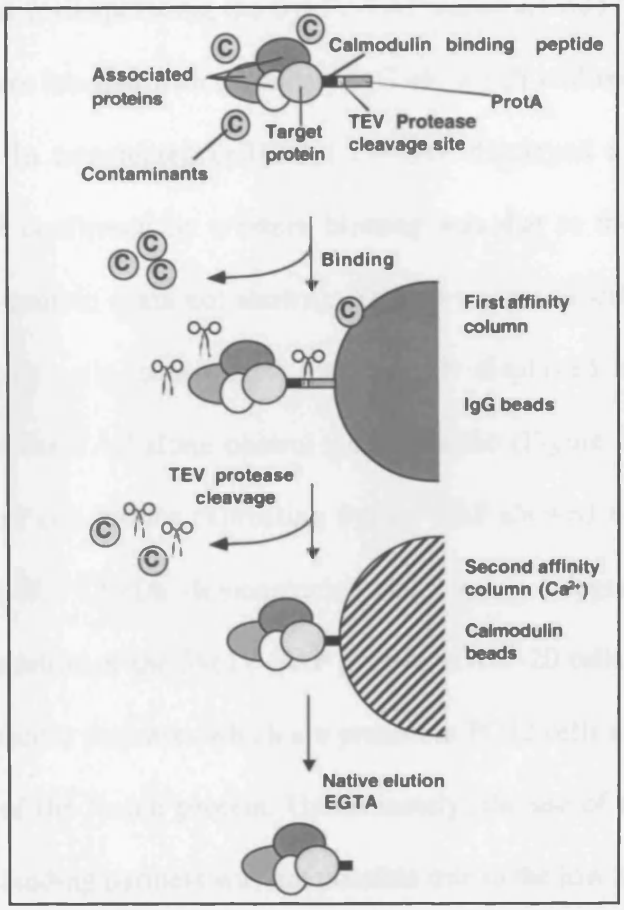

Figure 7.4.1: Tap tag purification method. Cells overexpressing the Tap tag fused to the target protein are lysed and subjected to the first purification step through an IgG-beads column. The fusion protein and its interactors will bind to the column via the protein A domain. After several washes the fusion protein is cleaved with the TEV protease and the protein is then released from the column. The released protein is then subjected to a second purification step through a calmodulin-beads column. Finally, after several washes, the protein and its binding partners are eluted with EGTA. The eluates are precipitated and lysed in sample buffer. Samples are loaded on SDS-PAGE and analysed by mass-spectrometry (Puig A et al 2001).

To apply this method for the identification of unknown binding partners to Syt IV, the TAP tag was fused to the full-length rat-Syt IV at the C-terminus of the protein (Figure 7.4.2 A). To check for expression, the Syt IV-TAP construct was transfected into PC12 cells, and cells were labelled with secondary IgG ab, which will recognise the protein A in the TAP tag. In transfected cells, Syt IV-TAP displayed a dispersed cytosolic staining, which I confirmed by western blotting was due to the degradation of the expressed fusion protein (data not shown). Another neuroendocrine cell line, AtT-20, was used. In these cells, transfected Syt IV-TAP displayed mostly a perinuclear staining, whereas the TAP alone control was cytosolic (Figure 7.4.2 B). In addition, western blotting of cell lysates expressing Syt IV-TAP showed a band at the expected molecular weight of ~ 72 kDa, demonstrating that it was not degraded (Figure 7.4.2 C). The lack of degradation of the Syt IV-TAP protein in AtT-20 cells is presumably due to the absence of specific proteases which are present in PC12 cells and are responsible for the degradation of the fusion protein. Unfortunately, the use of this technique for the identification of binding partners was not possible due to the low transfection efficiency obtained in AtT-20 cells. Scaling-up the number of cells did not yield enough material to be detected by mass-spectroscopy. Another drawback observed when using this technique is the high loss of the fusion protein and bound proteins, due to two successive purifications and several washes. This purification method is certainly very useful, but depends very much on the availability of large amounts of starting material, which are only obtainable from cells where a high transfection efficiency can be obtained.

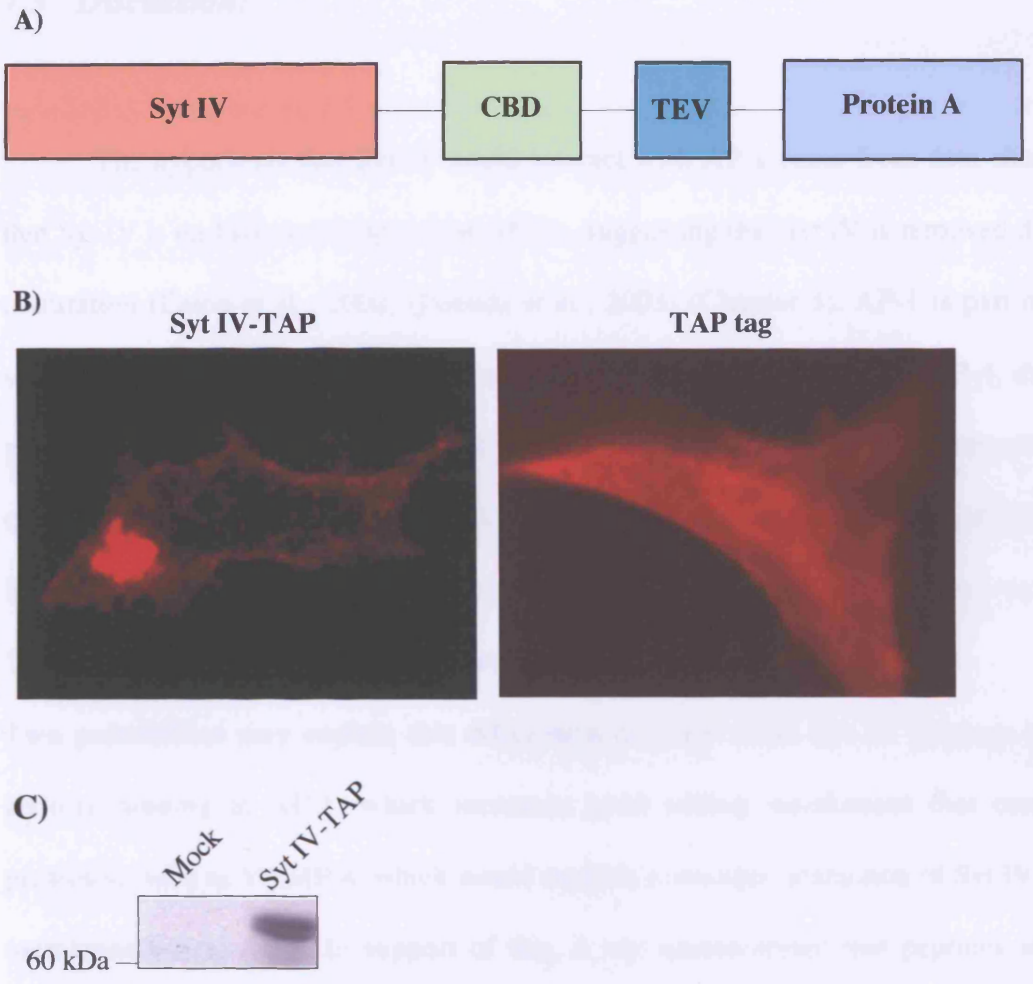

Figure 7.4.2: Expression of Syt IV-TAP and TAP tag in AtT-20 cells.
A) Full length Syt IV was fused to the TAP tag containing the calmodulin binding domain (CBD), the TEV cleavage site (Tabbaco Etch Virus site) and protein A (two IgG domains repeats). B) Syt IV-TAP and TAP tag (right) were transfected into AtT-20 cells using Lipofectamine 2000. Cells were then fixed with 3% PFA, permeabilised and labelled with the secondary anti-goat-Rhodamine-conjugated ab. Images were acquired using confocal microscopy and LSM 510 software. C)AtT-20 cells were Transfected with Syt IV-TAP or mock transfecd with transfection reagent alone. Cells were then lysed in Triton X-100-containing buffer and and loaded on an SDS-PAGE gel followed by blotting using HRP-labeled-secondary ab.

7.5 Discussion:

The hypothesis that Syt IV could interact with AP-1 came from data showing that Syt IV is on ISGs and absent from MSGs, suggesting that Syt IV is removed during maturation (Eaton et al., 2000) (Fukuda et al., 2003) (Chapter 3). AP-1 is part of the sorting machinery involved in a removal of ISG proteins, such as VAMP-4, during granule maturation (Hinners et al., 2003). GST-pull-down experiments performed with cytosol or membranes as sources of AP-1 revealed that Syt IV displays a preferential binding to the membrane-bound form. This was unexpected, as proteins, such as VAMP4 (Hinners et al., 2003), bind to cytosolic AP-1.

Two possibilities may explain this differential binding: First, Syt IV displays a low affinity binding to AP-1, which increases upon adding membranes that contains protein(s), such as VAMP-4, which would mediate a stronger interaction of Syt IV with membrane-bound AP-1. In support of this, it was demonstrated that peptides with a tyrosine-based endocytic motif, present in other cargo proteins, stimulated binding of AP-2 to Syt I, and enhanced AP-2 recruitment to the plasma membrane (Haucke and De Camilli, 1999). This suggested a mechanism by which the interaction of AP-2 with Syt I is enhanced by the presence of additional cargo proteins to be loaded in the nascent endocytic vesicle, making Syt I part of a docking complex for AP-2.

Proteins bind to AP-1 via tyrosine or di-leucine-based sorting motifs present in their cytoplasmic tails (Bonifacino and Traub, 2003). It is therefore possible that cargo proteins containing these motifs, which are loaded in CCVs forming from ISGs, could in the same way inhance the affinity of Syt IV with AP-1. This hypothesis can be tested by incubating the GST-Syt IV cytoplasmic domain with BAMC or PNS from PC12

cells in the presence of peptides containing either tyrosine or di-leucine motifs, and asking whether the binding of Syt IV to AP-1 can be stimulated in these conditions.

The second hypothesis arising from the finding that Syt IV displays stronger binding to membrane-bound compared to the cytosolic AP-1, is that Syt IV may bind specifically to the phosphorylated form of AP-1. It was demonstrated that AP-1, upon membrane binding, becomes phosphorylated on the μ1 subunit, and dephosphorylated on the β1 subunit (Ghosh and Kornfeld, 2003). The phosphorylation of the μ1 subunit of AP-1 enhances binding to the tyrosine sorting signal in the cytoplasmic tails of MPR cargo molecules, which was suggested to facilitate their capture and retention in the forming CCVs (Ghosh and Kornfeld, 2003). It will be interesting to investigate whether the same applies for Syt IV. Extracting AP-1 from purified CCVs with Protein phosphatase 2A (PP2A) and Hsc-70, which induce dephosphorylation of AP-1 and its subsequent release (Ghosh and Kornfeld, 2003), and testing whether it will decrease the binding to Syt IV, will help answer this question.

In addition, to determine whether the binding to AP-1 mediates the sorting of Syt IV from ISGs, it will be interesting to identify the motif within the Syt IV cytoplasmic domain responsible for this interaction. Proteins have been shown to mediate binding to μ1 subunit of AP-1 via both a tyrosine-based motif, such as that in CD-MPR (Ghosh and Kornfeld, 2004) and via a di-leucine-based motif, such as that in VAMP4 (Peden et al., 2001). Interestingly, the Syt IV-C2B domain contains a tyrosine–based motif ($_{297}$YQST$_{300}$) that could mediate the binding to AP-1. However, it is also possible that Syt IV could interact with AP-1 via an unusual unidentified motif present in its cytoplasmic domain. Indeed, the binding of Syt I to AP-2 is mediated via a double lysine motif (Chapman et al., 1998), which is also found in the SytIV cytoplasmic

domain. Mutation of the tyrosine and the double lysine motifs in Syt IV will reveal their requirement for AP-1 binding.

Addressing these questions will help further our understanding of how Syt IV is sorted from ISGs, and more importantly, how the differential binding to AP-1 contributes to the removal of proteins during granule maturation.

8 Chapter 8: Concluding remarks

The similar distribution of Syt IV to the SNAREs Stx6 and VAMP4 on ISGs, and not MSGs, in neuroendocrine cells (Eaton et al., 2000) (Wendler et al., 2001) (Chapter 3), prompted me to investigate whether Syt IV is part of a protein machinery involved in secretory granule maturation.

I showed using *in vitro* and *in vivo* approaches that the Syt IV cytoplasmic domain, as well as siRNA against Syt IV, inhibited ISG-ISG fusion as well as SgII processing, demonstrating that Syt IV is required for secretory granule maturation.

The interaction of Syt IV with Stx6 further suggested that they might be part of the same complex regulating ISG homotypic fusion, an essential step during granule maturation in PC12 cells. This study has identified a novel component of the putative complex involved in ISG-ISG fusion. It would be interesting to use Syt IV as a "bait" in interaction studies to characterise the full protein complex involved in ISG homotypic fusion. Identification of the complete complex will advance our understanding of this membrane fusion event in particular, and the regulation of ISG maturation in general.

Furthermore, the continued dissection of Syt IV function in ISG fusion, such as the fusion step it regulates or the mode of its binding to Stx6, will be additional questions to answer. Doing so will give further clues on the way this family of proteins regulate membrane fusion events. Moreover, comparing the mode of function between Syt IV and the calcium-dependent phospholipid-binding protein Syt I, will reveal similarities as well as differences in the way they regulate fusion.

It would also be of great interest to analyse Syt IV-knock-out mice. In particular, investigating whether the granule size or content is affected in the endocrine or

neuroendocrine cells of these mice will give additional proof that Syt IV is important for secretory granule maturation under physiological conditions.

Finally, this study has revealed a novel role for Syt IV in an intracellular membrane fusion event, and reinforces the notion that this family of proteins participate in distinct membrane trafficking events.

9 Chapter 9: References

Adolfsen, B., S. Saraswati, M. Yoshihara, and J.T. Littleton. 2004. Synaptotagmins are trafficked to distinct subcellular domains including the postsynaptic compartment. *J. Cell Biol.* 166:249-260.

Anderson, R.G., J.R. Falck, J.L. Goldstein, and M.S. Brown. 1984. Visualization of acidic organelles in intact cells by electron microscopy. *Proc Natl Acad Sci U S A.* 81:4838-42.

Anderson, R.G., and L. Orci. 1988. A view of acidic intracellular compartments. *J Cell Biol.* 106:539-43.

Andres, D.A., M.C. Seabra, M.S. Brown, S.A. Armstrong, T.E. Smeland, F.P. Cremers, and J.L. Goldstein. 1993. cDNA cloning of component A of Rab geranylgeranyl transferase and demonstration of its role as a Rab escort protein. *Cell.* 73:1091-9.

Arvan, P., and D. Castle. 1998. Sorting and storage during secretory granule biogenesis: looking backward and looking forward. *Biochem J.* 332 (Pt 3):593-610.

Austin, C., I. Hinners, and S.A. Tooze. 2000. Direct and GTP-dependent interaction of ADP-ribosylation factor 1 with clathrin adaptor protein AP-1 on immature secretory granules. *J Biol Chem.* 275:21862-9.

Baeuerle, P.A., and W.B. Huttner. 1987. Tyrosine sulfation is a trans-Golgi-specific protein modification. *J Cell Biol.* 105:2655-64.

Bai, J., and E.R. Chapman. 2004. The C2 domains of synaptotagmin--partners in exocytosis. *Trends Biochem Sci.* 29:143-51.

Bai, J., C.A. Earles, J.L. Lewis, and E.R. Chapman. 2000. Membrane-embedded synaptotagmin penetrates cis or trans target membranes and clusters via a novel mechanism. *J Biol Chem.* 275:25427-35.

Bai, J., W.C. Tucker, and E.R. Chapman. 2004a. PIP2 increases the speed of response of synaptotagmin and steers its membrane-penetration activity toward the plasma membrane. *Nat Struct Mol Biol.* 11:36-44.

Bai, J., C.T. Wang, D.A. Richards, M.B. Jackson, and E.R. Chapman. 2004b. Fusion pore dynamics are regulated by synaptotagmin*t-SNARE interactions. *Neuron.* 41:929-42.

Bai, J., P. Wang, and E.R. Chapman. 2002. C2A activates a cryptic Ca(2+)-triggered membrane penetration activity within the C2B domain of synaptotagmin I. *Proc Natl Acad Sci U S A.* 99:1665-70.

Bayer, M.J., C. Reese, S. Buhler, C. Peters, and A. Mayer. 2003. Vacuole membrane fusion: V0 functions after trans-SNARE pairing and is coupled to the Ca2+-releasing channel. *J Cell Biol.* 162:211-22.

Benjannet, S., N. Rondeau, R. Day, M. Chretien, and N.G. Seidah. 1991. PC1 and PC2 are proprotein convertases capable of cleaving proopiomelanocortin at distinct pairs of basic residues. *Proc Natl Acad Sci U S A.* 88:3564-8.

Bennett, M.K., N. Calakos, and R.H. Scheller. 1992. Syntaxin: a synaptic protein implicated in docking of synaptic vesicles at presynaptic active zones. *Science.* 257:255-9.

Berton, F., V. Cornet, C. Iborra, J. Garrido, B. Dargent, M. Fukuda, M. Seagar, and B. Marqueze. 2000. Synaptotagmin I and IV define distinct populations of neuronal transport vesicles. *Eur J Neurosci.* 12:1294-302.

Blott, E.J., and G.M. Griffiths. 2002. Secretory lysosomes. *Nat Rev Mol Cell Biol.* 3:122-31.

Bock, J.B., J. Klumperman, S. Davanger, and R.H. Scheller. 1997. Syntaxin 6 functions in trans-Golgi network vesicle trafficking. *Mol Biol Cell.* 8:1261-71.

Bock, J.B., H.T. Matern, A.A. Peden, and R.H. Scheller. 2001. A genomic perspective on membrane compartment organization. *Nature.* 409:839-41.

Bommert, K., M.P. Charlton, W.M. DeBello, G.J. Chin, H. Betz, and G.J. Augustine. 1993. Inhibition of neurotransmitter release by C2-domain peptides implicates synaptotagmin in exocytosis. *Nature.* 363:163-5.

Bonifacino, J.S., and B.S. Glick. 2004. The mechanisms of vesicle budding and fusion. *Cell.* 116:153-66.

Bonifacino, J.S., and L.M. Traub. 2003. Signals for sorting of transmembrane proteins to endosomes and lysosomes. *Annu Rev Biochem.* 72:395-447.

Bryant, N.J., and D.E. James. 2001. Vps45p stabilizes the syntaxin homologue Tlg2p and positively regulates SNARE complex formation. *Embo J.* 20:3380-8.

Burgoyne, R.D., and M.J. Clague. 2003. Calcium and calmodulin in membrane fusion. *Biochim Biophys Acta.* 1641:137-43.

Cain, C.C., D.M. Sipe, and R.F. Murphy. 1989. Regulation of endocytic pH by the Na+,K+-ATPase in living cells. *Proc Natl Acad Sci U S A.* 86:544-8.

Carty, S.E., R.G. Johnson, and A. Scarpa. 1982. Electrochemical proton gradient in dense granules isolated from anterior pituitary. *J Biol Chem.* 257:7269-73.

Chanat, E., and W.B. Huttner. 1991. Milieu-induced, selective aggregation of regulated secretory proteins in the trans-Golgi network. *J Cell Biol.* 115:1505-19.

Chanat, E., U. Weiss, and W.B. Huttner. 1994. The disulfide bond in chromogranin B, which is essential for its sorting to secretory granules, is not required for its aggregation in the trans-Golgi network. *FEBS Lett.* 351:225-30.

Chanat, E., U. Weiss, W.B. Huttner, and S.A. Tooze. 1993. Reduction of the disulfide bond of chromogranin B (secretogranin I) in the trans-Golgi network causes its missorting to the constitutive secretory pathways. *Embo J.* 12:2159-68.

Chapman, E.R. 2002. Synaptotagmin: a Ca(2+) sensor that triggers exocytosis? *Nat Rev Mol Cell Biol.* 3:498-508.

Chapman, E.R., S. An, J.M. Edwardson, and R. Jahn. 1996. A novel function for the second C2 domain of synaptotagmin. Ca2+-triggered dimerization. *J Biol Chem.* 271:5844-9.

Chapman, E.R., R.C. Desai, A.F. Davis, and C.K. Tornehl. 1998. Delineation of the oligomerization, AP-2 binding, and synprint binding region of the C2B domain of synaptotagmin. *J Biol Chem.* 273:32966-72.

Chapman, E.R., P.I. Hanson, S. An, and R. Jahn. 1995. Ca2+ regulates the interaction between synaptotagmin and syntaxin 1. *J Biol Chem.* 270:23667-71.

Chen, Y.A., S.J. Scales, S.M. Patel, Y.C. Doung, and R.H. Scheller. 1999. SNARE complex formation is triggered by Ca2+ and drives membrane fusion. *Cell.* 97:165-74.

Chen, Y.A., and R.H. Scheller. 2001. SNARE-mediated membrane fusion. *Nat Rev Mol Cell Biol.* 2:98-106.

Chieregatti, E., J.W. Witkin, and G. Baldini. 2002. SNAP-25 and synaptotagmin 1 function in Ca2+-dependent reversible docking of granules to the plasma membrane. *Traffic.* 3:496-511.

Christoforidis, S., H.M. McBride, R.D. Burgoyne, and M. Zerial. 1999a. The Rab5 effector EEA1 is a core component of endosome docking. *Nature.* 397:621-5.

Christoforidis, S., M. Miaczynska, K. Ashman, M. Wilm, L. Zhao, S.C. Yip, M.D. Waterfield, J.M. Backer, and M. Zerial. 1999b. Phosphatidylinositol-3-OH kinases are Rab5 effectors. *Nat Cell Biol.* 1:249-52.

Ciufo, L.F., J.W. Barclay, R.D. Burgoyne, and A. Morgan. 2005. Munc18-1 regulates early and late stages of exocytosis via syntaxin-independent protein interactions. *Mol Biol Cell.* 16:470-82.

Colombo, M.I., W. Beron, and P.D. Stahl. 1997. Calmodulin regulates endosome fusion. *J Biol Chem.* 272:7707-12.

Cool, D.R., E. Normant, F. Shen, H.C. Chen, L. Pannell, Y. Zhang, and Y.P. Loh. 1997. Carboxypeptidase E is a regulated secretory pathway sorting receptor: genetic obliteration leads to endocrine disorders in Cpe(fat) mice. *Cell.* 88:73-83.

Craxton, M. 2004. Synaptotagmin gene content of the sequenced genomes. *BMC Genomics.* 5:43.

Creutz, C.E., S.L. Snyder, and T.A. Schulz. 2004. Characterization of the yeast tricalbins: membrane-bound multi-C2-domain proteins that form complexes involved in membrane trafficking. *Cell Mol Life Sci.* 61:1208-20.

Dai, H., O.H. Shin, M. Machius, D.R. Tomchick, T.C. Sudhof, and J. Rizo. 2004. Structural basis for the evolutionary inactivation of Ca(2+) binding to synaptotagmin 4. *Nat Struct Mol Biol.* 11:844-849.

Davidson, H.W., C.J. Rhodes, and J.C. Hutton. 1988. Intraorganellar calcium and pH control proinsulin cleavage in the pancreatic beta cell via two distinct site-specific endopeptidases. *Nature.* 333:93-6.

Davletov, B.A., and T.C. Sudhof. 1993. A single C2 domain from synaptotagmin I is sufficient for high affinity Ca2+/phospholipid binding. *J Biol Chem.* 268:26386-90.

Desai, R.C., B. Vyas, C.A. Earles, J.T. Littleton, J.A. Kowalchyck, T.F. Martin, and E.R. Chapman. 2000. The C2B domain of synaptotagmin is a Ca(2+)-sensing module essential for exocytosis. *J Cell Biol.* 150:1125-36.

DiAntonio, A., K.D. Parfitt, and T.L. Schwarz. 1993. Synaptic transmission persists in synaptotagmin mutants of Drosophila. *Cell.* 73:1281-90.

Dittie, A.S., N. Hajibagheri, and S.A. Tooze. 1996. The AP-1 adaptor complex binds to immature secretory granules from PC12 cells, and is regulated by ADP-ribosylation factor. *J Cell Biol.* 132:523-36.

Dittie, A.S., J. Klumperman, and S.A. Tooze. 1999. Differential distribution of mannose-6-phosphate receptors and furin in immature secretory granules. *J Cell Sci.* 112 (Pt 22):3955-66.

Dittie, A.S., L. Thomas, G. Thomas, and S.A. Tooze. 1997. Interaction of furin in immature secretory granules from neuroendocrine cells with the AP-1 adaptor complex is modulated by casein kinase II phosphorylation. *Embo J.* 16:4859-70.

Dittie, A.S., and S.A. Tooze. 1995. Characterization of the endopeptidase PC2 activity towards secretogranin II in stably transfected PC12 cells. *Biochem J.* 310 (Pt 3):777-87.

Duden, R. 2003. ER-to-Golgi transport: COP I and COP II function (Review). *Mol Membr Biol.* 20:197-207.

Earles, C.A., J. Bai, P. Wang, and E.R. Chapman. 2001. The tandem C2 domains of synaptotagmin contain redundant Ca2+ binding sites that cooperate to engage t-SNAREs and trigger exocytosis. *J Cell Biol.* 154:1117-23.

Eaton, B.A., M. Haugwitz, D. Lau, and H.P. Moore. 2000. Biogenesis of regulated exocytotic carriers in neuroendocrine cells. *J Neurosci.* 20:7334-44.

Elferink, L.A., M.R. Peterson, and R.H. Scheller. 1993. A role for synaptotagmin (p65) in regulated exocytosis. *Cell.* 72:153-9.

Farquhar, M.G., and G.E. Palade. 1981. The Golgi apparatus (complex)-(1954-1981)-from artifact to center stage. *J Cell Biol.* 91:77s-103s.

Fasshauer, D., H. Otto, W.K. Eliason, R. Jahn, and A.T. Brunger. 1997. Structural changes are associated with soluble N-ethylmaleimide-sensitive fusion protein attachment protein receptor complex formation. *J Biol Chem.* 272:28036-41.

Fasshauer, D., R.B. Sutton, A.T. Brunger, and R. Jahn. 1998. Conserved structural features of the synaptic fusion complex: SNARE proteins reclassified as Q- and R-SNAREs. *Proc Natl Acad Sci U S A.* 95:15781-6.

Ferguson, G.D., S.G. Anagnostaras, A.J. Silva, and H.R. Herschman. 2000. Deficits in memory and motor performance in synaptotagmin IV mutant mice. *Proc Natl Acad Sci U S A.* 97:5598-603.

Ferguson, G.D., D.M. Thomas, L.A. Elferink, and H.R. Herschman. 1999. Synthesis degradation, and subcellular localization of synaptotagmin IV, a neuronal immediate early gene product. *J Neurochem.* 72:1821-31.

Fernandez, I., D. Arac, J. Ubach, S.H. Gerber, O. Shin, Y. Gao, R.G. Anderson, T.C. Sudhof, and J. Rizo. 2001. Three-dimensional structure of the synaptotagmin 1 C2B-domain: synaptotagmin 1 as a phospholipid binding machine. *Neuron.* 32:1057-69.

Fernandez-Chacon, R., A. Konigstorfer, S.H. Gerber, J. Garcia, M.F. Matos, C.F. Stevens, N. Brose, J. Rizo, C. Rosenmund, and T.C. Sudhof. 2001. Synaptotagmin I functions as a calcium regulator of release probability. *Nature.* 410:41-9.

Fuchs, R., S. Schmid, and I. Mellman. 1989. A possible role for Na+,K+-ATPase in regulating ATP-dependent endosome acidification. *Proc Natl Acad Sci U S A.* 86:539-43.

Fukuda, M. 2004. RNA interference-mediated silencing of synaptotagmin IX, but not synaptotagmin I, inhibits dense-core vesicle exocytosis in PC12 cells. *Biochem J.* 380:875-9.

Fukuda, M., E. Kanno, and K. Mikoshiba. 1999. Conserved N-terminal cysteine motif is essential for homo- and heterodimer formation of synaptotagmins III, V, VI, and X. *J Biol Chem.* 274:31421-7.

Fukuda, M., E. Kanno, Y. Ogata, C. Saegusa, T. Kim, Y.P. Loh, and A. Yamamoto. 2003. Nerve Growth Factor-dependent Sorting of Synaptotagmin IV Protein to Mature Dense-core Vesicles That Undergo Calcium-dependent Exocytosis in PC12 Cells. *J. Biol. Chem.* 278:3220-3226.

Fukuda, M., E. Kanno, M. Satoh, C. Saegusa, and A. Yamamoto. 2004. Synaptotagmin VII is targeted to dense-core vesicles and regulates their Ca2+ -dependent exocytosis in PC12 cells. *J Biol Chem.* 279:52677-84.

Fukuda, M., T. Kojima, and K. Mikoshiba. 1996. Phospholipid composition dependence of Ca2+-dependent phospholipid binding to the C2A domain of synaptotagmin IV. *J Biol Chem.* 271:8430-4.

Fukuda, M., J.A. Kowalchyk, X. Zhang, T.F. Martin, and K. Mikoshiba. 2002. Synaptotagmin IX regulates Ca2+-dependent secretion in PC12 cells. *J Biol Chem.* 277:4601-4.

Fukuda, M., and K. Mikoshiba. 2000a. Calcium-dependent and -independent hetero-oligomerization in the synaptotagmin family. *J Biochem (Tokyo).* 128:637-45.

Fukuda, M., and K. Mikoshiba. 2000b. Distinct self-oligomerization activities of synaptotagmin family. Unique calcium-dependent oligomerization properties of synaptotagmin VII. *J Biol Chem.* 275:28180-5.

Fukuda, M., and A. Yamamoto. 2004. Effect of forskolin on synaptotagmin IV protein trafficking in PC12 cells. *J Biochem (Tokyo).* 136:245-53.

Geppert, M., Y. Goda, R.E. Hammer, C. Li, T.W. Rosahl, C.F. Stevens, and T.C. Sudhof. 1994. Synaptotagmin I: a major Ca2+ sensor for transmitter release at a central synapse. *Cell.* 79:717-27.

Gerdes, H.H., P. Rosa, E. Phillips, P.A. Baeuerle, R. Frank, P. Argos, and W.B. Huttner. 1989. The primary structure of human secretogranin II, a widespread tyrosine-sulfated secretory granule protein that exhibits low pH- and calcium-induced aggregation. *J Biol Chem.* 264:12009-15.

Gerona, R.R., E.C. Larsen, J.A. Kowalchyk, and T.F. Martin. 2000. The C terminus of SNAP25 is essential for Ca(2+)-dependent binding of synaptotagmin to SNARE complexes. *J Biol Chem.* 275:6328-36.

Gerst, J.E. 2003. SNARE regulators: matchmakers and matchbreakers. *Biochim Biophys Acta.* 1641:99-110.

Ghosh, P., and S. Kornfeld. 2003. AP-1 binding to sorting signals and release from clathrin-coated vesicles is regulated by phosphorylation. *J Cell Biol.* 160:699-708.

Ghosh, P., and S. Kornfeld. 2004. The cytoplasmic tail of the cation-independent mannose 6-phosphate receptor contains four binding sites for AP-1. *Arch Biochem Biophys.* 426:225-30.

Gorvel, J.P., P. Chavrier, M. Zerial, and J. Gruenberg. 1991. rab5 controls early endosome fusion in vitro. *Cell.* 64:915-25.

Gowda, D.C., B. Goossen, R.K. Margolis, and R.U. Margolis. 1989. Chondroitin sulfate and heparan sulfate proteoglycans of PC12 pheochromocytoma cells. *J Biol Chem.* 264:11436-43.

Grass, I., S. Thiel, S. Honing, and V. Haucke. 2004. Recognition of a basic AP-2 binding motif within the C2B domain of synaptotagmin is dependent on multimerization. *J Biol Chem.* 279:54872-80.

Grimberg, E., Z. Peng, I. Hammel, and R. Sagi-Eisenberg. 2003. Synaptotagmin III is a critical factor for the formation of the perinuclear endocytic recycling compartment and determination of secretory granules size. *J Cell Sci.* 116:145-154.

Gumbiner, B., and R.B. Kelly. 1981. Secretory granules of an anterior pituitary cell line, AtT-20, contain only mature forms of corticotropin and beta-lipotropin. *Proc Natl Acad Sci U S A.* 78:318-22.

Haberman, Y., E. Grimberg, M. Fukuda, and R. Sagi-Eisenberg. 2003. Synaptotagmin IX, a possible linker between the perinuclear endocytic recycling compartment and the microtubules. *J Cell Sci.* 116:4307-18.

Haucke, V., and P. De Camilli. 1999. AP-2 recruitment to synaptotagmin stimulated by tyrosine-based endocytic motifs. *Science.* 285:1268-71.

Hayashi, T., H. McMahon, S. Yamasaki, T. Binz, Y. Hata, T.C. Sudhof, and H. Niemann. 1994. Synaptic vesicle membrane fusion complex: action of clostridial neurotoxins on assembly. *Embo J.* 13:5051-61.

Heinemann, C., R.H. Chow, E. Neher, and R.S. Zucker. 1994. Kinetics of the secretory response in bovine chromaffin cells following flash photolysis of caged Ca2+. *Biophys J.* 67:2546-57.

Heumann, R., V. Kachel, and H. Thoenen. 1983. Relationship between NGF-mediated volume increase and "priming effect" in fast and slow reacting clones of PC12 pheochromocytoma cells. Role of cAMP. *Exp Cell Res.* 145:179-90.

Hinners, I., F. Wendler, H. Fei, L. Thomas, G. Thomas, and S.A. Tooze. 2003. AP-1 recruitment to VAMP4 is modulated by phosphorylation-dependent binding of PACS-1. *EMBO Rep.* 4:1182-9.

Hu, C., M. Ahmed, T.J. Melia, T.H. Sollner, T. Mayer, and J.E. Rothman. 2003. Fusion of cells by flipped SNAREs. *Science.* 300:1745-9.

Hui, E., J. Bai, P. Wang, M. Sugimori, R.R. Llinas, and E.R. Chapman. 2005. Three distinct kinetic groupings of the synaptotagmin family: candidate sensors for rapid and delayed exocytosis. *Proc Natl Acad Sci U S A.* 102:5210-4.

Hutton, J.C. 1982. The internal pH and membrane potential of the insulin-secretory granule. *Biochem J.* 204:171-8.

Ibata, K., M. Fukuda, T. Hamada, H. Kabayama, and K. Mikoshiba. 2000. Synaptotagmin IV is present at the Golgi and distal parts of neurites. *J Neurochem.* 74:518-26.

Irminger, J.C., C.B. Verchere, K. Meyer, and P.A. Halban. 1997. Proinsulin targeting to the regulated pathway is not impaired in carboxypeptidase E-deficient Cpefat/Cpefat mice. *J Biol Chem.* 272:27532-4.

Jahn, R., and T.C. Sudhof. 1999. Membrane fusion and exocytosis. *Annu. Rev. Biochem.* 68:863-911.

Johnson, R.G., and A. Scarpa. 1976. Internal pH of isolated chromaffin vesicles. *J Biol Chem.* 251:2189-91.

Kee, Y., and R.H. Scheller. 1996. Localization of synaptotagmin-binding domains on syntaxin. *J Neurosci.* 16:1975-81.

Kimura, J.H., L.S. Lohmander, and V.C. Hascall. 1984. Studies on the biosynthesis of cartilage proteoglycan in a model system of cultured chondrocytes from the Swarm rat chondrosarcoma. *J Cell Biochem.* 26:261-78.

Klumperman, J., R. Kuliawat, J.M. Griffith, H.J. Geuze, and P. Arvan. 1998. Mannose 6-phosphate receptors are sorted from immature secretory granules via adaptor protein AP-1, clathrin, and syntaxin 6-positive vesicles. *J Cell Biol.* 141:359-71.

Klyachko, V.A., and M.B. Jackson. 2002. Capacitance steps and fusion pores of small and large-dense-core vesicles in nerve terminals. *Nature.* 418:89-92.

Kornfeld, S., and I. Mellman. 1989. The biogenesis of lysosomes. *Annu Rev Cell Biol.* 5:483-525.

Kreykenbohm, V., D. Wenzel, W. Antonin, V. Atlachkine, and G.F. von Mollard. 2002. The SNAREs vti1a and vti1b have distinct localization and SNARE complex partners. *Eur J Cell Biol.* 81:273-80.

Kromer, A., M.M. Glombik, W.B. Huttner, and H.H. Gerdes. 1998. Essential role of the disulfide-bonded loop of chromogranin B for sorting to secretory granules is revealed by expression of a deletion mutant in the absence of endogenous granin synthesis. *J Cell Biol.* 140:1331-46.

Kuliawat, R., and P. Arvan. 1992. Protein targeting via the "constitutive-like" secretory pathway in isolated pancreatic islets: passive sorting in the immature granule compartment. *J Cell Biol.* 118:521-9.

Kuliawat, R., and P. Arvan. 1994. Distinct molecular mechanisms for protein sorting within immature secretory granules of pancreatic beta-cells. *J Cell Biol.* 126:77-86.

Kuliawat, R., E. Kalinina, J. Bock, L. Fricker, T.E. McGraw, S.R. Kim, J. Zhong, R. Scheller, and P. Arvan. 2004. Syntaxin-6 SNARE involvement in secretory and

endocytic pathways of cultured pancreatic beta-cells. *Mol Biol Cell.* 15:1690-701.

Kuliawat, R., J. Klumperman, T. Ludwig, and P. Arvan. 1997. Differential sorting of lysosomal enzymes out of the regulated secretory pathway in pancreatic beta-cells. *J Cell Biol.* 137:595-608.

Ladinsky, M.S., J.R. Kremer, P.S. Furcinitti, J.R. McIntosh, and K.E. Howell. 1994. HVEM tomography of the trans-Golgi network: structural insights and identification of a lace-like vesicle coat. *J Cell Biol.* 127:29-38.

Lamango, N.S., E. Apletalina, J. Liu, and I. Lindberg. 1999. The proteolytic maturation of prohormone convertase 2 (PC2) is a pH-driven process. *Arch Biochem Biophys.* 362:275-82.

Littleton, J.T., J. Bai, B. Vyas, R. Desai, A.E. Baltus, M.B. Garment, S.D. Carlson, B. Ganetzky, and E.R. Chapman. 2001. synaptotagmin mutants reveal essential functions for the C2B domain in Ca2+-triggered fusion and recycling of synaptic vesicles in vivo. *J Neurosci.* 21:1421-33.

Littleton, J.T., T.L. Serano, G.M. Rubin, B. Ganetzky, and E.R. Chapman. 1999. Synaptic function modulated by changes in the ratio of synaptotagmin I and IV. *Nature.* 400:757-60.

Machado, H.B., W. Liu, L.J. Vician, and H.R. Herschman. 2004. Synaptotagmin IV overexpression inhibits depolarization-induced exocytosis in PC12 cells. *J Neurosci Res.* 76:334-41.

Mallard, F., B.L. Tang, T. Galli, D. Tenza, A. Saint-Pol, X. Yue, C. Antony, W. Hong, B. Goud, and L. Johannes. 2002. Early/recycling endosomes-to-TGN transport involves two SNARE complexes and a Rab6 isoform. *J Cell Biol.* 156:653-64.

Matthew, W.D., L. Tsavaler, and L.F. Reichardt. 1981. Identification of a synaptic vesicle-specific membrane protein with a wide distribution in neuronal and neurosecretory tissue. *J Cell Biol.* 91:257-69.

Mayer, A. 2001. What drives membrane fusion in eukaryotes? *Trends Biochem Sci.* 26:717-23.

Mbikay, M., N.G. Seidah, and M. Chretien. 2001. Neuroendocrine secretory protein 7B2: structure, expression and functions. *Biochem J.* 357:329-42.

McBride, H.M., V. Rybin, C. Murphy, A. Giner, R. Teasdale, and M. Zerial. 1999. Oligomeric complexes link Rab5 effectors with NSF and drive membrane fusion via interactions between EEA1 and syntaxin 13. *Cell.* 98:377-86.

McNew, J.A., F. Parlati, R. Fukuda, R.J. Johnston, K. Paz, F. Paumet, T.H. Sollner, and J.E. Rothman. 2000. Compartmental specificity of cellular membrane fusion encoded in SNARE proteins. *Nature.* 407:153-9.

Mills, I.G., A.T. Jones, and M.J. Clague. 1999. Regulation of endosome fusion. *Mol Membr Biol.* 16:73-9.

Mills, I.G., S. Urbe, and M.J. Clague. 2001. Relationships between EEA1 binding partners and their role in endosome fusion. *J Cell Sci.* 114:1959-65.

Misura, K.M., J.B. Bock, L.C. Gonzalez, Jr., R.H. Scheller, and W.I. Weis. 2002. Three-dimensional structure of the amino-terminal domain of syntaxin 6, a SNAP-25 C homolog. *Proc Natl Acad Sci U S A.* 99:9184-9.

Misura, K.M., R.H. Scheller, and W.I. Weis. 2000. Three-dimensional structure of the neuronal-Sec1-syntaxin 1a complex. *Nature.* 404:355-62.

Moore, H.P., J.M. Andresen, B.A. Eaton, M. Grabe, M. Haugwitz, M.M. Wu, and T.E. Machen. 2002. Biosynthesis and secretion of pituitary hormones: dynamics and regulation. *Arch Physiol Biochem.* 110:16-25.

Muller, L., X. Zhu, and I. Lindberg. 1997. Mechanism of facilitation of PC2 maturation by 7B2: Involvement in pro-PC2 transport and activation but not folding. *J. Cell Biol.* 139:625-638.

Munson, M., X. Chen, A.E. Cocina, S.M. Schultz, and F.M. Hughson. 2000. Interactions within the yeast t-SNARE Sso1p that control SNARE complex assembly. *Nat Struct Biol.* 7:894-902.

Natori, S., and W.B. Huttner. 1996. Chromogranin B (secretogranin I) promotes sorting to the regulated secretory pathway of processing intermediates derived from a peptide hormone precursor. *Proc Natl Acad Sci U S A.* 93:4431-6.

Nichols, B.J., C. Ungermann, H.R. Pelham, W.T. Wickner, and A. Haas. 1997. Homotypic vacuolar fusion mediated by t- and v-SNAREs. *Nature.* 387:199-202.

Nicholson-Tomishima, K., and T.A. Ryan. 2004. Kinetic efficiency of endocytosis at mammalian CNS synapses requires synaptotagmin I. *Proc Natl Acad Sci U S A.* 101:16648-52.

Nonet, M.L., K. Grundahl, B.J. Meyer, and J.B. Rand. 1993. Synaptic function is impaired but not eliminated in C. elegans mutants lacking synaptotagmin. *Cell.* 73:1291-305.

Orci, L. 1986. The morphology of proinsulin processing. *Ann N Y Acad Sci.* 488:292-316.

Orci, L., P. Halban, M. Amherdt, M. Ravazzola, J.D. Vassalli, and A. Perrelet. 1984. A clathrin-coated, Golgi-related compartment of the insulin secreting cell accumulates proinsulin in the presence of monensin. *Cell.* 39:39-47.

Orci, L., M. Ravazzola, M. Amherdt, D. Louvard, and A. Perrelet. 1985. Clathrin-immunoreactive sites in the Golgi apparatus are concentrated at the trans pole in polypeptide hormone-secreting cells. *Proc Natl Acad Sci U S A.* 82:5385-9.

Orci, L., M. Ravazzola, M.J. Storch, R.G. Anderson, J.D. Vassalli, and A. Perrelet. 1987. Proteolytic maturation of insulin is a post-Golgi event which occurs in acidifying clathrin-coated secretory vesicles. *Cell.* 49:865-8.

Osborne, S.L., J. Herreros, P.I. Bastiaens, and G. Schiavo. 1999. Calcium-dependent oligomerization of synaptotagmins I and II. Synaptotagmins I and II are localized on the same synaptic vesicle and heterodimerize in the presence of calcium. *J Biol Chem.* 274:59-66.

Oyler, G.A., G.A. Higgins, R.A. Hart, E. Battenberg, M. Billingsley, F.E. Bloom, and M.C. Wilson. 1989. The identification of a novel synaptosomal-associated protein, SNAP-25, differentially expressed by neuronal subpopulations. *J Cell Biol.* 109:3039-52.

Palade, G. 1975. Intracellular aspects of the process of protein synthesis. *Science.* 189:347-58.

Peden, A.A., G.Y. Park, and R.H. Scheller. 2001. The Di-leucine motif of vesicle-associated membrane protein 4 is required for its localization and AP-1 binding. *J Biol Chem.* 276:49183-7.

Peng, R., and D. Gallwitz. 2002. Sly1 protein bound to Golgi syntaxin Sed5p allows assembly and contributes to specificity of SNARE fusion complexes. *J Cell Biol.* 157:645-55.

Perin, M.S., N. Brose, R. Jahn, and T.C. Sudhof. 1991. Domain structure of synaptotagmin (p65). *J Biol Chem.* 266:623-9.

Perin, M.S., V.A. Fried, G.A. Mignery, R. Jahn, and T.C. Sudhof. 1990. Phospholipid binding by a synaptic vesicle protein homologous to the regulatory region of protein kinase C. *Nature.* 345:260-3.

Peters, C., M.J. Bayer, S. Buhler, J.S. Andersen, M. Mann, and A. Mayer. 2001. Trans-complex formation by proteolipid channels in the terminal phase of membrane fusion. *Nature.* 409:581-8.

Peters, C., and A. Mayer. 1998. Ca2+/calmodulin signals the completion of docking and triggers a late step of vacuole fusion. *Nature.* 396:575-80.

Pevsner, J., S.C. Hsu, J.E. Braun, N. Calakos, A.E. Ting, M.K. Bennett, and R.H. Scheller. 1994. Specificity and regulation of a synaptic vesicle docking complex. *Neuron.* 13:353-61.

Poskanzer, K.E., K.W. Marek, S.T. Sweeney, and G.W. Davis. 2003. Synaptotagmin I is necessary for compensatory synaptic vesicle endocytosis in vivo. *Nature.* 426:559-63.

Puig, O., F. Caspary, G. Rigaut, B. Rutz, E. Bouveret, E. Bragado-Nilsson, M. Wilm, and B. Seraphin. 2001. The tandem affinity purification (TAP) method: a general procedure of protein complex purification. *Methods.* 24:218-29.

Rapoport, T.A. 1992. Transport of proteins across the endoplasmic reticulum membrane. *Science.* 258:931-6.

Rickman, C., and B. Davletov. 2003. Mechanism of calcium-independent synaptotagmin binding to target SNAREs. *J Biol Chem.* 278:5501-4.

Robinson, I.M., R. Ranjan, and T.L. Schwarz. 2002. Synaptotagmins I and IV promote transmitter release independently of Ca(2+) binding in the C(2)A domain. *Nature.* 418:336-40.

Rosa, P., A. Hille, R.W. Lee, A. Zanini, P. De Camilli, and W.B. Huttner. 1985. Secretogranins I and II: two tyrosine-sulfated secretory proteins common to a variety of cells secreting peptides by the regulated pathway. *J Cell Biol.* 101:1999-2011.

Saegusa, C., M. Fukuda, and K. Mikoshiba. 2002. Synaptotagmin V is targeted to dense-core vesicles that undergo calcium-dependent exocytosis in PC12 cells. *J Biol Chem.* 277:24499-505.

Schiavo, G., Q.M. Gu, G.D. Prestwich, T.H. Sollner, and J.E. Rothman. 1996. Calcium-dependent switching of the specificity of phosphoinositide binding to synaptotagmin. *Proc Natl Acad Sci U S A.* 93:13327-32.

Schiavo, G., G. Stenbeck, J.E. Rothman, and T.H. Sollner. 1997. Binding of the synaptic vesicle v-SNARE, synaptotagmin, to the plasma membrane t-SNARE, SNAP-25, can explain docked vesicles at neurotoxin-treated synapses. *Proc Natl Acad Sci U S A.* 94:997-1001.

Schoonderwoert, V.T., J.C. Holthuis, S. Tanaka, S.A. Tooze, and G.J. Martens. 2000. Inhibition of the vacuolar H+-ATPase perturbs the transport, sorting, processing and release of regulated secretory proteins. *Eur J Biochem.* 267:5646-54.

Schulz, T.A., and C.E. Creutz. 2004. The tricalbin C2 domains: lipid-binding properties of a novel, synaptotagmin-like yeast protein family. *Biochemistry.* 43:3987-95.

Seidah, N.G., and A. Prat. 2002. Precursor convertases in the secretory pathway, cytosol and extracellular milieu. *Essays Biochem.* 38:79-94.

Shorter, J., M.B. Beard, J. Seemann, A.B. Dirac-Svejstrup, and G. Warren. 2002. Sequential tethering of Golgins and catalysis of SNAREpin assembly by the vesicle-tethering protein p115. *J Cell Biol.* 157:45-62.

Simonsen, A., J.M. Gaullier, A. D'Arrigo, and H. Stenmark. 1999. The Rab5 effector EEA1 interacts directly with syntaxin-6. *J Biol Chem.* 274:28857-60.

Simonsen, A., R. Lippe, S. Christoforidis, J.M. Gaullier, A. Brech, J. Callaghan, B.H. Toh, C. Murphy, M. Zerial, and H. Stenmark. 1998. EEA1 links PI(3)K function to Rab5 regulation of endosome fusion. *Nature.* 394:494-8.

Smith, R.E., and M.G. Farquhar. 1966. LYSOSOME FUNCTION IN THE REGULATION OF THE SECRETORY PROCESS IN CELLS OF THE ANTERIOR PITUITARY GLAND. *J. Cell Biol.* 31:319-347.

Sollner, T., M.K. Bennett, S.W. Whiteheart, R.H. Scheller, and J.E. Rothman. 1993. A protein assembly-disassembly pathway in vitro that may correspond to sequential steps of synaptic vesicle docking, activation, and fusion. *Cell.* 75:409-18.

Steegmaier, M., J. Klumperman, D.L. Foletti, J.S. Yoo, and R.H. Scheller. 1999. Vesicle-associated membrane protein 4 is implicated in trans-Golgi network vesicle trafficking. *Mol Biol Cell.* 10:1957-72.

Steiner, D.F., D. Cunningham, L. Spigelman, and B. Aten. 1967. Insulin biosynthesis: evidence for a precursor. *Science.* 157:697-700.

Sugita, S., W. Han, S. Butz, X. Liu, R. Fernandez-Chacon, Y. Lao, and T.C. Sudhof. 2001. Synaptotagmin VII as a plasma membrane Ca(2+) sensor in exocytosis. *Neuron.* 30:459-73.

Sugita, S., Y. Hata, and T.C. Sudhof. 1996. Distinct Ca(2+)-dependent properties of the first and second C2-domains of synaptotagmin I. *J Biol Chem.* 271:1262-5.

Sugita, S., O.H. Shin, W. Han, Y. Lao, and T.C. Sudhof. 2002. Synaptotagmins form a hierarchy of exocytotic Ca(2+) sensors with distinct Ca(2+) affinities. *Embo J.* 21:270-80.

Sun-Wada, G.H., Y. Wada, and M. Futai. 2004. Diverse and essential roles of mammalian vacuolar-type proton pump ATPase: toward the physiological understanding of inside acidic compartments. *Biochim Biophys Acta.* 1658:106-14.

Sutton, R.B., B.A. Davletov, A.M. Berghuis, T.C. Sudhof, and S.R. Sprang. 1995. Structure of the first C2 domain of synaptotagmin I: a novel Ca2+/phospholipid-binding fold. *Cell.* 80:929-38.

Sutton, R.B., D. Fasshauer, R. Jahn, and A.T. Brunger. 1998. Crystal structure of a SNARE complex involved in synaptic exocytosis at 2.4 A resolution. *Nature.* 395:347-53.

Thomas, D.M., G.D. Ferguson, H.R. Herschman, and L.A. Elferink. 1999. Functional and biochemical analysis of the C2 domains of synaptotagmin IV. *Mol Biol Cell.* 10:2285-95.

Toonen, R.F., K.J. de Vries, R. Zalm, T.C. Sudhof, and M. Verhage. 2005. Munc18-1 stabilizes syntaxin 1, but is not essential for syntaxin 1 targeting and SNARE complex formation. *J Neurochem.* 93:1393-400.

Tooze, J., M. Hollinshead, R. Frank, and B. Burke. 1987. An antibody specific for an endoproteolytic cleavage site provides evidence that pro-opiomelanocortin is packaged into secretory granules in AtT20 cells before its cleavage. *J Cell Biol.* 105:155-62.

Tooze, J., and S.A. Tooze. 1986. Clathrin-coated vesicular transport of secretory proteins during the formation of ACTH-containing secretory granules in AtT20 cells. *J Cell Biol.* 103:839-50.

Tooze, S.A., T. Flatmark, J. Tooze, and W.B. Huttner. 1991. Characterization of the immature secretory granule, an intermediate in granule biogenesis. *J Cell Biol.* 115:1491-503.

Tooze, S.A., and W.B. Huttner. 1990. Cell-free protein sorting to the regulated and constitutive secretory pathways. *Cell.* 60:837-47.

Tooze, S.A., G.J. Martens, and W.B. Huttner. 2001. Secretory granule biogenesis: rafting to the SNARE. *Trends Cell Biol.* 11:116-22.

Trimble, W.S., D.M. Cowan, and R.H. Scheller. 1988. VAMP-1: a synaptic vesicle-associated integral membrane protein. *Proc Natl Acad Sci U S A.* 85:4538-42.

Tsuboi, T., and G.A. Rutter. 2003. Multiple forms of "kiss-and-run" exocytosis revealed by evanescent wave microscopy. *Curr Biol.* 13:563-7.

Tucker, W.C., and E.R. Chapman. 2002. Role of synaptotagmin in Ca2+-triggered exocytosis. *Biochem J.* 366:1-13.

Tucker, W.C., J.M. Edwardson, J. Bai, H.J. Kim, T.F. Martin, and E.R. Chapman. 2003. Identification of synaptotagmin effectors via acute inhibition of secretion from cracked PC12 cells. *J Cell Biol.* 162:199-209.

Tucker, W.C., T. Weber, and E.R. Chapman. 2004. Reconstitution of Ca2+-regulated membrane fusion by synaptotagmin and SNAREs. *Science.* 304:435-8.

Ubach, J., Y. Lao, I. Fernandez, D. Arac, T.C. Sudhof, and J. Rizo. 2001. The C2B domain of synaptotagmin I is a Ca2+-binding module. *Biochemistry.* 40:5854-60.

Ubach, J., X. Zhang, X. Shao, T.C. Sudhof, and J. Rizo. 1998. Ca2+ binding to synaptotagmin: how many Ca2+ ions bind to the tip of a C2-domain? *Embo J.* 17:3921-30.

Ungermann, C., K. Sato, and W. Wickner. 1998. Defining the functions of trans-SNARE pairs. *Nature.* 396:543-8.

Urbe, S., A.S. Dittie, and S.A. Tooze. 1997. pH-dependent processing of secretogranin II by the endopeptidase PC2 in isolated immature secretory granules. *Biochem J.* 321 (Pt 1):65-74.

Urbe, S., L.J. Page, and S.A. Tooze. 1998. Homotypic fusion of immature secretory granules during maturation in a cell-free assay. *J Cell Biol.* 143:1831-44.

Verhage, M., A.S. Maia, J.J. Plomp, A.B. Brussaard, J.H. Heeroma, H. Vermeer, R.F. Toonen, R.E. Hammer, T.K. van den Berg, M. Missler, H.J. Geuze, and T.C. Sudhof. 2000. Synaptic assembly of the brain in the absence of neurotransmitter secretion. *Science.* 287:864-9.

Vician, L., I.K. Lim, G. Ferguson, G. Tocco, M. Baudry, and H.R. Herschman. 1995. Synaptotagmin IV is an immediate early gene induced by depolarization in PC12 cells and in brain. *Proc Natl Acad Sci U S A.* 92:2164-8.

Voets, T., R.F. Toonen, E.C. Brian, H. de Wit, T. Moser, J. Rettig, T.C. Sudhof, E. Neher, and M. Verhage. 2001. Munc18-1 promotes large dense-core vesicle docking. *Neuron.* 31:581-91.

von Poser, C., K. Ichtchenko, X. Shao, J. Rizo, and T.C. Sudhof. 1997. The evolutionary pressure to inactivate. A subclass of synaptotagmins with an amino acid substitution that abolishes Ca2+ binding. *J Biol Chem.* 272:14314-9.

Walch-Solimena, C., K. Takei, K.L. Marek, K. Midyett, T.C. Sudhof, P. De Camilli, and R. Jahn. 1993. Synaptotagmin: a membrane constituent of neuropeptide-containing large dense-core vesicles. *J Neurosci.* 13:3895-903.

Wang, C.T., R. Grishanin, C.A. Earles, P.Y. Chang, T.F. Martin, E.R. Chapman, and M.B. Jackson. 2001. Synaptotagmin modulation of fusion pore kinetics in regulated exocytosis of dense-core vesicles. *Science.* 294:1111-5.

Wang, C.T., J.C. Lu, J. Bai, P.Y. Chang, T.F. Martin, E.R. Chapman, and M.B. Jackson. 2003a. Different domains of synaptotagmin control the choice between kiss-and-run and full fusion. *Nature.* 424:943-7.

Wang, P., M.C. Chicka, A. Bhalla, D.A. Richards, and E.R. Chapman. 2005. Synaptotagmin VII Is Targeted to Secretory Organelles in PC12 Cells, Where It Functions as a High-Affinity Calcium Sensor. *Mol Cell Biol.* 25:8693-702.

Wang, P., C.T. Wang, J. Bai, M.B. Jackson, and E.R. Chapman. 2003b. Mutations in the effector binding loops in the C2A and C2B domains of synaptotagmin I disrupt exocytosis in a nonadditive manner. *J Biol Chem.* 278:47030-7.

Weber, T., B.V. Zemelman, J.A. McNew, B. Westermann, M. Gmachl, F. Parlati, T.H. Sollner, and J.E. Rothman. 1998. SNAREpins: minimal machinery for membrane fusion. *Cell.* 92:759-72.

Wendler, F., L. Page, S. Urbe, and S.A. Tooze. 2001. Homotypic fusion of immature secretory granules during maturation requires syntaxin 6. *Mol Biol Cell.* 12:1699-709.

Whyte, J.R., and S. Munro. 2002. Vesicle tethering complexes in membrane traffic. *J Cell Sci.* 115:2627-37.

Wu, M.M., M. Grabe, S. Adams, R.Y. Tsien, H.P. Moore, and T.E. Machen. 2001. Mechanisms of pH regulation in the regulated secretory pathway. *J Biol Chem.* 276:33027-35.

Wu, Y., Y. He, J. Bai, S.R. Ji, W.C. Tucker, E.R. Chapman, and S.F. Sui. 2003. Visualization of synaptotagmin I oligomers assembled onto lipid monolayers. *Proc Natl Acad Sci U S A.* 100:2082-7.

Xu, H., and D. Shields. 1993. Prohormone processing in the trans-Golgi network: endoproteolytic cleavage of prosomatostatin and formation of nascent secretory vesicles in permeabilized cells. *J Cell Biol.* 122:1169-84.

Yin, J.C., J.S. Wallach, M. Del Vecchio, E.L. Wilder, H. Zhou, W.G. Quinn, and T. Tully. 1994. Induction of a dominant negative CREB transgene specifically blocks long-term memory in Drosophila. *Cell.* 79:49-58.

Yuste, R., R.B. Miller, K. Holthoff, S. Zhang, and G. Miesenbock. 2000. Synapto-pHluorins: chimeras between pH-sensitive mutants of green fluorescent protein and synaptic vesicle membrane proteins as reporters of neurotransmitter release. *Methods Enzymol.* 327:522-46.

Zerial, M., and H. McBride. 2001. Rab proteins as membrane organizers. *Nat Rev Mol Cell Biol.* 2:107-17.

Zhang, X., M.J. Kim-Miller, M. Fukuda, J.A. Kowalchyk, and T.F. Martin. 2002. Ca2+-dependent synaptotagmin binding to SNAP-25 is essential for Ca2+-triggered exocytosis. *Neuron.* 34:599-611.

Zhou, A., G. Webb, X. Zhu, and D.F. Steiner. 1999. Proteolytic processing in the secretory pathway. *J Biol Chem.* 274:20745-8.